AD_____

Award Number: DAMD17-01-1-0688

TITLE: Novel Tissue Models of Junctional Epidermolysis Bullosa to Characterize Functional Mechanisms of Sulfur Mustard Injury to Human Skin

PRINCIPAL INVESTIGATOR: Jonathan A. Garlick, Ph.D.

CONTRACTING ORGANIZATION: The Research Foundation of SUNY State University of New York
Stony Brook, New York 11794-3362

REPORT DATE: May 2003

TYPE OF REPORT: Annual

PREPARED FOR: U.S. Army Medical Research and Materiel Command
Fort Detrick, Maryland 21702-5012

REPORT DOCUMENTATION PAGE

Form Approved
OMB No. 074-0188

1. AGENCY USE ONLY (Leave blank)	2. REPORT DATE	3. REPORT TYPE AND DATES COVERED
	May 2003	Annual (1 May 2002 - 30 Apr 2003)

4. TITLE AND SUBTITLE
Novel Tissue Models of Junctional Epidermolysis Bullosa to Characterize Functional Mechanisms of Sulfur Mustard Injury to Human Skin

5. FUNDING NUMBERS
DAMD17-01-1-0688

6. AUTHOR(S)
Jonathan A. Garlick, Ph.D.

7. PERFORMING ORGANIZATION NAME(S) AND ADDRESS(ES)
The Research Foundation of SUNY State
University of New York
Stony Brook, New York 11794-3362

E-Mail: jgarlick@notes.cc.sunysb.edu

8. PERFORMING ORGANIZATION REPORT NUMBER

9. SPONSORING / MONITORING AGENCY NAME(S) AND ADDRESS(ES)
U.S. Army Medical Research and Materiel Command
Fort Detrick, Maryland 21702-5012

10. SPONSORING / MONITORING AGENCY REPORT NUMBER

11. SUPPLEMENTARY NOTES
Original contains color plates: All DTIC reproductions will be in black and white.

12a. DISTRIBUTION / AVAILABILITY STATEMENT
Approved for Public Release; Distribution Unlimited

12b. DISTRIBUTION CODE

13. ABSTRACT (Maximum 200 Words)

In the second year of our research, our laboratory has extensively studied skin pathophysiology in response to SM by adapting *in vivo*, human skin/nude mouse chimera to further understand mechanisms of SM-induced vesication of human skin (TASK 1). We have established dose/time responses of these skin-like tissues following exposure to SM vapor and have characterized prevesicating and post-vesicating changes in basement membrane and apoptosis that lead to early cell injury and subsequent dermal-epidermal separation. Furthermore, we have developed and tested new tissue models designed to study how basement membrane proteins alter SM-induced selectivity of basal cell injury (TASK 8) and how wound response is impaired after SM exposure (TASK 6). These studies delineated key factors and pathways that direct the survival and growth of human, skin-like tissues, such as the processing of laminin 5 and activation of AKT signaling, that will now serve as an important baseline for subsequent studies that will determine the effect of SM. In addition, we have refined our organotypic model of wound healing to include components found immediately after SM injury so that effects of SM on re-epithelialization can now be studied in a more *in vivo*-like environment.

14. SUBJECT TERMS
Sulfur mustard, basement membrane, organotypic culture, keratinocytes

15. NUMBER OF PAGES
70

16. PRICE CODE

17. SECURITY CLASSIFICATION OF REPORT	18. SECURITY CLASSIFICATION OF THIS PAGE	19. SECURITY CLASSIFICATION OF ABSTRACT	20. LIMITATION OF ABSTRACT
Unclassified	Unclassified	Unclassified	Unlimited

Table of Contents

INTRODUCTION

Due to ethical reasons, limited studies have been carried out in understanding the detailed mechanistic actions of SM using human skin. Therefore, an ideal approach to identify molecular and biochemical pathways of sulfur mustard (SM)-induced vesication would be to use engineered human skin which mimics the clinical and histologic features of this tissue. During the course of the past year, **our laboratory has extensively studied skin pathophysiology in response to SM by adapting in vivo, human skin/nude mouse chimera, which display many features of human skin to further our understanding of mechanisms of SM-induced vesication of human skin.** In doing so, we have established dose/time responses of these human, skin-like tissues following exposure to SM vapor and have characterized prevesicating and post-vesicating doses leading to early cell injury and which in turn initiate events leading to subsequent dermal-epidermal separation. We have accomplished this by establishing the baseline response of normal skin keratinocytes to SM by identifying apoptotic and basement membrane changes that are associated with the earliest events in lesion formation. Our studies have provided important proof of concept that novel *in vivo* skin-like tissue models mimic tissue alteration previously found in animal models of SM response of skin. **Furthermore, we have developed and tested new tissue models designed to study how basement membrane proteins alter SM-induced selectivity of basal cells and how wound response is impaired after exposure to SM**. These human tissue models will be of great help in understanding the functional mechanisms of SM injury and in testing new countermeasures to limit morbidity and mortality due to SM.

BODY – PART ONE

Task 8: To develop and construct novel human tissue models with and without basement membrane to determine the role of basement membrane components on the survival of human keratinocytes in response to sulfur mustard.

Task 8: To determine how the presence or absence of basement membrane effects the response of skin-like tissues to SM exposure.

INTRODUCTION - The maintenance of human epidermis is dependent on the regulation of keratinocyte proliferation, terminal differentiation and survival. The findings described above have demonstrated that not all basal keratinocytes in human skin exposed to sulfur mustard were susceptible to cellular damage and apoptosis. This suggested that interactions between basal keratinocytes and basement membrane or extracellular matrix proteins might control the capacity of cells to survive exposure to SM. Conversely, other cellular interactions with connective tissue components may be linked to the inability to survive exposure to SM. A very important goal of our studies is to determine cellular signals that direct the survival response to SM exposure. Since we found in our *in vivo* studies that only specific subsets of basal keratinocytes underwent cellular damage leading to apoptosis, we are well-poised to define which extracellular matrix (ECM) or basement membrane (BM) components can provide survival signals which would protect cells when challenged with SM.

The cutaneous basement membrane zone is a complex network of macromolecules that promotes cell adhesion, tissue organization and modulates keratinocyte growth and differentiation. A central goal of our research is to use our knowledge of basement membrane biology, and specifically the role of

individual BM components to further understand how basement membrane directs the survival or death of cells exposed to SM. To address this directly, we have developed and characterized novel organotypic tissue models for human epidermis over the last year in which keratinoctyes were grown on polycarbonate membranes coated with purified ECM or BM components placed on a contracted collagen gel which has been repopulated with dermal fibroblasts. Using these tissue models, we have determined the response of normal human keratinocytes to the ECM and BM substrates as a preliminary study before determining their response to SM. To accomplish this, we have used immunohistochemical, morphologic and biochemical analyses to characterize the influence of these ECM and BM subtrates on the morphogenesis, survival, differentiation and growth of NHK. We have observed that the presence of individual BM components, such as Type IV and laminin 1, supports keratinocyte growth and survival in a way similar to that of tissues grown on intact BM on de-epidermalized dermis. In contrast, tissues grown in organotypic cultures on ECM components that are not found in basement membrane did not fully support cell growth and survival of these tissues. We are now well-poised to use these ECM/BM substrate-specific human tissue models to determine the differential susceptibility of tissues grown on various connective tissue substrates to SM damage.

EXPERIMENTAL RESULTS :

1 - Basement Membrane and Extracellular Matrix Components Modify Epidermal Morphogenesis – The morphology of epithelial tissues generated on a variety of connective tissue substrates was compared in order to determine the effect of the extracellular matrix microenvironment on normalization of tissue architecture. When keratinocytes were grown on an acellular, de-epidermalized dermis containing pre-existing basement membrane components Collagen IV, VII and laminin 1 (Andriani et al., in press, see appendix), the epithelium demonstrated *in vivo*-like tissue architecture and organization, as seen by the presence of cuboidal basal cells nested in undulating rete pegs and well-defined spinous, granular layers and an orthokeratinized stratum corneum (Figure 1A). A slightly altered pattern of morphologic differentiation was seen when cells were grown directly on a contracted Type I collagen gel containing dermal fibroblatsts. However, the transition between strata was not as distinct as was seen in AlloDerm cultures and no polarization of the basal layer was observed (Figure 1B). When keratinocytes were seeded onto the ECM or BM-coated polycarbonate membranes the morphology of epithelial tissues varied as a function of the connective tissue substrate. Tissues grown on membranes coated with the BM components Type IV Collagen (Figure 1E) or Laminin 1 (Figure 1F) demonstrated morphologic features most similar to cultures grown on de-epidermalized dermis. These tissues were well-stratified with polarized basal cells and a well-formed spinous layer In contrast, cultures grown on fibronectin-coated membranes, demonstrated tissues that were somewhat thinner and less organized than cultures grown on de-epidermalized dermis or on the BM proteins that demonstrated flattened basal cells and poorly-organized spinous layer (Figure 1H). The most aberrant morphology was seen on a Type I collagen substrate (Figure 1D), where the cultures demonstrated a thin epithelium characterized by non-polarized, flattened basal cells and very thin spinous layer and stratum corneum. These results demonstrated that epithelial morphogenesis and tissue architecture were dependent on the nature of ECM or BM proteins at the dermal-epidermal interface. The presence of basement membrane proteins enhanced tissue organization and resulted in normalization of tissue morphology.

2 - Reduced cell growth and elevated apoptosis were present only in tissues grown on proteins not found in basement membrane (fibronectin and Type I collagen) - Growth of tissues on coated insets was determined after cultures were incubated with BrdU for 6 hours and the fraction of basal cells in S-phase

nuclei was measured following staining with an anti-BrdU antibody (Labelling Index = LI) (Figures 2 and 5). Tissues grown on Type IV collagen demonstrated elevated LIs (27%) that were comparable to proliferative indices seen for AlloDerm controls (28%) grown on pre-existing basement membrane components. Proliferation rate was greater in these cultures in comparison to cells grown either on contracted collagen gels (26%) or on Laminin 1 (23%). Lower LIs were seen for cultures grown on fibronectin (16.5%) and Type I collagen (15%). These findings demonstrated that all substrates maintained the growth of keratinocytes and that levels of proliferation were roughly correlated with overall tissue thickness. However, the presence of basement membrane components, such as Type IV collagen, sustained cell growth at significantly higher levels than was seen in the presence of proteins that are not normally found in the basement membrane, such as fibronectin and Type I collagen.

In situ TUNEL assay was used to determine the number and distribution of keratinocytes that have undergone apoptotic cell death when tissues were grown on different connective tissue substrates. No TUNEL-positive basal cells were seen when cultures were grown on Type IV collagen substrates, and apoptotic cells were only seen in the upper layers of the epithelium (Figure 3, arrow), as is seen in normal, human epithelium. In contrast, roughly 6% of basal cells were TUNEL-positive and nearly 3-fold more apoptotic basal cells (17.5%) were seen when tissues were grown on fibronectin (Figure 4 and 5). These findings demonstrated that the BM component Type IV collagen promoted keratinocyte survival while ECM components that are not normally found in basement membrane were not able to prevent apoptotic cell death of basal cells. The improved tissue architecture seen on Type IV collagen-coated membranes have demonstrated that normalization of tissue morphogenesis was associated with sustained cell proliferation and the absence of basal cell death (Figure 5).

3- Type IV collagen immediately activates AKT survival signaling pathway – A very important goal of our studies is to determine cellular signals that direct the survival response to SM exposure. Since we found in Part I that only specific subsets of basal keratinocytes underwent cellular damage leading to apoptosis, we next hoped to define which ECM or BM components would provide survival signals which would protect cells when challenged with SM. In an effort to further understand the role of Type IV collagen in the stimulation of keratinocyte growth and survival that was seen in organotypic cultures, we have assayed activity of AKT in monolayer and organotypic cultures. AKT is a serine/threonine kinase that is known to stimulate cell survival and proliferation when in a phosphorylated, activated form. We utilized an assay for AKT activity which measures the ability of this kinase to phosphorylate glycogen synthase kinase 3β (GSK3β). Elevated activity of AKT would thus be demonstrated by an increased degree of GSK3β phosphoryation. We have performed two assays to determine which ECM or BM coating could stimulate AKT-mediated signaling. In order to determine the response of AKT when keratinocytes were grown in monolayer culture, cells were seeded in serum-free media on plates coated with either laminin 1, Type IV collagen, fibronectin, Type I collagen or on uncoated, tissue culture plastic and harvested after 4 and 24 hours. Only cells seeded on Type IV collagen demonstrated AKT activation 4 hours after seeding while other substrates demonstrated very minimal or no activation (Figure 6A). Since the anti-apoptotic phenotype demonstrated by Type IV collagen was shown in organotypic culture, it was important to also determine whether AKT activation occured when cells were seeded onto coated polycarbonate membranes. Only Type IV collagen showed AKT activity within 30 minutes after harvesting cells (Figure 6B). By 2 hours after seeding, cells seeded on fibronectin also demonstrated AKT activity that was equivalent to cells grown on Type IV collagen. By 4 hours after seeding, low levels of AKT activity were seen for cells grown on Type I collagen, well. However, by 8 hours after seeding, AKT levels were more highly elevated in cells grown on fibronectin and Type IV

collagen. These findings demonstrated that keratinocyte survival on Type IV collagen was associated with the immediate upregulation of AKT activity. In this light, AKT activity has proven to be a useful marker in determining survival response of keratinocytes to SM.

4 - *Only Type IV collagen is permissive for synthesis and deposition of proteins required for basement membrane assembly* – Tissues fabricated on coated polycarbonate membranes were stained using immunohistochemistry technique to determine the synthesis and deposition of basement membrane components. Tissues grown on Type I collagen, Type IV collagen and fibronectin all demonstrated linear deposition of laminin 5 when stained with an antibody that detects the intact laminin 5 heterotrimer (Figure 7). This pattern was similar to that seen for cultures grown on AlloDerm (Figure 8) and contracted collagen gels and showed that laminin 5 secretion was independent of the nature of ECM proteins present when cultures were initiated. A similar pattern of expression and deposition was seen when cultures were stained with an antibody directed against the γ2 chain of laminin 5 (Figure 8). In contrast, only tissues grown on Type IV collagen substrates demonstrated a significant upregulation of the α6 integrin subunit, which is the basement membrane receptor for laminin 5. Expression of this subunit was significantly elevated in basal keratinocytes grown on Type IV collagen-coated inserts, which demonstrated intense, cytoplasmic staining in basal cells (Figure 9) and some deposition on the coated membrane (Figure 9). This intensity of stain was similar to that seen for tissues grown on AlloDerm, which showed linear deposits of α6 integrin subunit and was more continuous than the punctuate staining seen when tissues were grown on contracted collagen gels. In contrast, tissues grown on Type I collagen-coated membranes demonstrated minimal production of α6 integrin that was limited to the cytoplasm while fibronectin-coated membranes showed no synthesis or deposition of α6 integrin. This showed that while all substrates were permissive for the deposition of laminin 5, co-localization with its integrin pair was only seen when pre-existing basement membrane proteins or Type IV collagen were present. Since we have previously shown that AlloDerm tissues that co-localization of α6 integrin and laminin 5 were associated with BM assembly (Andriani et al, see appendix), this suggests that only the presence of pre-existing BM components, such as Type IV collagen, will allow this to occur.

Western blot analysis of tissues grown on coated inserts, contracted collagen gels and AlloDerm were performed to determine the absolute amounts of laminin5 produced on these substrates. This was accomplished by performing immunoblot analysis using an antibody recognizing the short arm of the γ2 chain of laminin 5 to demonstrate the unprocessed (155kD) and unprocessed (105kD) forms of this molecule. Total laminin 5 was significantly upregulated for cultures grown on AlloDerm and contracted collagen gels. Lower levels of laminin 5 production were seen for cultures grown on Type IV collagen and fibronectin, which synthesized similar amounts of this protein. These levels of expression were 4-fold greater than those seen for cultures grown on Type I collagen. When the ratio of processed to unprocessed forms were calculated, very little processed form of the γ2 chain of laminin 5 was seen for cultures grown on Type 1 collagen membranes (ratio=1.06). A three-fold increase in processing was seen for cultures grown on Type IV collagen membranes (ratio=3.04) and fibronectin (ratio=2.01). This demonstrated that while total production of laminin 5 was highest on AlloDerm and contracted collagen gels, Type IV collagen substrates induced a greater degree of synthesis and processing than tissues grown on Type I collagen.

The presence of other proteins found in basement membrane showed a variable pattern of expression. Laminin 1 (Figure 12) and Type VII collagen (Figure 13) were found in basal cells grown on fibronenctin and Type I and IV collagens. However, the distribution of these proteins was restricted to the cytoplasm

and was not deposited at the basement membrane interface, as was seen for tissues grown on AlloDerm and on contracted collagen gels. In distinction, deposition of Type IV Collagen (Figure 14) was not seen in tissues grown on fibronectin and Type I collagen . These findings suggested that proteins present in native basement membrane, such as Type IV Collagen, were required for the normalized deposition of other BM components. In this light, the synthesis, secretion and processing of a broader complement of these proteins could only occur in the presence of pre-existing basement membrane components.

5 - Expression of epidermal differentiation markers- To determine if differences in tissue architecture seen when cultures were grown on different stromal substrates were associated with aberrant keratinocyte differentiation, immunofluorescent studies were performed to map the distribution of markers of early (keratin 1=K1) and late (filaggrin) markers of keratinocyte differentiation. All cultures grown on coated membranes demonstrated normalized, strata-specific expression of K1 and FIL. Expression of these markers occurred regardless of the overall thickness of the tissue and were similar to the distribution seen in AlloDerm controls (Figure 15). For example, well-organized, thicker tissues such as those grown on Type IV Collagen, laminin 1 and on a mixture of fibronectin and collagen 1 demonstrated expression of K1 in immediate suprabasal layers of the epithelium in a pattern similar to those seen for cultures grown on AlloDerm and directly on the contracted Type I collagen gel. Interestingly, thinner and more poorly-organized tissues, such as those grown on fibrillar Type 1 collagen, Type I collagen and fibronectin also showed K1 expression that was limited to suprabasal cells as seen by the presence of this protein in cells immediately above the basal layer. This demonstrated that appropriate K1 expression was independent on ECM or BM substrate or on overall tissue thickness. In a similar manner, expression of FIL was seen in tissues grown on all substrates in a distribution which extended from the mid-spinous to the surface layers, in a pattern which mimicked that seen in AlloDerm and collagen gels (Figure 11). Taken together, these findings show that expression of markers of keratinocyte differentiation was independent of the presence of particular ECM or BM components.

PROBLEMS ENCOUNTERED: The development of the tissue models described have proceeded without significant problems or delays. At the outset, we attempted to establish these cultures in the presence of fibroblasts that grew directly on the plastic surface under the insert containing the epithelial cells, without embedding fibroblasts in contracted gels, that would serve as controls. However, these tissues underwent minimal stratification, indicating that fibroblasts needed to be in contracted collagen gels for optimization of tissue growth and morphology. As a result, all experiments were conducted by placing contracted collagen gels under the coated polycarbonate membranes. We are now ready to begin conducting studies using SM in our own facility to test the response of these tissues to SM doses. The onset of this work has been delayed for several months by unexpected delays in the construction of our facility. Thanks to the diligence of Mr. Ben Casole and his staff, we were recently approved for the use of SM in our lab and expect to begin this work this month.

NEXT: The establishment of three-dimensional tissue models of normal human keratinocytes grown on individual basement membrane components or extracellular matrix proteins has opened new avenues for directly assessment of cellular pathways that are associated with targeted cell injury induced by SM. Our next step will be to determine SM doses which will allow us to model cell and tissue alterations seen in our *in vivo* studies. Once dose ranges have been established for these in vitro studies, we will be able to assess SM response to tissues grown on intact BM, partially-formed basement membrane or on individual proteins which are either components of BM (Type IV collagen) or are not found in BM (Type I collagen). The studies listed above will serve as an important baseline to measure the tissue response to

SM and all assays have been well-established to determine cell survival, growth and differentiation in response to SM exposure as outlined in TASK 8B of the Statement of Work.

BODY – PART TWO

TASK 1: To determine the dose/time responses of normal human skin-like tissues comprised of normal keratinocytes following exposure to SM.

TASK 1: To determine the alterations in basement membrane structure and function and associated changes in apoptotic cell death following exposure of grafted human skin-like transplants to sulfur mustard

INTRODUCTION: The goal of these studies was to determine the pathophysiology of SM–induced cutaneous lesions on human skin grafts that were generated as three-dimensional, organotypic cultures that were transplanted to nude mice. Until now, a variety of animal models have been the mainstay of studies directed at determining the effects of SM on human skin. Our previous studies have shown that this human tissue model demonstrates features that are remarkably similar to the response seen in these models of SM-exposure. This has been accomplished by performing time-course studies that have characterized the morphologic, immunohistochemical and apoptotic response to SM.

EXPERIMENTAL RESULTS:

1.Grafting organotypic cultures to nude mice and exposing grafts to neat Sulfur Mustard - Organotypic cultures were fabricated and transplanted to nude mice, forming stable surface grafts with the clinical appearance of normal skin and all histologic features of normal epithelial and dermal compartments. The rapid normalization of the epidermal and stromal compartments of these grafts, the ultrastructural evidence of intact basement membrane (see Appendix, *in press*) and the presence of stem cells in their normal, basal position allows study of SM effects on this tissue. A total of 115 animals were grafted and 78 were used for the SM exposure experiments. These experiments were performed at Medical Research and Materiel Command in Aberdeen, MD by Dr. John Petrali and Tracey Hamilton. Animals were shipped to Aberdeen three to six weeks after grafting. Mice were anesthetized and the graft was exposed to a vapor of neat SM or to a sham exposure with no SM. Grafts were exposed to SM vapor by wetting a disc of Whatman filter paper (#2) that was placed into a polyethylene cap (Colubia Diagnostics Inc, Springfield, VA) with 10ul of neat SM. These vapor caps were placed over the graft site and adjacent mouse skin and were secured with double-sided tape. The dose of SM administered was established by varying the duration of exposure to the HD vapor. After removal of the caps, mice were placed in individual holding cages under a connecting hood to allow elimination of any residual SM. At the appropriate post-exposure times (see below), mice were euthanized and grafts and a border of adjacent mouse skin were removed with a dermatologic punch. Skin specimens were cut in half and either fixed in 10% neutral buffered formalin or snap frozen in liquid nitrogen after being placed in 2M sucrose overnight. Morphology was studied after H and E staining and immunohistochemical stains were performed from either paraffin-embedded specimens (Laminin 1) or from non-fixed, frozen specimens (laminin 5, Type IV collagen, Type VII collagen). In situ TUNEL assay was performed using ISOL (in situ oligo ligation) end-labeling and immunoperoxidase detection of apoptotic cells in paraffin sections.

Numbers of apoptotic cells were calculated by counting 1000 nuclei present in four serial sections that were each 100 um apart.

2. Preliminary experiments to determine effective dose of SM – Since the SM dose at which tissue damage of human grafts would occur was not known, it was first important to establish the dose of SM vapor exposure and times after exposure that would demonstrate meaningful pathologic alterations in grafted skin. Based on previous work, the following parameters of exposure were first tested in 27 nude mice to test each condition in triplicate.

Time after exposure	Length of exposure		
12 hours	2 min	5 min	10 min
48 hours	2 min	5 min	10 min
14 days	2 min	5 min	10 min

Grafts were exposed to SM for two minutes and were excised after either 12 hours or 48 hours yielded little damage to the epithelium (Figure 16). While no alterations in epithelial architecture or in individual cells was seen 12 hours after exposure, several pyknotic nuclei were seen in the epithelium 48 hours after exposure. This suggested a positive correlation between tissue damage and the length of time after exposure. However, it was clear that higher exposure times were required for SM to induce significant changes in tissue structure. Five minute exposures produced tissue alterations that were limited to the basal cell layer and were characterized by the presence of pyknotic nuclei that were seen 12 hours after exposure. By 14 days after SM exposure, pyknotic nuclei were seen at this dose and a small area of microvesiculation was visible beneath the basal layer. This suggested that tissue damage was increased as the length of time after exposure was increased. Highest doses of SM (10 minutes) demonstrated significant tissue alterations. By 48 hours after exposure, microvesicles were seen that contained numerous changes in the overlying epidermal cells. These changes included scattered necrotic basal cells that had separated from adjacent cells and basement membrane zone and the presence of pyknotic nuclei in the basal and superficial layers of the epithelium. By 14 days after exposure, the epidermis had completely separated from the dermis and eschar was seen on the surface of the grafts. These grafts demonstrated large numbers of pyknotic fibroblasts in themost superficial layer of the dermis. Interestingly, none of the exposures demonstrated a significant degree of inflammatory infiltrate or connective tissue edema, suggesting that the effect seen on the epithelium was due to direct effects on the epithelium and not to secondary effects induced by release of mediators from inflammatory cells. Higher exposures (5 min and 10 min) did demonstrate altered fibroblasts in the most superficial layer of the dermis that included the presence of pyknotic nuclei.

3. A prevesication phase characterized by selective basal cell death is induced shortly after SM exposure (6 hours) while a post-vesication phase is only seen at longer latencies (24 hours) - Based on the findings from the first experiment, a second group of grafted mice were exposed to SM in order to determine if prevesication and post-vesication phases of SM-induced damage could be seen in grafted tissues. The

goal was to enable examination of "initiating" damage to the epithelium that preceeded vesicating damage, so that in early changes at the basement membrane interface could be seen. It was decided that the 2 minute exposures did not provide useful tissue changes, but that exposures in the range of 5 to 10 minutes provided such a window through which the two phases of tissue damage could be documented. In addition, since significant basal cell damage was seen after 12 hours and microblisters were seen as early as 48 hours after exposure, it was decided to study the effects of SM as early as 6 hours after exposure. This experiment was performed as follows on a total of 27 grafted mice:

Time after exposure	Length of exposure		
6 hours	8 min	10 min	12 min
24 hours	5 min	8 min	10 min

1. Morphologic response 6 hours after SM exposures - Three mice were exposed for either 8 minutes (Figure 17), 10 minutes (Figure 18) or 12 minutes (Figure 19) and were analyzed by Hematoxylin and Eosin staining. When seen 6 hours after SM exposure, cellular damage was completely confined to the basal cell layer of the epidermis as suprabasal layers showed normal tissue integrity and no structural alterations or damaage. Pyknotic nuclei were confined to the basal layer and were not accompanied by evidence of changes in the cytoplasm suggestive of necrosis. The distinct compartmentalization of damaged cells to the basal layer was very striking. In addition, the damage to basal cells appeared to be selective, as isolated individual cells and clusters of basal cells demonstrated evidence of nuclear damage. Changes in nuclear morphology did not vary significantly between exposure times. In contrast, control, sham-exposed grafts demonstrated normal tissue morphology. Pyknotic nuclei were present as solitary cells and in small clumps along the basal layer of each graft. This demonstrated that early cellular damage in response to SM was selective in several regards – selectively nuclear, selective to the basal compartment and selective to groups of cells within the basal layer. This suggests that there is a tissue susceptibility that drives early events in SM-induced injury in which subsets of basal cells are susceptible to cell death while others are protected, perhaps by intracellular survival signals.

2. **Morphologic reponse 24 hours after SM exposures** - In contrast to the specimens which were sampled at 6 hours after exposure, grafts studied 24 hours after exposures to SM showed significantly greater degrees of tissue damage. These changes were seen even after relatively short exposure times (5 min) and included the presence of pyknotic nuclei in all layers of the epithelium that were especially concentrated in the basal and suprabasal layers (Figure 21). These tissues demonstrated necrosis and ballooning degeneration of basal cells that were associated with their separation from the basement membrane zone. These areas of separation appeared as well-defined microvesicles after both 8 minute (Figure 22) and 10 minute exposures (Figure 23). This demonstrated, a dose-dependent effect on tissue damage that was correlated to SM dose 24 hours after exposure to the agent. In addition, the degree of epidermal necrosis was correlated with dermal-epidermal separation as seen by areas of microscopic vesication seen with necrosis of the overlying epidermis. Fibroblasts in the upper dermis demonstrated large numbers of pyknotic nuclei. Inflammatory infiltrate was still somewhat sparse, but was greater than in tissues sampled 6 hours after exposure. These findings demonstrated that a time interval of greater

than 6 hours was needed to induce vesication at the dermal-epidermal interface. This showed that the pre-vesication phase of tissue damage seen at 6 hours was necessary to initiate lesions but was not sufficient to cause vesication. This suggested that vesication was not an immediate response to SM exposure but was rather preceded by precursor lesions in the basal layer that were targeted to specific subsets of basal cells. This early initiating damage represents an early window of cellular changes that may represent the target population of cells that are susceptible to early damage. Subsequently, a short latent period was required for the more complete manifestation of SM-induced tissue damage.

4 – Dose-independent, apoptotic cell death was restricted to selected populations of basal cells shortly after SM exposure (6 hours) while vesication-associated apoptosis occurs in a dose-dependent manner after longer latencies (24 hours) - We performed a time-course study in which tissues from the above Experiment 2 were stained by *in situ* TUNEL assay to detect apoptotic cells. Measures of TUNEL-positive cells were calculated as both the percentage of total numbers of apoptotic cells seen throughout the tissue in basal and suprabasal layers (Figure 24) and as the percentage of basal cells that were apoptotic (Figure 25). Sham-exposed grafts were used as controls. By 6 hours after the 8 min SM exposure, roughly 5% of basal cells were TUNEL-positive. Interestingly, percentages of apoptotic cells did not increase with increased length of exposure, suggesting that there was a threshold number of basal cells that were targeted for early apoptosis in these tissues. On the other hand, a sharp increase in the percentage of TUNEL-positive basal cells was seen after 24 hours when the exposure time was increased from 5 to 8 and 10 minutes. An even more dramatic dose-dependency was seen when the percentage of total apoptotic cells in the tissue was calculated. The percentage of TUNEL-positive cells seen 24 hours after SM exposure was 5% for exposures of 5 min, 15% for exposures of 8 min and 35 % for 10 minute exposures. All of the apoptotic cells seen after 5 minute exposures were found in the basal cell layer and were associated with a lack of vesication. In contrast, most apoptotic cells seen after 8 and 10 minute exposures were found in the suprabasal layers and were associated with vesication. The finding that only a small subset of cells was effected 6 hours after exposure in a dose-independent manner suggested that a limited number of cells was susceptible to the initial effects during the prevesicant stage. The significantly greater numbers of apoptotic cells seen 24 hours after SM exposure suggested that a majority of these damaged cells were the result of secondary effects and were not directly caused by SM exposure. We have found that at the prevesication stage, subsets of basal cells have already been targeted for cell death and have undergone apoptosis. This represents only a fraction of the total number of apoptotic cells that are present a the subsequent vesication stage, suggesting that additional apoptotic events occur after this initiating damage. These findings confirm previous results performed in hairless guinea pigs that demonstrated that apoptotic pathways are involved in the cytotoxic death of basal cells.

5. Immunohistochemical analysis of basement membrane proteins after SM exposure demonstrated that initial apoptotic response to SM occurs before significant basement membrane disruption - Immunohistochemical stains for basement membrane proteins were performed on exposed grafts in order to correlate specific alterations in these proteins with prevesication and post-vesication damage in these tissues. Specifically, tissues were stained for laminin 5, Type VII Collagen and Type IV Collagen, using the antibodies listed in the Table below. Non-fixed, frozen sections were stained using the GB3 antibody to detect the intact laminin 5 heterotrimer. At 6 hours after exposure, neither grafts exposed for 8 min nor 10 min demonstrated any disruption of laminin 5 staining (Figure 26). Laminin 5 was deposited in a linear distribution along the basement membrane zone in a pattern which was identical to that seen in sham-exposed controls. Staining with an antibody directed against the γ2 chain of laminin 5 (SE144) revealed similar findings (data not shown). Similarly, staining for Type VII Collagen was linear and not

disrupted during this prevesication stage (6 hours post-exposure) after both 8 min and 10 min exposures in a pattern similar to sham-exposed controls (Figure 26). In contrast, at 24 hours post-exposure both laminin 5 and Type VII Collagen was disrupted. This distribution was characterized by skip areas in which no stain was seen, as well as areas of broadened and diffuse staining and decreased linear staining. These results suggested that the initial apoptotic response to SM seen in basal cells occured before significant basement membrane disruption and is independent of it. These results were supported by stains with an antibody directed against laminin 1, which were performed on pararffin-embedded tissues after pepsin digestion (Figure 27). Tissues stained after being exposed to SM for either 8 min or 12 min did not show disruption of laminin 1, 6 hours after exposure and appeared similar to sham-treated controls. In contrast, grafts exposed to SM for either 5 min, 8 min or 10 min showed focal areas of disruption of Type IV collagen deposition 24 hours after SM exposure. This was particularly at the 8 minute exposure, where less immunoreactive material was seen along the basement membrane at the floor of the microvesicle. When TUNEL and laminin 1 stains were performed on adjacent serial sections of 24 hour post-exposure grafts, a discontinuous laminin 1 stain was found to be associated with the presence of numerous apoptotic cells that had detached from the basement membrane (Figure 28). In contrast, laminin 1 stain was still continuous during the prevesication stage (6 hours post SM-exposure), where several basal, apoptotic cells were seen. This supported the view that basement membrane was largely intact during events leading to basal cell apoptosis and disruption of this structure only occurred after a period of latency.

Antibodies used to detect basement membrane components

Antibody	Specificity	Source
GB-3	Complete heterotrimer of laminin-5	G. Meneguzzi
SE-144	Gamma 2 subunit laminin-5	G. Meneguzzi
MoAb	Type IV collagen	Sigma Inc.
MoAb	Type VII collagen	Sigma Inc.
MoAb	Laminin-1	Sigma

PROBLEMS ENCOUNTERED - Considering the logistical challenge posed by grafting animals in our facility and exposing them at Aberdeen, the progress of this work has been extremely good. This is due to the outstanding logistical assistance given by Dr. John Petrali and Tracey Hamilton, who performed the exposures in their facility. Several grafted animals died in transit and several other grafts were lost before exposures could be given. With this in mind, we will ensure that grafts are stable before shipping the next sets of mice that will be grafted with JEB cells and normal keratinocytes. This will ease the logistical burden by knowing in advance the number of mice that will be exposed to SM.

NEXT - Having constructed skin-like models containing JEB keratinocytes during Year I of these studies (Task 2) and by establishing dose/time levels of SM which can induce subvesicating (prevesication phase) injury and vesicating injury with grafts of normal keratinocytes, we are now prepared to test the effects of these SM doses on grafted JEB keratinocytes (Tasks 3, 5 and 6). In addition, our important observation that only subsets of basal cells are targeted by early (6 hour) SM exposure will direct studies to determine the cellular and molecular basis for this sensitivity to or protection from SM injury. By furthering our understanding of the molecular basis of this phenomenon through studies described above using *in vitro* models (Task 8), we will

attempt to genetically modify cells to augment their survival potential when challenged by SM. If successful in identifying these pathways, we will next graft tissues constructed from cells whose genetic modification would allow a significant survival advantage to SM exposure *in vivo*. We feel that the finding of selective basal cell damage and survival may be a critical determinant in the response to SM exposure and we will intensively pursue the mechanism through which this occurs.

BODY – PART THREE

Task 6: Assay the response of organotypic cultures and grafts to high, vesicating doses of SM and conduct phenotypic assays of wound healing response.

INTRODUCTION - Blisters induced by SM heals very slowly and can revesicate after healing This wound healing response is characterized by delayed reepithelialization of aberrant keratinocytes, persistence of apoptotic epithelium in the wound and disordered maturation of the reestablished epithelium. In addition, the persistent loss of immunoreactivity of laminin 5 after SM exposure suggests that alkylated fragments of laminin 5 may both inhibit reepithelialization after injury and prevent reestablishment of normal BM, thereby leading to further ulceration of the epithelium. Such altered healing responses to SM injury are serious complications and result in prolonged hospitalizations and post-injury care. The mechanism of such altered wound healing must be understood for the development of measures designed to accelerate this process to proceed. An ideal approach to study these events following SM injury to human skin would be to use tissue models which mimic the response to wounding in its *in vivo* counterpart. We have developed techniques for construction of a model for wound healing of human keratinocytes *in vitro* which has been generated by adapting organotypic cultures to follow the response of stratified epithelium to an incisional woud. Using this system, we have previously found that the chronology of events during re-epithelialization is similar to that reported in skin during wound healing. However, this model did not contain components that would normally be found in an acute wound environment that has been exposed to SM, such as fibrin and fibronectin and platelet-derived products. In an effort to improve the organotypic wounding model and adapt it to study response to SM exposure, we have developed techniques to follow the response to a wound generated in the presence of serum components which form a clot immediately after wounding. This was accomplished by adding gelled plugs of platelet-poor and platelet-rich plasma directly to *in vitro* wounds. The presence of these components accelerated re-epithelialization and provides a more in vivo-like environment for studying the response of wounded epithelium to SM. Understanding the role of mechanistic factors involved in SM-associated delay of wound response will allow planning and implementation of treatment designed to accelerate re-epithelialization and enable more rapid reestablishment of tissue integrity.

1 - Healing response of wounded organotypic cultures is accelerated in the presence of in-vivo factors found in clots generated with platelet-rich and platelet-poor plasma - In order to determine the response of wounded organotypic cultures in the presence of plasma-derived factors, the *in vitro* wound model previously developed in the laboratory was modified to include a clot composed of platelet-rich (PRP) or platelet-poor plasma (PPP). This was accomplished by using plasma from freshly sampled blood from volunteers that was centrifuged (Harvest Inc.) to isolate the platelet-rich and platelet-poor plasma fractions. These fractions were mixed with calcium and thrombin and immediately placed into wounds

generated in organotypic cultures. These components immediately gelled in the wound bed to generate an incisional wound that could undergo healing in the presence a clot containing factors usually present in acute wounds (platelet-derived factors, fibronectin and fibrin). Wounds were generated by incision of an organotypic culture and were transferred to a second collagen gel. Wounds were allowed to re-epithelialize for 48 and 96 hours and wound response was compared to wounded controls which did not have serum factors added to the wound bed. Wounds were bisected and one-half was processed for Hematoxylin and Eosin staining and morphologic study and one-half was preserved for immunohistochemical staining.

Analysis of wounded samples revealed that the presence of both PPP and PRP greatly accelerated re-epithelialization compared to control wounds grown without either of these plasma products. At 48 hours after wounding, wounds generated in the presence of PRP demonstrated an epithelial monolayer that had just completed covering the wound surface (Figure 29). This was seen as a thin cell monolayer that covered a fibrinous, cellular material (PRP) found just beneath it (Figure 29, 40X). A similar degree of re-epitheilalization was seen on PPP (Figure 30), which showed a cell monolayer covering an acellular, homogeneous material (PPP). In contrast, wounds without PRP or PPP treatment showed no epithelial tongue 48 hours after wounding (Figure 31). By 96 hours, wounds covered with either PRP (Figure 32) or PPP (Figure 33) demonstrated complete coverage of the fibrinous material with a multilayer tissue. This was evidence that the stratification phase of healing had ensued. In contrast, re-epithelialization in the absence of PRP or PPP showed only minimal coverage of the wound, as seen by the migrating tongue of epithelium that was seen near the center of the wound (Figure 34). Immunohistochemical staining for laminin 5 with a GB-3 antibody showed pericellular staining in cells at the wound edge that had yet to begin migration when no PRP or PPP was present 48 hours after wounding. In contrast, wounds stained 48 hours after incision demonstrated deposition of laminin 5 at the basal surface of their migrating tongue of cells with either PRP (Figure 35) or with PPP (Figure 36). A similar pattern of deposition was seen in the migrating epithelial tongue 96 hours after wounding in the absence of PRP or PPP (Figure 37) In contrast, laminin 5 was deposited along the newly forming basement membrane zone in both PPP-treated (Figure 38) and PRP-treated wounds (Figure 39). These results demonstrated that a more *in-vivo* like wound environment, that had incorporated serum components normally present in a wound, was able to greatly accelerate wound re-epithelialization. This modification and refinement of our existing wound-healing assay, is now able to more closely simulate the events that occur during wound response after SM-exposure. Since the components present in PRP or PPP, such as fibrin, fibronectin and serum and platelet-derived growth factors, would be expected to play a role in normal re-epithelialization and would be damaged by SM, their presence in simulating re-epitheliazation in response to SM is critical. We are now well-poised to begin to determine the response of this *in vitro* wounding model to SM.

PROBLEMS : No problems were encountered while accomplishing this work.

NEXT : We are now well-prepared to perform experiments designed to study the effects of SM on the re-epithelialization of organotypic wounds generated in an *in vivo*-like environment. By demonstrating the acceleration of wound response on a substrate that mimics the environment that would be present in an acute wound following SM exposure, we will be able to directly determine the effects of SM directly on this substrate and on the delay of wound response. We will first perform these studies with normal keratinocytes and then on tissues constructed with JEBV keratinocytes (Tasks 6 and 7). Once we determine the phenotype of SM-exposed cells in this environment, it will be possible to directly determine response of these tissues when grafted, wounded and exposed to SM (Task 6 and 7).

KEY RESEARCH ACCOMPLISHMENTS:

TASK ONE

1 - We established dose/time responses of human, skin-like tissues composed of normal keratinocytes and grafted to nude mice following exposure to SM vapor. Strikingly, these human tissue models mimic previous studies performed in animals to a high degree. Studies based on these findings will shortly be submitted for publication.
2 – We have determined the consequences of SM doses on the early, initial changes that lead to selective apoptosis of basal cells and precede dermal-epidermal separation.
3 - We have identified characteristic alterations in basement membrane components associated with lesion formation when grafts of normal skin keratinocytes were exposed to SM.
4 – We have found that at relatively short intervals after SM exposure (6h), a prevesication phase was seen that demonstrated early, initiating damage that was limited to selective apoptosis of the basal cell layer that was independent of SM dose.
5 – We determined that at longer intervals after SM-exposure (24h), a dose-dependent vesication phase was seen whose response to SM was characterized by significantly greater tissue damage that included microvesicle formation, cellular necrosis and a sharp increase numbers of apoptotic cells throughout the tissue
6 – We have found that SM-induced apoptosis was restricted to distinct, subpopulations of basal cells, thus demonstrating a mechanism of selective basal cell death in response to SM.
7 - We found that short intervals after SM exposure (6h) demonstrated a similar fraction of apoptotic cells in the tissue that was similar for all doses applied. This suggested that a threshold number of cells was targeted as the "initiating" lesion seen in response to SM.

TASK EIGHT

8 - We developed novel human, three dimensional tissue models that allow direct study of the effects of SM on skin-like tissues grown on purified extracellular matrix and basement membrane components. As a baseline for these studies, we have found epidermal morphogenesis and tissue architecture were dependent on the type of BM or ECM protein present. These studies have been summarized and will shortly be submitted for publication.
9 - We have determined that the nature of proteins present at the dermal-epidermal interface of three-dimensional human tissues determine the level of apoptosis or cell survival in that tissue. This parameter of cell death has established its utility in studies that will shortly begin to determine the role of these proteins in the susceptibility of skin-like tissues to SM exposure.
10 - We have found that AKT survival signaling pathways are selectively activated by basement membrane components such as Type IV collagen and are not stimulated by proteins that are not found in basement membrane. We expect to use AKT activity in these tissue models as a marker of keratinocyte survival in response to SM.
11 - We have found that the synthesis, deposition and processing of basement membrane components such as laminin 5 is dependent on the nature of the connective tissue substrate on which three dimensional cultures are grown. We expect to use this finding as a valuable marker as we assess tissue response to SM.

TASK SIX

12 - We have developed an advanced wound healing model to study the effects of SM on reepithelialization of skin-like tissues in the presence of factors normally found in an acute wound environment (platelet-derived factors, fibronectin and fibrinogen). This will permit study of the effect of SM on these components during wound healing in organotypic culture for the first time.
12 - We have found that the healing response in an environment which mimics acute wound response, through the presence of platelet-derived factors, fibronectin and fibrinogen, greatly enhances re-epithelialization of wounded tissues in organotypic cultures. This will allow direct determination of the mechanisms through which SM may impede this event.

REPORTABLE OUTCOMES

MANUSCRIPTS

1) Frank Andriani, Alexander Margulis, Ning Lin, Sy Griffey, and Jonathan A. Garlick. Analysis of microenvironmental factors contributing to basement membrane assembly and normalized epidermal phenotype (In press, *Journal of Investigative Dermatology*)

2) Shari Greenberg, Ning Lin, John Petrali, Tracey Hamilton and Jonathan A. Garlick. Pathogenesis of skin lesions caused by sulfur mustard in three-dimensional human tissues grafted to nude mice (in preparation)

3) Frank Andriani, Nadav Segal, Ning Lin, Larry Pfeiffer and Jonathan A. Garlick. Basement membrance components are required for epidermal organization and survival of human keratinocytes in organotypic culture (in preparation)

ABSTRACTS: Tissue Engineering Meeting, Cold Spring Harbor, 2002

1) Frank Andriani, Alexander Margulis, Ning Lin, Sy Griffey, and Jonathan A. Garlick. Microenvironmental factors contribute to basement membrane assembly and normalize epidermal phenotype in an improved human skin equivalent model

2) Frank Andriani, Nadav Segal, Ning Lin, Larry Pfeiffer and Jonathan A. Garlick. Basement membrance components are required for epidermal organization and survival of human keratinocytes in organotypic culture

CONCLUSIONS:

The long-term goals of our research is to further understand the initiating site of SM action leading to blister formation and delayed wound healing and to elucidate mechanisms that direct these events. In the second year of our research, we have accomplished several of the tasks described in the Statement of Work that have significantly advanced our ability to accomplish these goals. During the course of the past year, our laboratory has extensively studied skin pathophysiology in response to SM by adapting *in*

vivo, human skin/nude mouse chimera, which display many features of human skin, to further our understanding of mechanisms of SM-induced vesication of human skin. In doing so, we have established dose/time responses of these human, skin-like tissues following exposure to SM vapor and have characterized prevesicating and post-vesicating doses leading to early cell injury that initiate events leading to subsequent dermal-epidermal separation. We have accomplished this by establishing the baseline response of grafted normal skin keratinocytes, which form normalized human skin, to SM by identifying apoptotic and basement membrane changes that are associated with the earliest events in lesion formation. Our studies have provided important proof of concept that these novel *in vivo,* skin-like tissues can serve as an excellent model to study the pathogenesis of SM injury on human skin. In addition, these studies show that the responses of these human, skin-like tissues mimic tissue alterations previously found in animal models of SM injury of skin.

Importantly, we have developed and tested new tissue models designed to study how basement membrane proteins alter SM-induced selectivity of basal cell injury and how wound response is impaired after SM exposure. These studies delineated key factors and pathways that direct the survival and growth of human, skin-like tissues. Identification of these pathways will now serve as an important baseline for subsequent studies that will determine the effect of SM on these parameters. We have established that basement membrane proteins, but not proteins not normally found in basement membrane, can specifically direct survival and growth of human, three-dimensional, skin-like tissues. In addition, we have learned that cellular and molecular processes, such as the processing of laminin 5 and activation of AKT signaling, mediate these events. Importantly, we expect that such evidence of survival-signaling mediated by basement membrane will help elucidate how the selective basal cell damage occurs upon initiation of an SM-induced lesion. In addition, we have refined our organotypic model of wound healing to include components found immediately after SM injury (fibrin, fibronectin and platelet-derived factors so that effects of SM on re-epithelialization can now be studied in a more *in vivo*-like environment. We are well-poised to immediately study these events by conducting *in vitro* experiments in our SM-approved research facility.

APPENDIX

1. ARTICLES AND ABSTRACTS

2. FIGURES

Analysis of Microenvironmental Factors Contributing to Basement Membrane Assembly and Normalized Epidermal Phenotype

Frank Andriani,* Alexander Margulis,* Ning Lin,* Sy Griffey,‡ and Jonathan A. Garlick*†

*Department of Oral Biology & Pathology, School of Dental Medicine, SUNY at Stony Brook, Stony Brook, New York, USA;
†Department of Dermatology, School of Medicine, SUNY at Stony Brook, Stony Brook, New York, USA;
‡LifeCell Corporation, One Millenium Way, Branchburg, New Jersey, USA

To understand further the role of the dynamic interplay between keratinocytes and stromal components in the regulation of the growth, differentiation, morphogenesis, and basement membrane assembly of human stratified squamous epithelium, we have generated novel, three-dimensional organotypic cultures in which skin keratinocytes were grown in the absence or presence of pre-existing basement membrane components and/or dermal fibroblasts. We found that keratinocytes cultured in the presence of pre-existing basement membrane components and dermal fibroblasts for 9 d showed rapid assembly of basement membrane, as seen by a nearly complete lamina densa, hemidesmosomes, and the polarized, linear distribution of laminin 5 and a6 integrin subunit. Basement membrane assembly was somewhat delayed in the absence of dermal fibroblasts, but did occur at discrete nucleation sites when pre-existing basement membrane components were present. No basement membrane developed in the absence of pre-existing basement membrane components, even in the presence of dermal fibroblasts. Bromodeoxyuridine incorporation studies showed that early keratinocyte growth was independent of mesenchymal support, but by 14 d, both fibroblasts and assembled basement membrane were required to sustain growth. Normalization of keratinocyte differentiation was independent of both dermal fibroblasts and structured basement membrane. These results indicated that epithelial and mesenchymal components play a co-ordinated role in the generation of structured basement membrane and in the regulation of normalized epithelial growth and tissue architecture in an *in vitro* model of human skin. ***Key words: basement membrane/epithelial–mesenchymal interactions/fibroblasts/laminin 5/organotypic culture. J Invest Dermatol 120:00–00, 2003***

Microenvironmental factors, such as the dynamic cross-talk between epithelium and connective tissue, are known to regulate epidermal morphogenesis and homeostasis. Diffusible factors produced by keratinocytes and mesenchymal cells are known to support epidermal growth and differentiation through the reciprocal modulation of paracrine-acting growth-regulatory factors (Smola *et al*, 1993; Szabowski *et al*, 2000). Epithelial–mesenchymal interactions have also been shown to mediate the synthesis of basement membrane constituents and to contribute to basement membrane formation (Fleischmajer *et al*, 1998; Smola *et al*, 1998b). Interactions between keratinocytes and extracellular matrix proteins at the basement membrane zone maintain tissue integrity and modulate keratinocyte adhesion, proliferation, migration, and gene expression (Fusenig, 1994; Jones *et al*, 1995).

Manuscript received May 6, 2002; revised August 22, 2002; accepted for publication August 26, 2002

Reprint requests to: Dr Jonathan A. Garlick, Department of Oral Biology and Pathology, School of Dental Medicine, SUNY at Stony Brook, Stony Brook, New York 11794-8702, USA. Email: jgarlick@notes.cc.sunysb.edu

Abbreviations: BrdU, bromodeoxyuridine; LI, labeling index

Epithelial basement membranes are composed of an intricate network of extracellular matrix proteins that interact at the epithelial–stromal interface (Christiano and Uitto, 1996). Interactions between the major constituents of basement membrane, including types IV and VII collagens, several members of the laminin family (laminins 1, 5, 6, and 7) and nidogen, mediate basement membrane stability and adhesion through complex molecular interactions. For example, laminin 5 within anchoring filaments links a6ß4 integrin to type VII collagen to promote epithelial attachment mediated by hemidesmosomes (Rousselle *et al*, 1997), whereas laminin 5 complexed to laminins 6 and 7 interacts with a3ß1 to contribute to basement membrane assembly and stabilization (Champliaud *et al*, 1996; Dipersio *et al*, 1997). Interactions between type IV collagen and ß1 integrins (Fleischmajer *et al*, 1997), as well as those between these integrins and laminins (Fleischmajer *et al*, 1998), have been shown to provide an early scaffold for basement membrane organization. Deposition and assembly of basement membrane is thought to occur concurrently with the normalization of epithelial growth, morphogenesis, and differentiation (Bohnert *et al*, 1986; Marinkovich *et al*, 1993); however, mechanisms of basement membrane assembly that are mediated by epithelial and mesenchymal factors and the concomitant regulation of epidermal phenotype remain unclear.

The integrated events that occur during basement assembly need to be studied in biologic systems in which a high degree of

Journal: JID | ☑ Disk used | ED: Ramesh H | Pgn by:terry | Scan: Pai
Article: BWUS_JID_12235 | Pages: 9 | Despatch Date: 19/4/2003 | Color: Fig 4, 6
BWUS_JID_12235.PDF 19-Apr-03 17:4 2136488 Bytes 9 PAGES

tissue complexity can be achieved. For example, whereas the synthesis of basement membrane components by keratinocytes and fibroblasts has most commonly been studied in monolayer cultures (Stanley *et al*, 1982; Bohnert *et al*, 1986; Woodley *et al*, 1988; Olsen *et al*, 1989), keratinocytes do not express their differentiated phenotype and signals from a structured extracellular matrix are not present in these cultures. To overcome this limitation, three-dimensional organotypic cultures, which mimic many of the *in vivo* features of human skin, have been used to investigate the role of epithelial–mesenchymal cross-talk in epidermal biology (Marinkovich *et al*, 1993; Zieske *et al*, 1994; Fleischmajer *et al*, 1998; Smola *et al*, 1998b; Hildebrand *et al*, 2002); however, the dynamics of basement membrane assembly have not been fully explored due to the failure of organotypic cultures to demonstrate morphologically identifiable basement membrane (Prunieras *et al*, 1983; Bohnert *et al*, 1986; Grinnell *et al*, 1986; O'Keefe *et al*, 1987; Contard *et al*, 1993; Ohji *et al*, 1994). As intact basement membrane is known to be a critical signal for the normal control of epidermal growth and differentiation (Stoker *et al*, 1990; Fleischmajer *et al*, 1993; Marinkovich *et al*, 1993), it is important to generate organotypic tissues that can develop normalized basement membrane structure.

In this study, we have optimized the growth and differentiation of skin-like, organotypic cultures by combining the two components thought to be critical in the normalization of epidermal homeostasis: dermal fibroblasts and basement membrane. These organotypic cultures allow us to ask how basement membrane components and/or dermal fibroblasts direct the assembly and organization of structured basement membrane and the concomitant normalization of epidermal phenotype. This was accomplished by growing keratinocytes on an acellular, human dermal substrate (AlloDerm) that was repopulated with human fibroblasts. We have found that organotypic cultures grown with dermal fibroblasts on pre-existing basement membrane components demonstrated a high degree of tissue normalization and formed a structured, mature basement membrane. In contrast, keratinocytes grown in the absence of pre-existing basement membrane components were well-stratified, but did not form structured basement membrane and showed aberrant tissue organization. In the absence of dermal fibroblasts, basement membrane assembly occurred at discrete initiation sites, as long as pre-existing basement membrane components were present. Maturation of well-structured basement membrane was found to be associated with the linear deposition of the receptor-ligand pair in hemidesmosomes, laminin 5 and α6 integrin. Furthermore, sustained keratinocyte growth required both intact basement membrane and dermal fibroblasts, whereas normalized tissue differentiation was independent of these components. This novel human tissue model recapitulates the morphology of the *in vivo* tissue to a large degree and has facilitated further clarification of the contributions made by basement membrane components and dermal fibroblasts to normal epidermal morphogenesis.

MATERIALS AND METHODS

Monolayer cell culture Normal human epidermal keratinocytes were cultured from newborn foreskin by the method of Rheinwald and Green (1975) in keratinocyte medium described by Wu *et al* (1982). Cultures were established through trypsinization of foreskin fragments and grown on irradiated 3T3 fibroblasts. 3T3 cells were maintained in Dulbecco's modified Eagle's medium containing 10% bovine calf serum. Human dermal fibroblasts were derived from foreskins and grown in media containing Dulbecco's modified Eagle's medium and 10% fetal calf serum.

Organotypic culture Organotypic cultures grown in the absence of pre-existing basement membrane components ("collagen raft" cultures) were prepared as previously described (Vaccariello *et al*, 1999). Briefly, early passage human dermal fibroblasts were added to neutralized type I collagen (Organogenesis, Canton, Massachusetts) to a final concentration of 2.5×10^4 cells per mL. Three milliliters of this mixture was added to each 35 mm well insert of a six-well plate and incubated for 4–6 d in media containing Dulbecco's modified Eagle's medium and 10% fetal calf serum, until the collagen matrix showed no further shrinkage. At this time, a total of 5×10^5 normal human epidermal keratinocytes were seeded directly on the contracted collagen gel. Organotypic cultures were grown in the presence of pre-existing basement membrane components ("AlloDerm cultures") by seeding keratinocytes on AlloDerm, a de-epidermalized, acellular cadaver dermis derived from human skin, which was treated to remove the surface epithelium and stromal cells while still retaining basement membrane components on its surface (LifeCell Corp., Branchburg, New Jersey). This de-epidermalized dermis was layered on the contracted collagen gel described above with the basement membrane facing up, and fibroblasts migrated from the gel below into the AlloDerm. Cultures were prepared in the absence of fibroblasts by incubating contracted collagen gels with distilled water for 3 h. Cultures were maintained submerged in low calcium epidermal growth media for 2 d, submerged for 2 d in normal calcium epidermal growth media and raised to the air–liquid interface by feeding from below with normal calcium cornification medium for an additional 3–10 d (Vaccariello *et al*, 1999). Cultures were maintained for 2, 9, and 14 d and were performed in triplicate. For proliferation assays, bromodeoxyuridine (BrdU) (Sigma, St Louis, MO) was added to organotypic cultures 8 h prior to harvesting at a final concentration of 10 μM.

Immunofluorescence Specimens were frozen in embedding media (Triangle Biomedical, Durham, North Carolina) in liquid nitrogen vapors after being placed in 2 M sucrose for 2 h at 4°C. Tissues were serial sectioned at 6 μm and mounted on to gelatin-chrome alum-coated slides. Tissue sections were washed with phosphate-buffered saline and blocked with 10 μg goat IgG per mL, 0.05% goat serum, and 0.2% bovine serum albumin, vol/vol in phosphate-buffered saline without fixation. Sections were incubated with monoclonal antibodies to laminin 5 (GB-3, Gift of Dr G. Meneguzzi), α6 integrin subunit (G0H3, Chemicon International Inc., Temecula, California), bromodeoxyuridine (Boehringer Mannheim, Indianapolis, Indiana) and filaggrin (Biomedical Technologies Inc., Stoughton, Massachusetts) and detected with Alexa 594™-conjugated goat anti-rat or anti-mouse IgG (Molecular Probes, Eugene, Oregon). Slides were coverslipped with Vectashield containing 1 μg per mL DAPI (Vector Laboratories, Burlingame, California). Fluorescence was visualized using a Nikon Eclipse 600 microscope and photomicroscopy was performed using a Texas Red filter. For routine light microscopy, tissues were fixed in 10% neutral buffered formalin, embedded in paraffin, and 4 μm sections were stained with hematoxylin and eosin.

Transmission electron microscopy Organotypic cultures were cut into small pieces of approximately 2 × 2 mm and fixed in 2% glutaraldehyde in 0.1 M cacodylate and 0.1 M sucrose at pH 7.2. The samples were then postfixed in 2% osmium tetroxide in 0.1 M cacodylate and 1% tannic acid in 0.1 M cacodylate. Following fixation the samples were dehydrated in graded ethanol, cleared with propylene oxide and infiltrated with Spurr's resin. Following polymerization of the resin, thick sections were produced using a Reichert Ultracut E microtome and sections were stained with toluidine blue to determine orientation. The blocks were then thin sectioned at approximately 90 nm and mounted on copper grids. Grids were stained with 5% uranyl acetate in deionized water and Reynold's lead citrate. Stained grids were examined at various magnifications using a Hitachi H-600 transmission electron microscope.

RESULTS

Basement membrane components and dermal fibroblasts optimize epidermal morphogenesis The organotypic tissue model was fabricated by growing human keratinocytes on an acellular, human dermal substrate (AlloDerm) that was repopulated with human fibroblasts that migrated into the dermis from an underlying contracted collagen gel (**Fig 1*A***). Keratinocytes grown on AlloDerm generated an epithelium with an *in vivo*-like tissue architecture after 9 d (**Fig 1*B***). In the presence of fibroblasts, these cultures demonstrated an orthokeratinized epithelium with polarized, columnar basal cells nested in rete pegs and well-formed spinous and granular layers (**Fig 1*B***, layer A). The upper part of the connective tissue showed papillary dermis composed of a fine, collagenous network (**Fig 1*B***, layer B1) and the lower reticular dermis composed of denser collagen bundles (**Fig 1*B***, layer B2). Fibroblasts seeded into the contracted type I collagen gel (**Fig 1*B***, layer C) repopulated the AlloDerm by migrating into its lower surface. AlloDerm tissues have been found to retain the pre-existing

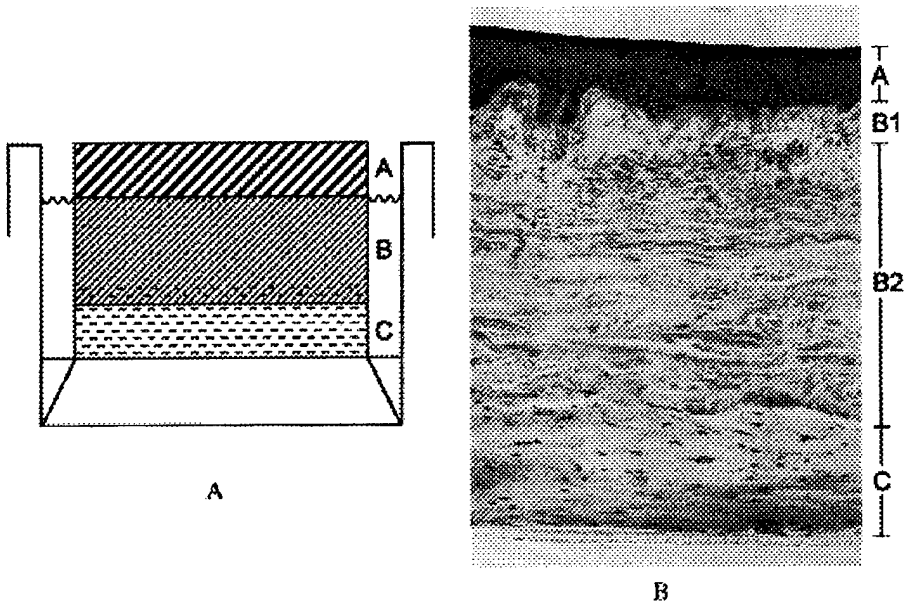

Figure 1. Schematic representation of the AlloDerm culture model and tissue morphology of AlloDerm cultures. As seen in (*A*), a type I collagen gel that contained dermal fibroblasts (*C*) was fabricated and allowed to contract for 7 d. AlloDerm, a de-epidermalized, acellular human dermis (*B*), was then laid on this gel to allow fibroblasts to migrate into the dermis. Twenty-four hours later, keratinocytes (*A*) were seeded on the pre-existing basement membrane components present on the surface of the AlloDerm. Cultures were submerged in media for 4 d and then grown at an air–liquid interface for either 3 or 10 additional days. "Collagen raft" cultures were grown directly on the collagen gel (*C*), without the intervening AlloDerm substrate. In (*B*), the morphologic components of the AlloDerm culture model are seen after 9 d in culture. An orthokeratinized stratified squamous epithelium is seen that shows polarized basal cells and rete pegs (*A*). Basal keratinocytes are resting on a papillary dermis composed of fine, collagen fibrils (*B1*) that is overlying a reticular dermis containing dense collagen bundles (*B2*). Beneath the dermis is the contracted, type I collagen gel, which was seeded with fibroblasts (*C*). Fibroblasts that have migrated from the gel into the dermis. The polycarbonate membrane that supports these cultures is seen under the collagen gel.

basement membrane components types IV and VII collagen and laminin 1 on their upper surface (data not shown). In the absence of fibroblasts, keratinocytes cultured for 9 d in AlloDerm cultures, showed a thin epithelium that demonstrated all morphologic strata (**Fig 2*A***). In comparison, the incorporation of fibroblasts (**Fig 2*B***, *arrows*) into these cultures resulted in a fully stratified epithelium, which showed normal morphologic differentiation and tissue architecture (**Fig. 2*B***). A considerably thinner epithelium demonstrating less prominent morphologic strata was seen when cultures were grown without fibroblasts and without pre-existing basement membrane components (collagen raft cultures) for 9 d (**Fig 2*C***). These cultures demonstrated altered tissue architecture that was characterized by flattened basal cells and a lack of clear transition between morphologic strata. In contrast, cultures grown without basement membrane components but with fibroblasts for 9 d showed a well-stratified epithelium (**Fig 2*D***). The lower layers of this epithelium showed altered tissue organization, however, suggesting that pre-existing basement membrane components present in the AlloDerm were needed to polarize basal keratinocytes and achieve optimal tissue architecture.

When grown on AlloDerm with fibroblasts for 14 d, the epithelium continued to mature and showed a well-polarized basal layer and surface hyperorthokeratosis (**Fig 2*F***). In contrast, the epithelium remained thin when AlloDerm cultures were grown without fibroblasts for 14 d (**Fig 2*E***), suggesting that little growth had occurred beyond day 9 in cultures grown without fibroblasts. Alterations in morphology were evident in 14 d cultures grown without fibroblasts or basement membrane components (**Fig 2*G***). In these cultures, basal cells were widely spaced and flattened, the surface layer was parakeratotic and no clear transition between morphologic strata could be identified. Tissue stratification improved when these cultures were grown in the presence of fibroblasts for 14 d but the tissue remained highly disorganized (**Fig 2*H***). A summary of the morphologic findings for all cultures is seen in **Table I**. These findings demonstrated that the presence of both pre-existing basement membrane components and dermal fibroblasts were required to generate an epithelium with optimal morphology and tissue organization. Dermal fibroblasts were needed to support full stratification, whereas basement membrane components were required to improve tissue architecture.

Pre-existing basement membrane components direct the assembly of structured basement membrane The ultrastructural appearance of the basement membrane zone in organotypic cultures grown with and without fibroblasts and/or pre-existing basement membrane components was studied by transmission electron microscopy (**Fig 3**). No lamina densa or basement membrane structure was seen when collagen rafts were grown with fibroblasts for 9 d (**Fig 3*A***). The dermal–epidermal interface of these cultures showed electron-dense condensations that did not display structural features of hemidesmosomes (**Fig 3*A***, *arrows*). In contrast, cultures grown for 9 d on AlloDerm with fibroblasts demonstrated extended stretches of lamina densa (**Fig 3*B***). Isolated areas showed hemidesmosomes, consisting of inner and outer plaques associated with keratin filaments intracellularly (**Fig 3*B***, *inset, white arrow*) and fine bridging structures representing anchoring filaments on their extracellular surface (**Fig 3*B***, *inset, black arrows*). When grown in the absence of fibroblasts for 9 d, however, AlloDerm cultures did not show a continuous lamina densa, but rather demonstrated evenly spaced hemidesmosomes (**Fig 3*C***). Under higher magnification, these regions showed focal areas of lamina densa and hemidesmosomes (**Fig 3*C***, inset), which were adjacent to keratin filament bundles intracellularly (**Fig 3*C***, *inset, white arrows*) and filamentous structures that spanned to the lamina densa (**Fig 3*C***, *inset, black arrow*). Further maturation of basement membrane structure was seen by the presence of a more continuous lamina densa in AlloDerm cultures grown for 14 d without fibroblasts (**Fig 3*D***). Hemidesmosomes were seen at

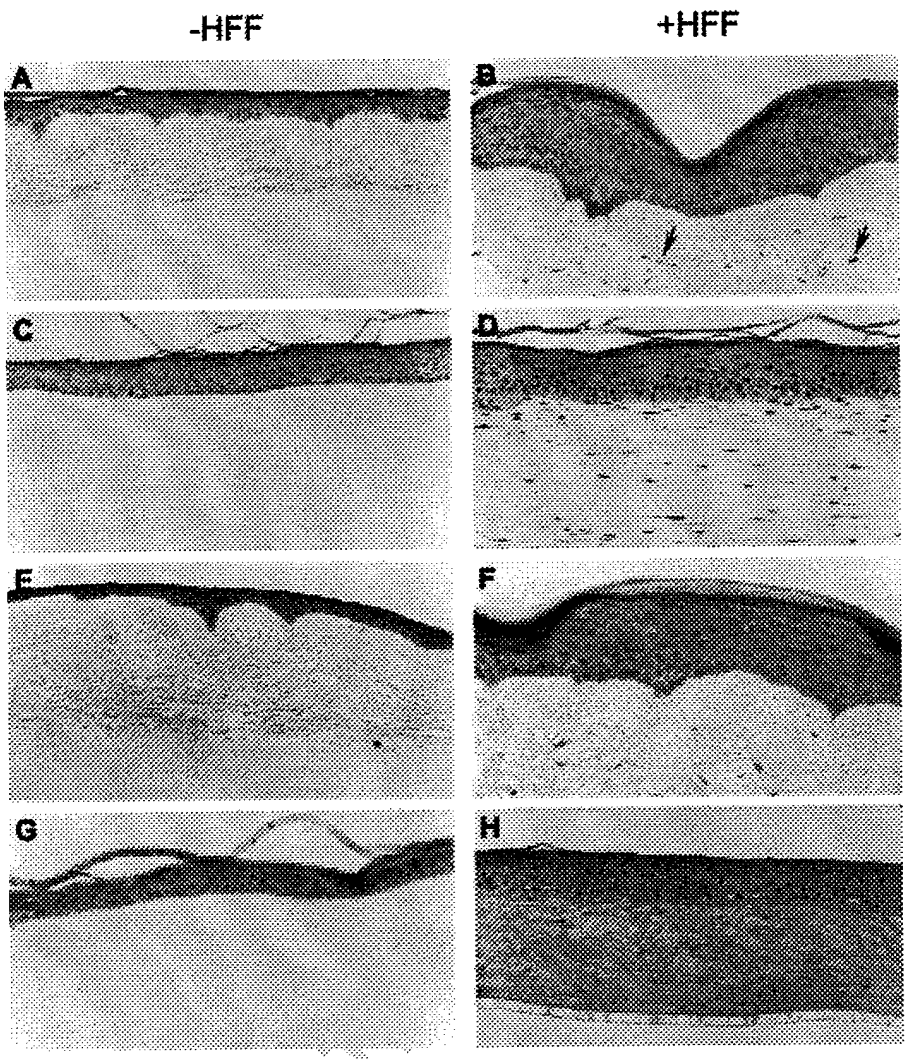

Figure 2. Morphogenesis of stratified squamous epithelium in the presence or absence of pre-existing basement membrane components and dermal fibroblasts. Keratinocytes were grown in organotypic culture for either 9 d (*A–D*) or 14 d (*E–H*) in the absence (*C,D,G,H*) or presence (*A,B,E,F*) of pre-existing basement membrane components. In the presence of basement membrane components and fibroblasts, a fully stratified epithelium was seen that demonstrated normal morphologic differentiation and tissue architecture (*B,F*), whereas cultures were considerably thinner without fibroblasts (*A,E*). In the absence of pre-existing basement membrane components, cultures underwent greater stratification with fibroblasts (*D*) than without fibroblasts (*C*), but both conditions showed altered tissue architecture characterized by disorganization of basal cells. These architectural alterations were more evident in 14 d cultures (*G,H*).

Table I. Summary of morphology, basement membrane components, and assembly, growth, and differentiation of organotypic epithelia Q20

regularly spaced intervals (**Fig 3*D***, *dark arrows*) and anchoring fibrils were seen adjacent to the lamina densa (**Fig 3*D***, *white arrow*). This demonstrated that, whereas fibroblasts could accelerate basement membrane maturation, they were not required for the development of structured basement membrane as long as pre-existing basement membrane components were present. Cultures grown in the presence of fibroblasts for 14 d showed a lamina densa that was more electron dense and continuous than that seen in 9 d AlloDerm cultures with fibroblasts (**Fig 3*E***). Interestingly, the electron-dense material of the lamina densa in these 9 and 14 d AlloDerm cultures was similar to that seen on the surface of AlloDerm that was analyzed after it was prepared and not placed in culture (**Fig 3*F***). This suggested that basement membrane organization took place on this surface, which served as a structural template for the assembly of basement membrane. It was concluded that pre-existing basement membrane components, but not dermal fibroblasts, were required for the assembly of structured basement membrane and hemidesmosomes. As seen in collagen raft cultures, however, the presence of fibroblasts alone was not permissive for the generation of a structured basement membrane.

Normalized deposition of hemidesmosomal components is dependent upon pre-existing basement membrane components and is accelerated by dermal fibroblasts The

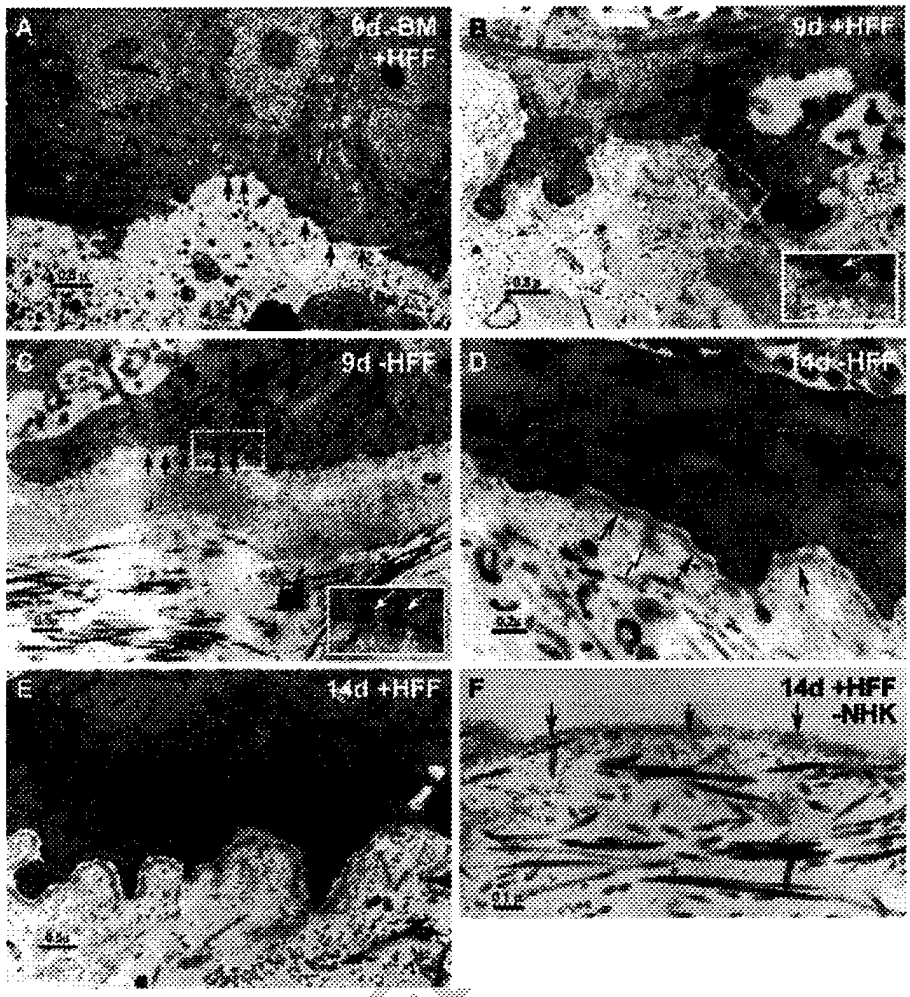

Figure 3. Ultrastructural assembly of the basement membrane zone in organotypic cultures. Cultures grown either in the absence (*A*) or presence of pre-existing basement membrane components (*B–E*) were studied after 9 d (*A–C*) and 14 d (*D,E*). Cultures were grown either with both keratinocytes and fibroblasts (*A,B,E*) or with keratinocytes and no fibroblasts (*C,D*). AlloDerm was also analyzed after it was freshly prepared without growing it in culture (*F*). Electron-dense condensations are seen in the absence of pre-existing basement membrane components (*A, arrows*) but no other basement membrane structures were seen (*A*). Lamina densa and hemidesmosomes were seen in (*B*), as evidenced by electron-dense plaques (*inset*) showing intracellular (*white arrow*) and extracellular (*black arrow*) filamentous structures. Focal areas of well-organized lamina densa and hemidesmosomes were seen in (*C*) (*black arrows*). Under higher magnification, these areas showed regularly spaced, electron-dense plaques (*inset*), which were associated with intracellular bundles of keratin filaments (*inset, white arrow*) and filamentous structures, which extended to the lamina densa (*inset, black arrow*). A more continuous basement membrane demonstrating anchoring fibrils (*white arrow*) and hemidesmosomes (*black arrow*) were seen in (*D*), whereas a continuous lamina densa was seen in (*E*). Electron-dense material was seen on the upper surface of freshly prepared AlloDerm, which was not used in cultures (*F, arrows*).

role of basement membrane components and dermal fibroblasts in the assembly of basement membrane was also characterized by determining the distribution of laminin 5 and its receptor, α6β4 integrin, by immunohistochemical stain. Basement membrane normalization was assessed by the degree to which these proteins were deposited in a polarized, linear pattern at the basement membrane zone. In the absence of dermal fibroblasts, 9 d AlloDerm cultures demonstrated a patchy, discontinuous deposition of laminin 5 at the dermal–epidermal interface (**Fig 4*A***). In contrast, cultures grown on AlloDerm in the presence of fibroblasts for 9 d demonstrated continuous and linear deposition of laminin 5 that was strictly polarized along the basement membrane zone (**Fig 4*B***). This suggested that the normalized deposition and organization of laminin 5 was accelerated when fibroblasts were incorporated into AlloDerm cultures. In contrast, a discontinuous pattern of laminin 5 deposition was seen for cultures grown on collagen rafts in the absence of pre-existing basement membrane components both without or with fibroblasts. In the absence of fibroblasts, laminin 5 was limited to the cytoplasm of basal cells and was not deposited in the basement membrane zone after 9 d (**Fig 4*C***). The addition of fibroblasts to these cultures resulted in the extracellular deposition of laminin 5, but the staining distribution remained punctate and discontinuous (**Fig 4*D***).

Even in the absence of fibroblasts, AlloDerm cultures showed a polarized and linear distribution of laminin 5 after 14 d (**Fig 4*E***). This supports the view that normalized laminin 5 deposition and basement membrane formation did not require dermal fibroblasts, as long as keratinocytes were grown on an interface containing pre-existing basement membrane proteins. In contrast, cultures grown without basement membrane components but with fibroblasts for 14 d continued to show patchy deposition of laminin 5 (**Fig 4*G,H***). When these cultures were grown without fibroblasts, only faint laminin 5 staining was seen, suggesting that this protein had been degraded in the absence of fibroblasts (**Fig 4*G***). It appears that, whereas laminin 5 was synthesized in the absence of pre-existing basement membrane components, these components were needed to direct the deposition of laminin 5 into the assembling basement membrane.

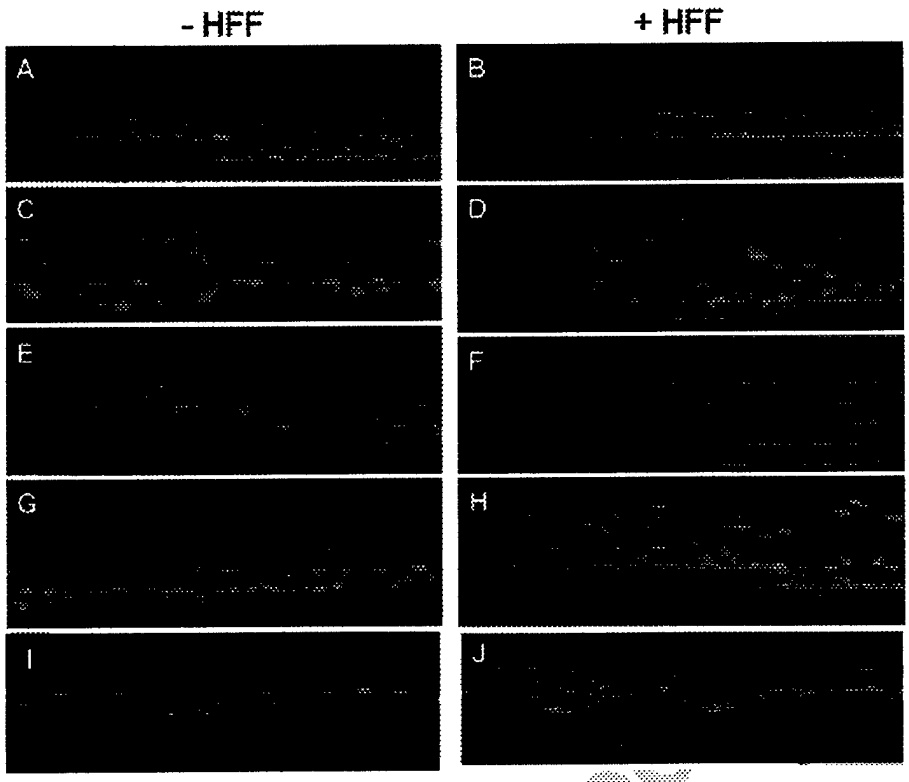

Figure 4. Pre-existing basement membrane components and fibroblasts enhance the deposition and polarization of laminin 5 and the a6 integrin subunit. Immunofluorescent stain for laminin 5 was performed on 9 and 14 d organotypic cultures in the presence of pre-existing basement membrane components with (*B,F*) and without (*A,E*) fibroblasts and in the absence of pre-existing basement membrane with (*D,H*) and without (*C,G*) fibroblasts. Staining for the a6 integrin subunit was performed on 14 d organotypic cultures in the presence of pre-existing basement membrane components with (*J*) and without (*I*) fibroblasts. Nine day cultures grown in the presence of pre-existing basement membrane without fibroblasts (*A*) demonstrated a patchy, discontinuous pattern of laminin 5 compared with cultures grown in the presence of fibroblasts (*B*), which showed continuous and linear deposition of laminin 5. Linear deposition was seen in 14 d cultures that contained pre-existing basement membrane components grown both with (*F*) or without (*E*) fibroblasts. In contrast, cultures grown in the absence of pre-existing basement membrane components with (*D,H*) and without (*C,G*) fibroblasts demonstrated laminin 5 expression that was discontinuous and pericellular at both 9 and 14 d. The linear deposition of a6 integrin subunit was seen in a pattern similar to laminin 5 when 14 d cultures were grown without (*I*) and with (*J*) fibroblasts in the presence of pre-existing basement membrane components.

The distribution of the a6 integrin subunit closely paralleled that of laminin 5 (**Table I**). Cultures grown on AlloDerm without fibroblasts for 9 d demonstrated staining that was both linear, yet pericellular in the suprabasal layers (**Table I**). Five days later (day 14), cultures grown without fibroblasts showed further basement membrane maturation as evidenced by the restriction of a6 integrin to a linear and polarized distribution at the basement membrane zone (**Fig 4*I***). This linear pattern was similar to that seen when cultures were grown in the presence of pre-existing basement membrane proteins and dermal fibroblasts, both at 9 d (**Table I**) and 14 d (**Fig 4*J***), suggesting that the presence of dermal fibroblasts accelerated the normalized distribution of this protein. In contrast, cultures grown in the absence of pre-existing basement membrane components demonstrated a pericellular distribution without fibroblasts and a patchy, extracellular deposition with fibroblasts (**Table I**). These findings demonstrated that the spatial and temporal deposition of laminin 5 and a6 integrin were similar during the maturation of the basement membrane. Thus, the normalized deposition of this integrin-ligand pair was fibroblast independent, but required the presence of pre-existing basement membrane components. The progressive maturation of basement membrane seen by the transition from the pericellular and patchy, to the linear, polarized deposition of these components in AlloDerm cultures, closely matched the temporal sequence of events through which ultrastructural assembly of basement membrane occurred.

Sustained keratinocyte growth requires fibroblasts and basement membrane, whereas normalized differentiation is fibroblast independent Growth of keratinocytes in organotypic cultures was determined by measuring the percentage of basal cells that incorporated BrdU during a 8 h pulse [labeling index (LI)]. Two day after seeding, keratinocyte cultures demonstrated elevated levels of proliferation regardless of the presence of dermal fibroblasts or basement membrane components (**Fig 5**). These cultures showed LI between 28 and 36%, suggesting that the initial growth of keratinocytes was independent of mesenchymal stimulation. Only keratinocytes cultured in the presence of AlloDerm and fibroblasts, however, were able to maintain proliferative activity after 14 d in culture. Keratinocytes grown directly on collagen rafts, with or without fibroblasts, as well as cells grown on AlloDerm without fibroblasts, showed a 1.5–2-fold decrease in LI after 9 d and nearly complete suppression of growth 14 d after seeding (**Fig 5**). In contrast, AlloDerm cultures grown for 14 d with fibroblasts showed a LI that continued to decrease to a range that was more similar to that seen *in vivo*, suggesting that full maturation of basement membrane structure was coupled to the normalization of keratinocyte growth. This demonstrated that the presence of both structured basement membrane and dermal fibroblasts were required to sustain keratinocyte growth in organotypic culture.

Normalization of keratinocyte differentiation was independent of dermal fibroblasts and basement membrane. When grown

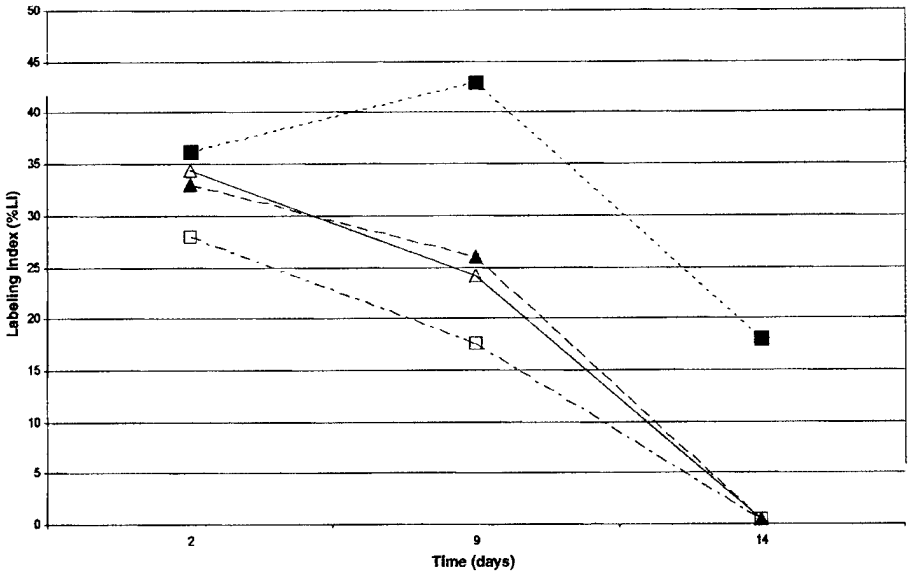

Figure 5. Keratinocyte growth is sustained by fibroblasts and basement membrane interactions. Organotypic cultures were grown for 2, 9, and 14 d and pulsed with 10 mM BrdU for their last 8 h. LI was determined by counting BrdU-positive, basal cell nuclei after immunohistochemical stain with an anti-BrdU antibody. Only cultures containing both assembled basement membrane and fibroblasts were able to sustain keratinocyte growth for 14 d (¦ ... .¦... .¦). Cultures grown with fibroblasts and without basement membrane components (?....?....?), without fibroblasts and with basement membrane components (? –? –?), and without either fibroblasts and basement membrane components (? –? –?) showed elevated growth initially, but no proliferative activity at 14 d.

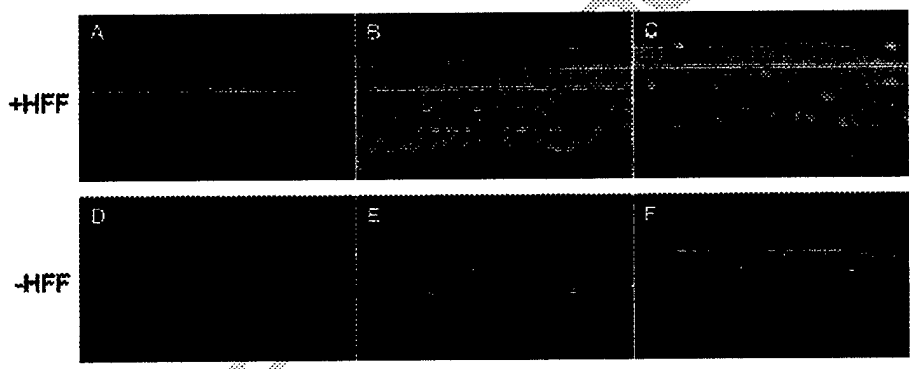

Figure 6. Differentiation of organotypic cultures is independent of pre-existing basement membrane components and dermal fibroblasts. Immunofluorescent stain for filaggrin demonstrated a normal pattern of expression limited to the stratum granulosum and stratum corneum when cultures were grown in the presence of fibroblasts both with (*A,B*) or without (*C*) pre-existing basement membrane components and when cultures were grown in the absence of fibroblasts with (*D,E*) or without (*F*) pre-existing basement membrane components.

with fibroblasts for 9 d and 14 d, filaggrin was expressed in the upper third of the epithelium in a pattern similar to that seen in human skin. This was the case for both AlloDerm cultures grown for 9 d (**Fig 6*A***) and 14 d (**Fig 6*B***) and for collagen raft cultures grown for 9 d (**Fig 6*C***). In the absence of dermal fibroblasts, AlloDerm cultures (**Fig 6*D,E***) and collagen raft cultures (**Fig 6*F***) grown for 9 and 14 d were considerably thinned, but demonstrated a normal pattern of filaggrin distribution. These findings showed that sustained keratinocyte growth was dependent on the presence of both structured basement membrane and dermal fibroblasts, whereas normalized differentiation was independent of both of these microenvironmental factors.

DISCUSSION

We have developed novel organotypic cultures of human stratified squamous epithelium to investigate how microenvironmental factors such as pre-existing basement membrane components and dermal fibroblasts direct the organization, assembly, and maturation of basement membrane and modulate epidermal phenotype. Using these engineered human tissues, we have found that these components play a co-ordinated part in the generation of a well-structured basement membrane, regulate keratinocyte growth and differentiation, and normalize epithelial tissue architecture. In the absence of pre-existing basement membrane components such as laminin 1 and type IV and VII collagen, fibroblasts were not sufficient to generate structured basement membrane or to normalize epithelial phenotype. When these proteins were present at the time keratinocytes were seeded (AlloDerm cultures), a well-structured basement membrane formed both with and without dermal fibroblasts. The incorporation of fibroblasts into the AlloDerm cultures accelerated basement membrane assembly, sustained keratinocyte growth, and normalized epidermal tissue architecture. We have achieved this by repopulating an acellular human dermis with viable fibroblasts that migrated from an underlying contracted type I collagen gel.

This novel, human tissue model recapitulates the morphology of the *in vivo* tissue to a large degree and contributes to our understanding of the role of epithelial–mesenchymal cross-talk in the normalization of basement membrane structure and the morphogenesis of human skin.

Our ultrastructural and immunohistochemical evidence clearly point to the rapid assembly of basement membrane when keratinocytes were cultured on AlloDerm that was repopulated with fibroblasts. Structured basement membrane was seen at 9 d as a nearly continuous lamina densa and was paralleled by the linear and polarized distribution of laminin 5 and the a6 integrin subunit. In the absence of fibroblasts, basement membrane assembly was initially seen as regularly spaced areas of lamina densa adjacent to hemidesmosomes, which may represent nucleation sites for basement membrane assembly. The patchy, but linear distribution of laminin 5 and α6 integrin seen by immunohistochemical stain supports the view that initial basement membrane organization can occur at discrete sites (Fleischmajer *et al*, 1998). It is thought that formation of structured basement membrane is a self-assembly process (Smola *et al*, 1998b; Colognato and Yurchenco, 2000), which occurs as the local concentration of basement membrane proteins reaches a critical threshold and enables these components to interact physically (Yurchenco and O'Rear, 1994). Marinkovich *et al* (1993) have shown that fibroblasts play a part in this process by secreting proteins that reorganize the extracellular matrix or stabilize previously assembled basement membrane. That study showed that when grown in organotypic culture with human foreskin keratinocytes, dermal fibroblasts synthesized and deposited three major components of basement membrane: laminin 1 and collagen types IV and VII (Marinkovich *et al*, 1993). It has been shown that these components need to be assembled prior to the formation of a mature basement membrane in order to bind to cell surface integrins and serve as nucleation sites for the self-assembly of basement membrane (Fleischmajer *et al*, 1998).

Our finding of discrete sites of basement membrane organization in the absence of fibroblasts strongly suggests that the pre-existing basement membrane components present on AlloDerm cultures provided a template on which basement membrane development could rapidly occur. It has recently been shown that hemidesmosomes form around pre-existing anchoring fibrils when foreskin keratinocytes were grown on a de-epidermalized bovine tongue connective tissue without fibroblasts (Hildebrand *et al*, 2002). Similarly, cell suspensions (Friend *et al*, 1982) and viable sheets of adult rabbit corneal epithelium (Gipson *et al*, 1983; Payne *et al*, 2000) have been shown to assemble hemidesmosomes rapidly when grown on corneal stroma that contains intact basal laminae. It was found that hemidesmosome assembly occurred at sites where pre-existing anchoring fibrils inserted into the lamina densa, suggesting that these were likely nucleation sites for hemidesmosome organization (Gipson *et al*, 1983). We observed that no basement membrane assembly was seen when keratinocytes were grown in organotypic culture without pre-existing basement membrane components, even when fibroblasts were incorporated. Thus, the presence of these pre-existing basement membrane proteins provides an important permissive cue for the rapid formation and maturation of ultrastructurally complete basement membrane.

We have incorporated fibroblasts into our tissue model by facilitating their migration to repopulate a previously acellular dermis. These fibroblasts moved from the underlying contracted, type I collagen gel and were retained in the reticular dermis (Lee *et al*, 2000). We have shown that epidermal morphogenesis and growth were significantly compromised by the absence of dermal fibroblasts. Similarly, previous studies have shown that keratinocyte growth and differentiation were improved when fibroblasts were incorporated into dermal equivalents (Limat *et al*, 1989; Rosdy and Clauss, 1990; Ponec and Kempenaar, 1995). In addition to the role of fibroblasts in the production of basement membrane components, it has been shown that diffusible factors produced by fibroblasts play a part in extracellular matrix metabolism and modulate keratinocyte production of basement membrane components (Smola *et al*, 1998b). This may help explain the more rapid assembly of basement membrane on AlloDerm grown in the presence of fibroblasts when compared with cultures from which fibroblasts were excluded. The cooperation between specific fibroblast-derived soluble factors and basement membrane assembly has recently been established (Li *et al*, 2001).

Organotypic tissue models have previously been adapted to study epithelial–mesenchymal interactions (Boxman *et al*, 1993; Smola *et al*, 1994; Berking and Herlyn, 2001) on a variety of connective tissue substrates that served as dermal equivalents. A well-stratified epithelium was seen when cultures were grown on dermal equivalents fabricated as type 1 collagen gels, which were populated with fibroblasts (Bell *et al*, 1981; Asselineau *et al*, 1989; Parenteau *et al*, 1991). Porous membranes seeded with fibroblasts or coated with extracellular matrix proteins have been used to generate skin-like organotypic cultures (Rosdy and Clauss, 1990). Alternatively, fibroblasts have been incorporated into a three-dimensional scaffold, where these cells could secrete and organize an extracellular matrix (Fleischmajer *et al*, 1998). Whereas organotypic cultures of stratified epithelium have been shown to express basement membrane components in organotypic culture (Prunieras *et al*, 1983; Bohnert *et al*, 1986; Grinnell *et al*, 1986; Contard *et al*, 1993; Ohji *et al*, 1994), limited success has been achieved in attaining structured basement membrane (Marinkovich *et al*, 1993; Zieske *et al*, 1994; Smola *et al*, 1998). As it is known that basement membrane components play a functional part in the regulation of epidermal growth and differentiation (Stoker *et al*, 1990), it is important to generate cultures that have a well-structured basement membrane. Furthermore, it has previously been shown that the correct spatial organization and polarity of basal cells was associated with functional hemidesmosomes and basement membrane integrity (Dowling *et al*, 1996). Our findings support these observations as only tissues with well-structured basement membrane showed optimal epithelial tissue architecture.

The goal of organotypic cultures of human skin is to fabricate and maintain a stratified epithelium that demonstrates *in vivo*-like features of epidermal morphology, growth, and differentiation (Berking and Herlyn, 2001). We have optimized these cultures by combining the two components thought to be critical in epidermal normalization: dermal fibroblasts and structured basement membrane. Dermal fibroblasts were required to stimulate stratification and accelerate basement membrane formation, whereas pre-existing basement membrane components were required to initiate and promote basement membrane assembly. Both of these microenvironmental factors were needed to sustain keratinocyte growth and optimize epithelial architecture. Our cultures demonstrated significantly improved basement membrane organization, stratification, growth, and differentiation when compared with cultures that lacked human fibroblasts, pre-existing basement membrane proteins or both of these components. This novel, composite culture system mimics the essential morphologic features of human skin to a high degree and demonstrates that this human culture model will be a valuable tool for future studies.

We would like to thank Sujata Pawagi, Michael Scalia, Heather Sawka, Nadav Segal, Lina Nguyen, and Larry Pfeiffer for technical assistance, Dr Lorne Taichman for critical comments, Jackie Garfield for performing transmission electron microscopy and to Karen Henrickson for preparation of illustrations. In addition, we thank Dr G. Meneguzzi for his generous gift of laminin 5 antibodies. This work was supported by grants no. DAMMD17-01-1-0688 from the US Army Medical Research and Materiel Command and no. 2RO1DE011250-06 from the National Institutes of Dental and Craniofacial Research.

REFERENCES

Asselineau D, Bernard BA, Bailly C, Darmon M: Retinoic acid improves epidermal morphogenesis. *Dev Biol* 133:322–335, 1989

Bell E, Ehrich P, Butte DJ, Nakatsuji T: Living tissue formed *in vitro* and accepted as skin-equivalent tissue of full thickness. *Science* 211:1052–1054, 1981

Berking C, Herlyn M: Human skin reconstruct models: a new application for studies of melanocyte and melanoma biology. *Histol Histopathol* 16:669–674, 2001

Bohnert A, Hornung J, Mackenzie IC, Fusenig NE: Epithelial–mesenchymal interactions control basement membrane production and differentiation in cultured and transplanted mouse keratinocytes. *Cell Tissue Res* 244:413–429, 1986

Boxman I, Lowik C, Aarden L, Ponec M: Modulation of IL-6 production and IL-1 activity by keratinocyte–fibroblast interaction. *J Invest Dermatol* 101:316–324, 1993

Champliaud MF, Lunstrum GP, Rousselle P, Nishiyama T, Keene DR, Burgeson RE: Human amnion contains a novel laminin variant, laminin 7, which like laminin 6, covalently associates with laminin 5 to promote stable epithelial-stromal attachment. *J Cell Biol* 132:1189–1198, 1996

Christiano AM, Uitto J: Molecular complexity of the cutaneous basement membrane zone: Revelations from the paradigms of epidermolysis bullosa. *Exp Dermatol* 5:1–11, 1996

Colognato H, Yurchenco PD: Form and function: the laminin family of heterotrimers. *Dev Dyn* 218:213–234, 2000

Contard P, Bartel RL, Jacobs L, *et al*: Culturing keratinocytes and fibroblasts in a three-dimensional mesh results in epidermal differentiation and formation of a basal lamina-anchoring zone. *J Invest Dermatol* 100:35–39, 1993

Dipersio CM, Hodivala-Dilke KM, Jaenisch ED, Perlish R, Kreidberg JA, Hynes RO: α3β1 integrin is required for normal development of the epidermal basement membrane. *J Cell Biol* 137:729–742, 1997

Dowling J, Yu Q-C, Fuchs E: β4 integrin is required for hemidesmosome formation, cell adhesion and cell survival. *J Cell Biol* 134:559–572, 1996

Fleischmajer R, Kuhn K, Sato Y, *et al*: There is temporal and spatial expression of alpha1 (IV), alpha2 (IV), alpha5 (IV), alpha6 (IV) collagen chains and beta1 integrins during the development of the basal lamina in an "*in vitro*" skin model. *J Invest Dermatol* 109:527–533, 1997

Fleischmajer R, MacDonald ED, Contard P, Perlish JS: Immunochemistry of a keratinocyte-fibroblast co-culture model for reconstruction of human skin. *J Histochem Cytochem* 41:1359–1366, 1993

Fleischmajer R, Utani A, MacDonald ED, *et al*: Initiation of skin basement membrane formation at the epidermo-dermal interface involves assembly of laminins through binding to cell membrane receptors. *J Cell Sci* 111 (14):1929–1940, 1998

Friend J, Kinoshita S, Thoft RA, Eliason JA: Corneal epithelial cell cultures on stromal carriers. *Invest Ophthalmol Vis Sci* 23:41–49, 1982

Fusenig NE: Epithelial–mesenchymal interactions regulate keratinocyte growth and differentiation *in vitro*. In: Leigh I, Lane B, Watt F (eds). *The Keratinocyte Handbook*. 1994, pp 71–97

Gipson IK, Grill SM, Spurr SJ, Brennan SJ: Hemidesmosome formation *in vitro*. *J Cell Biol* 97:849–857, 1983

Grinnell F, Takashima A, Lamke-Seymour C: Morphological appearance of epidermal cells cultured on fibroblast-reorganized collagen gels. *Cell Tissue Res* 246:13–21, 1986

Hildebrand HC, Hakkinen L, Wiebe CB, Larjava HS: Characterization of organotypic keratinocyte cultures on de-epithelialized bovine tongue mucosa. *Histol Histopathol* 17:151–153, 2002

Jones PH, Harper S, Watt FM: Stem cell patterning and fate in human epidermis. *Cell* 80:83–93, 1995

Lee DY, Ahn HT, Cho KHA: new skin equivalent model: dermal substrate that combines de-epidermized dermis with fibroblast-populated collagen matrix. *J Dermatol Sci* 23:132–137, 2000

Li X, Chen Y, Scheele S, Arman E, Haffner-Krausz R, Ekblom P, Lonai P: Fibroblast growth factor signaling and basement membrane assembly are connected during epithelial morphogenesis of the embryoid body. *J Cell Biol* 153:811–822, 2001

Limat A, Hunziker T, Boillat C, Bayreuther K, Noser F: Post-mitotic human dermal fibroblasts efficiently support the growth of human follicular keratinocytes. *J Invest Dermatol* 92:758–762, 1989

Marinkovich MP, Keene DR, Clytie SR, Burgeson RE: Cellular origin of the dermal-epidermal basement membrane. *Dev Dyn* 197:255–267, 1993

O'Keefe EJ, Woodley DT, Falk RJ, Gammon WR, Briggaman RA: Production of fibronectin by epithelium in a skin equivalent. *J Invest Dermatol* 88:634–639, 1987

Ohji M, SundarRaj N, Hassell JR, Thoft RA: Basement membrane synthesis by human corneal epithelial cells *in vitro*. *Invest Ophthalmol Vis Sci* 35:479–485, 1994

Olsen D, Nagayoshi T, Fazio M, *et al*: Human laminin: cloning and sequence analysis of cDNAs encoding A, B1 and B2 chains, and expression of the corresponding genes in human skin and cultured cells. *Lab Invest* 60:772–782, 1989

Parenteau NL, Nolte CM, Bilbo P, *et al*: Epidermis generated *in vitro*: practical considerations and applications. *J Cell Biochem* 45:245–251, 1991

Payne J, Gong H, Trinkhaus-Randall V: Tyrosine phosphorylation: a critical component in the formation of hemidesmosomes. *Cell Tissue Res* 300:401–411, 2000

Ponec M, Kempenaar J: Use of human skin recombinants as an in vitro model for testing the irritation potential of cutaneous irritants. *Skin Pharmacol* 8:49–59, 1995

Pruniéras M, Regnier M, Fougere S, Woodley D: Keratinocytes synthesize basal-lamina proteins in culture. *J Invest Dermatol* 81:74s–81s, 1983

Rheinwald JG, Green H: Serial cultivation of strains of human epidermal keratinocytes: the formation of keratinocyte colonies from single cells. *Cell* 6:331–344, 1975

Rosdy M, Clauss L-C: Terminal epidermal differentiation of human keratinocytes grown in chemically defined medium on inert filter substrates at the air–liquid interface. *J Invest Dermatol* 95:409–414, 1990

Rousselle P, Keene DR, Ruggiero F, Champliaud MF, Rest M, Burgeson RE: Laminin 5 binds the NC-1 domain of type VII collagen. *J Cell Biol* 138:719–728, 1997

Smola H, Stark HJ, Thiekotter G, Mirancea N, Krieg T, Fusenig NE: Dynamics of basement membrane formation by keratinocyte–fibroblast interactions in organotypic skin culture. *Exp Cell Res* 239:399–410, 1998

Smola H, Thiekotter G, Baur M, Stark HJ, Breitkreutz D, Fusenig NE: Organotypic and epidermal-dermal cocultures of normal human keratinocytes and dermal cells: Regulation of transforming growth factor α, β1 and β2 mRNA levels. *Toxicol In Vitro* 8:641–650, 1994

Smola H, Thiekotter G, Fusenig NE: Mutual induction of growth factor gene expression by epidermal–dermal cell interaction. *J Cell Biol* 122:417–429, 1993

Stanley JR, Hawley-Nelson P, Yaar M, Martin GR, Katz SI: Laminin and bullous pemphigoid antigen are distinct basement membrane proteins synthesized by epidermal cells. *J Invest Dermatol* 78:456–459, 1982

Stoker AW, Streuli CH, Martins-Green M, Bissell MJ: Designer microenvironments for the analysis of cell and tissue function. *Current Opinion Cell Biol* 2:864–874, 1990

Szabowski A, Maas-Szabowski N, Andrecht S, Kolbus A, Schorpp-Kistner M, Fusenig NE, Angel P: c-Jun and JunB antagonistically control cytokine-regulated mesenchymal–epidermal interaction in skin. *Cell* 103:745–755, 2000

Vaccariello M, Javaherian A, Garlick JA: *A Skin Substitute Model for Wound Healing. Tissue Engineering Methods and Protocols*. Totowa: Humana Press, 1999, pp 391–406

Woodley DT, Stanley JR, Reese MJ, O'Keefe EJ: Human dermal fibroblasts synthesize laminin. *J Invest Dermatol* 90:679–683, 1988

Wu Y-J, Parker LM, Binder NE, Beckett MA, Sinard JH, Griffiths CT, Reinwald JG: The mesothelial keratins: a new family of cytoskeletal proteins identified in cultured mesothelial cells nonkeratinizing epithelia. *Cell* 31:693–703, 1982

Yurchenco PD, O'Rear JJ: Basement membrane assembly. *Methods Enzymol* 245: 489–518, 1994

Zieske JD, Mason VS, Wasson ME, *et al*: Basement membrane assembly and differentiation of cultured corneal cells: importance of culture environment and endothelial cell interaction. *Exp Cell Res* 214:621–633, 1994

Tissue Engineering Meeting

Cold Spring Harbor

November 2002

Tissue Engineering
Poster

BASEMENT MEMBRANE COMPONENTS ARE REQUIRED FOR EPIDERMAL ORGANIZATION AND SURVIVAL OF HUMAN KERATINOCTYES IN ORGANOTYPIC CULTURE. Frank Andriani, Nadav Segal, Sue Pawagi, Ning Lin, Lina Nguyen and Jonathan Garlick (SUNY Stony Brook, School of Dental Medicine)

Epithelial-mesenchymal interactions promote morphogenesis and homeostasis of human skin. However, the role of individual basement membrane components (BMC) or extracellular matrix components (EMC) on the normalization of epidermal phenotype is not well-understood. The goal of this study was to develop human, organotypic tissue models to directly study the role of these connective tissue components on epidermal tissue architecture and keratinocyte differentiation, survival and growth. To accomplish this, we developed a novel organotypic tissue model by growing human keratinocytes on polycarbonate membranes coated with purified BMCs or EMCs that were placed on contracted Type I collagen gels populated with dermal fibroblasts. We found that only keratinocytes grown on membranes coated with BMCs (Type IV collagen or laminin 1) generated well-stratified epithelia demonstrating all morphologic layers. In contrast, tissues grown on EMCs not usually found in basement membrane (fibronectin, Type I collagen and fibrillar Type I collagen) demonstrated aberrant tissue architecture that was characterized by non-polarized basal cells and a poorly-formed spinous layer. Furthermore, only keratinocytes grown on BMC demonstrated a normalized, linear pattern of deposition of the basement membrane component laminin 5 and an elevated synthesis and processing of the $\gamma 2$ chain of laminin 5 upon Western analysis. This demonstrated that while pre-existing BMCs enabled proper organization of basement membrane, EMCs were not permissive for such assembly. *In situ* TUNEL assay revealed that no TUNEL-positive keratinocytes were seen in the basal layer when cultures were grown on BMCs while elevated levels of TUNEL-stained cells were seen in a basal position for tissues generated on EMCs. This showed that BMCs such as Type IV collagen promoted keratinocyte survival. Expression of markers of keratinocyte differentiation (keratin 10 and filaggrin) were normalized for tissues grown on both BMCs and EMCs, suggesting that keratinocyte differentiation was independent of these components. These studies have demonstrated that BMCs are critical microenvironmental factors that are needed to sustain keratinocyte survival and optimize epithelial architecture. This human culture model allows dissection of the role of connective tissue components on the regulation of epidermal phenotype and will be a valuable tool for future studies in epidermal biology.
(Supported by grants #2RO1DE011250-06 from the National Institutes of Dental and Craniofacial Research, #DAMMD17-01-1-0688 from the US Army Medical Research and Materiel Command.)

Tissue Engineering
Oral

GARLICK

MICROENVIRONMENTAL FACTORS CONTRIBUTE TO BASEMENT MEMBRANE ASSEMBLY AND NORMALIZE EPIDERMAL PHENOTYPE IN AN IMPROVED HUMAN SKIN EQUIVALENT MODEL

Frank Andriani, Alexander Margulis, Ning Ling, Jackie Garfield*, Larry Pfeiffer, Sy Griffey*, and Jonathan Garlick (SUNY Stony Brook, School of Dental Medicine, *Life Cell Inc.)

To further understand the role of the dynamic interplay between keratinocytes and stromal components in the regulation of the growth, differentiation, morphogenesis and basement membrane assembly of human stratified squamous epithelium, we have generated novel, three-dimensional organotypic cultures in which skin keratinocytes were grown in the absence or presence of pre-existing basement membrane components and/or dermal fibroblasts. We found that keratinocytes cultured in the presence of pre-existing basement membrane components and dermal fibroblasts for 9 days showed rapid assembly of basement membrane, as seen by a nearly complete lamina densa, hemidesmosomes and the polarized, linear distribution of laminin 5 and α6 integrin subunit. Basement membrane assembly was somewhat delayed in the absence of dermal fibroblasts, but did occur at discrete nucleation sites when pre-existing basement membrane components were present. No basement membrane developed in the absence of pre-existing basement membrane components, even in the presence of dermal fibroblasts. BrdU-incorporation studies showed that early keratinocyte growth was independent of mesenchymal support, but by 14 days, both fibroblasts and assembled basement membrane were required to sustain growth. Normalization of keratinocyte differentiation was independent of both dermal fibroblasts and structured basement membrane. These results indicated that epithelial and mesenchymal components play a coordinated role in the generation of structured basement membrane and in the regulation of normalized epithelial growth and tissue architecture in an *in vitro* model of human skin (Supported by grants #2RO1DE011250-06 from the National Institutes of Dental and Craniofacial Research, #DAMMD17-01-1-0688 from the US Army Medical Research and Materiel Command and LifeCell Inc.)

Figure 1

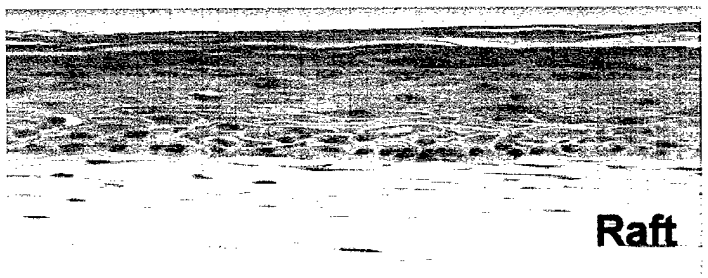

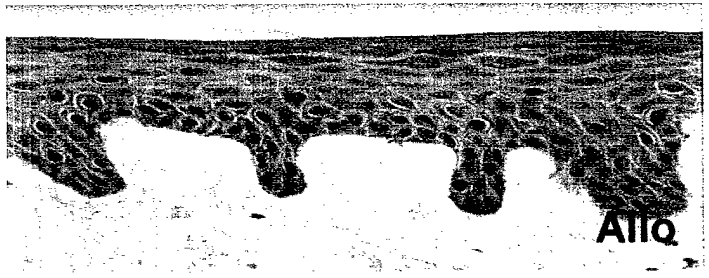

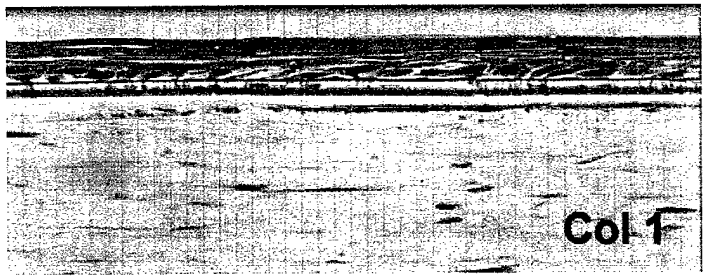

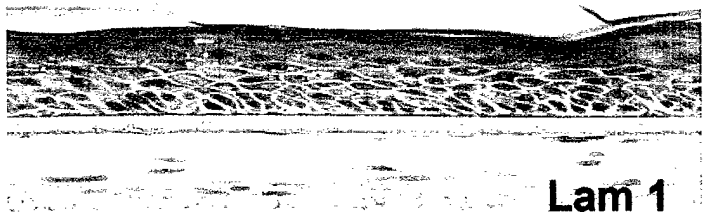

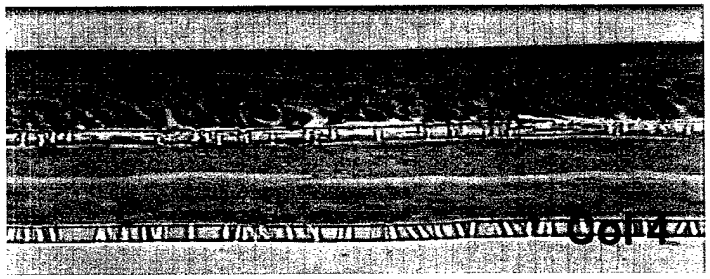

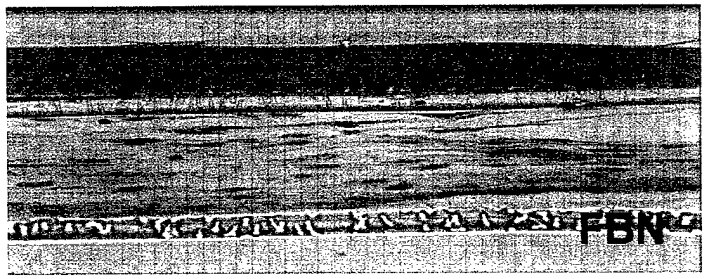

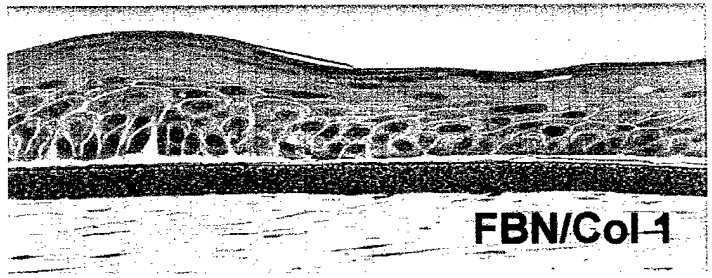

Figure 2

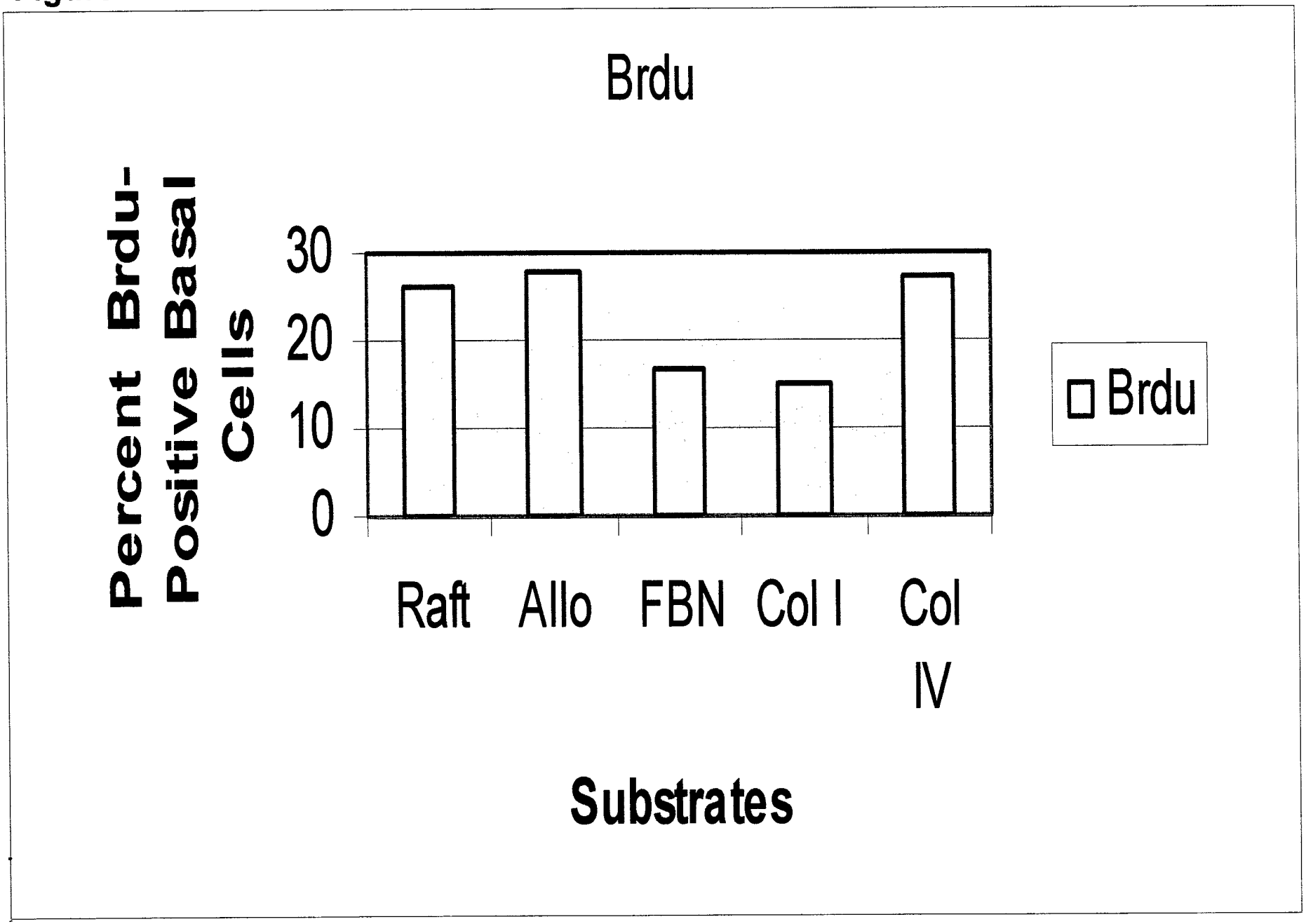
Brdu
Percent Brdu-Positive Basal Cells
30
20
10
0
Raft
Allo
FBN
Col I
Col IV
Brdu
Substrates

Figure 3

Apoptosis

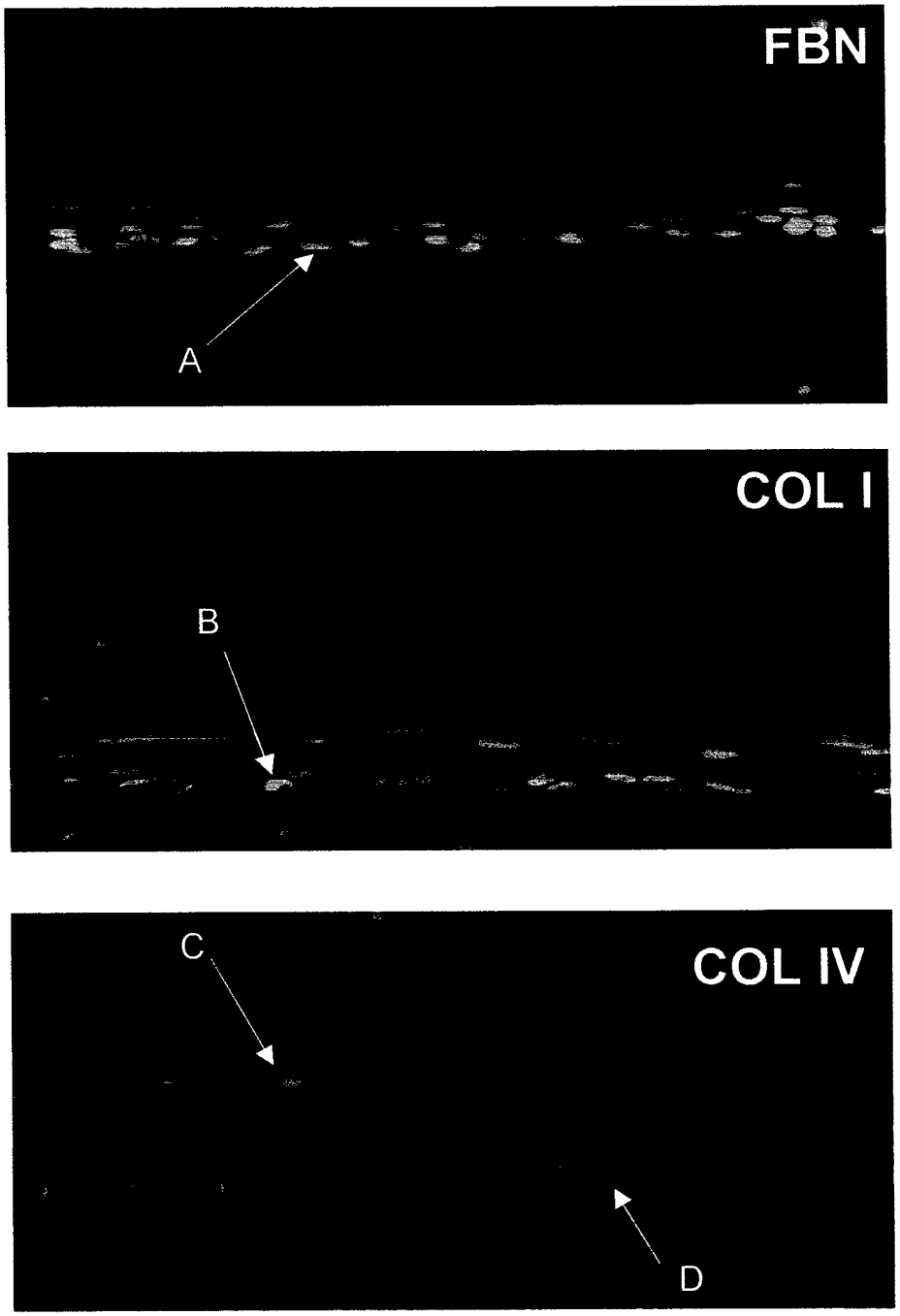

Figure 4

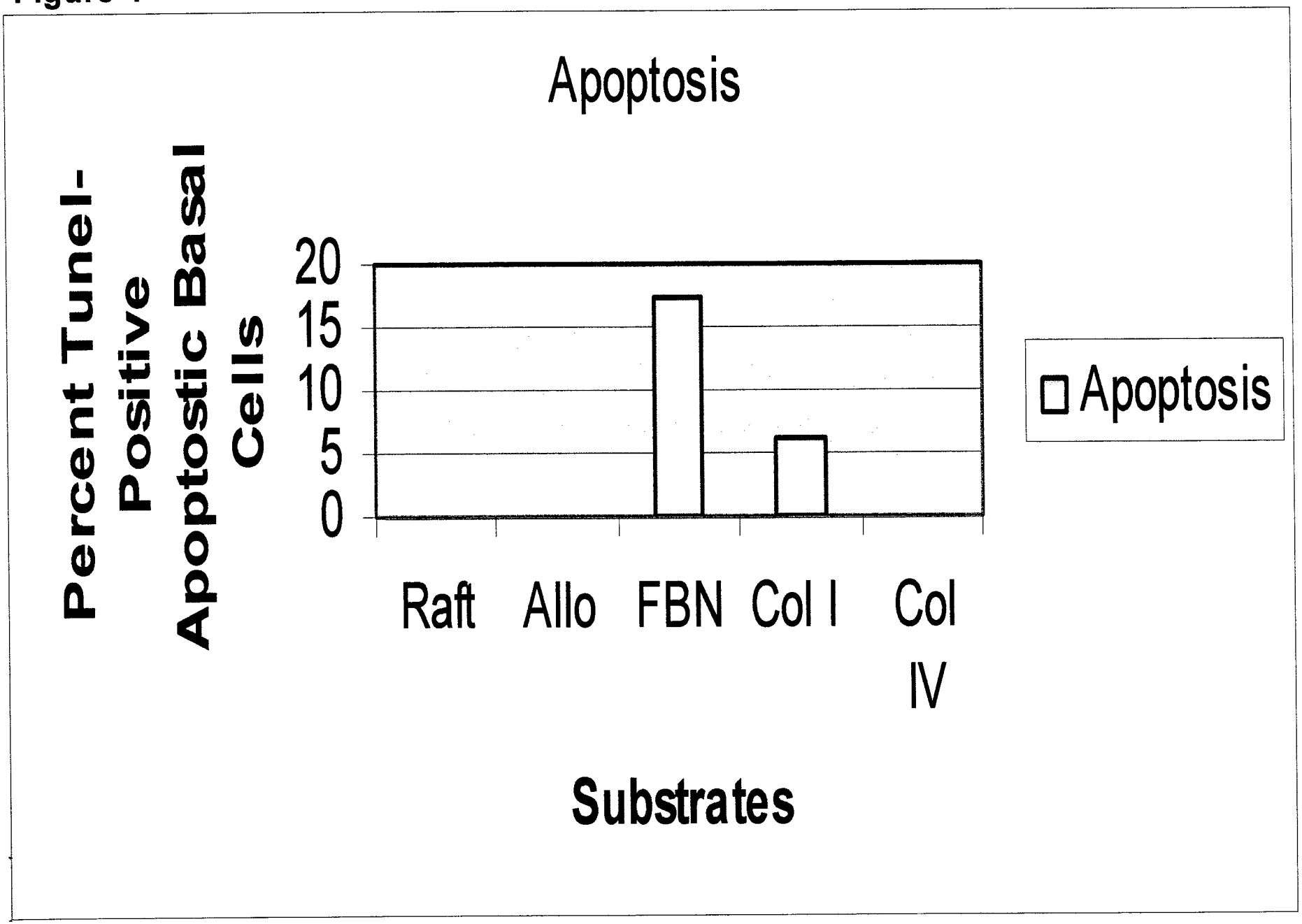
Apoptosis
Percent Tunel-Positive Apoptostic Basal Cells
20
15
10
5
0
Raft
Allo
FBN
Col I
Col IV
Substrates
Apoptosis

Figure 5

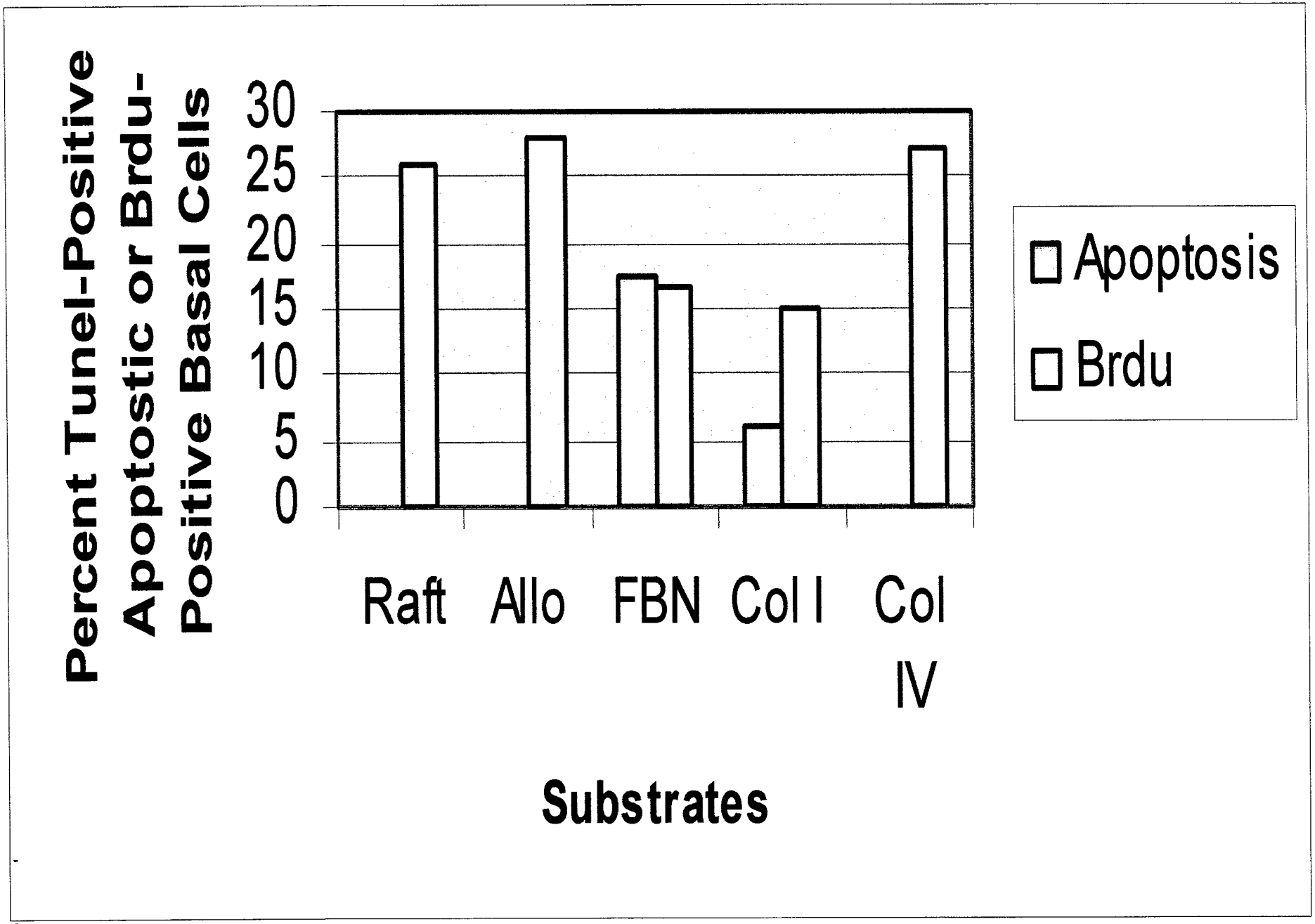
Percent Tunel-Positive Apoptostic or Brdu-Positive Basal Cells
30
25
20
15
10
5
0
Raft
Allo
FBN
Col I
Col IV
Substrates
Apoptosis
Brdu

Figure 6A

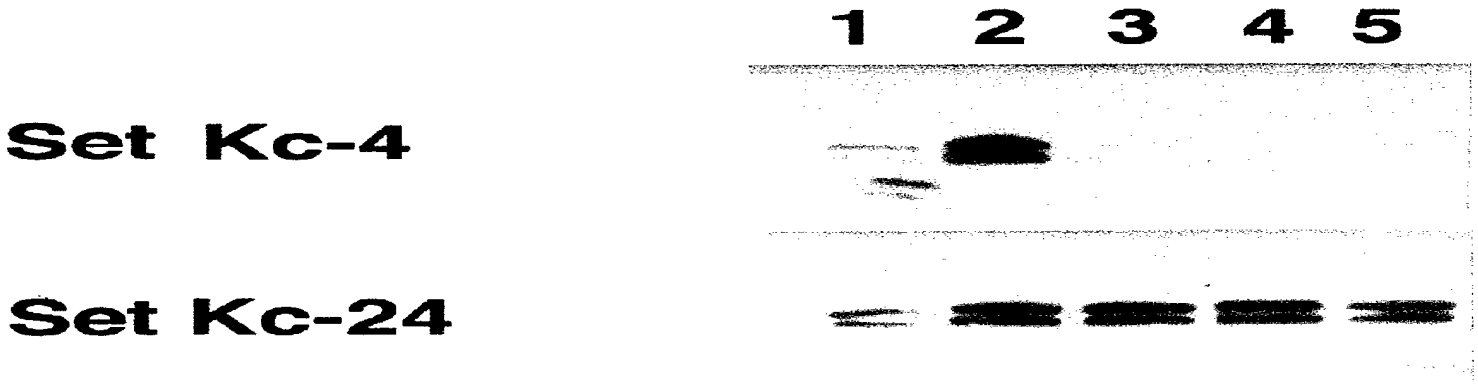

Figure 6B

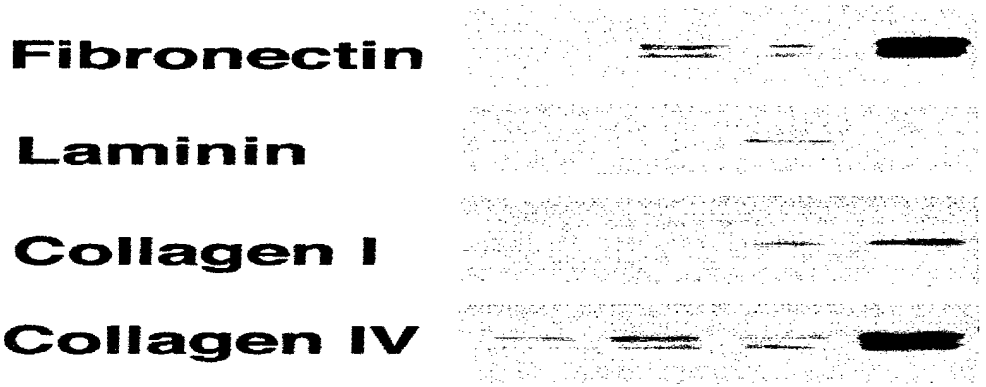

Figure 7

Laminin 5 (GB3)

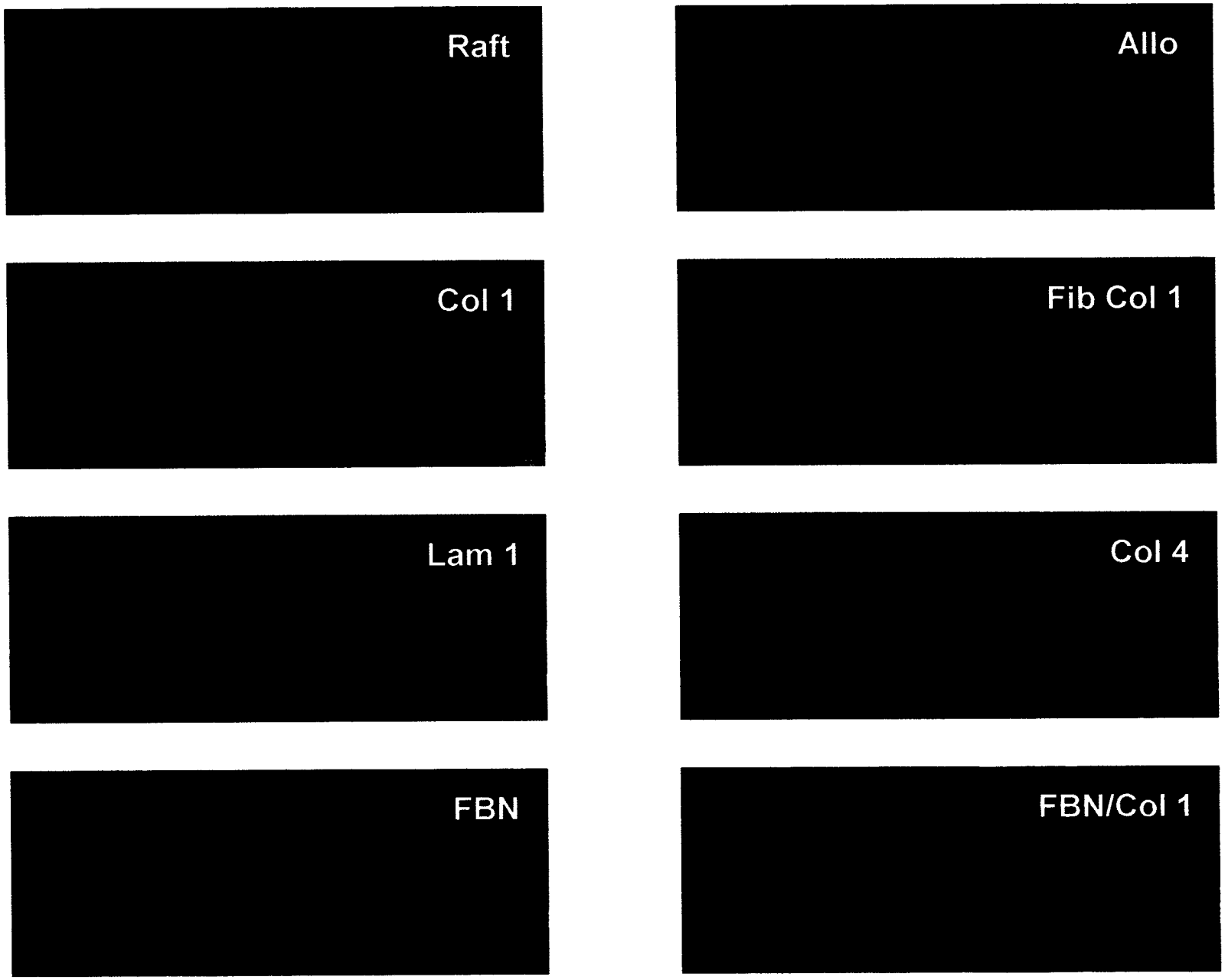

Figure 8

Laminin 5 (SE144)

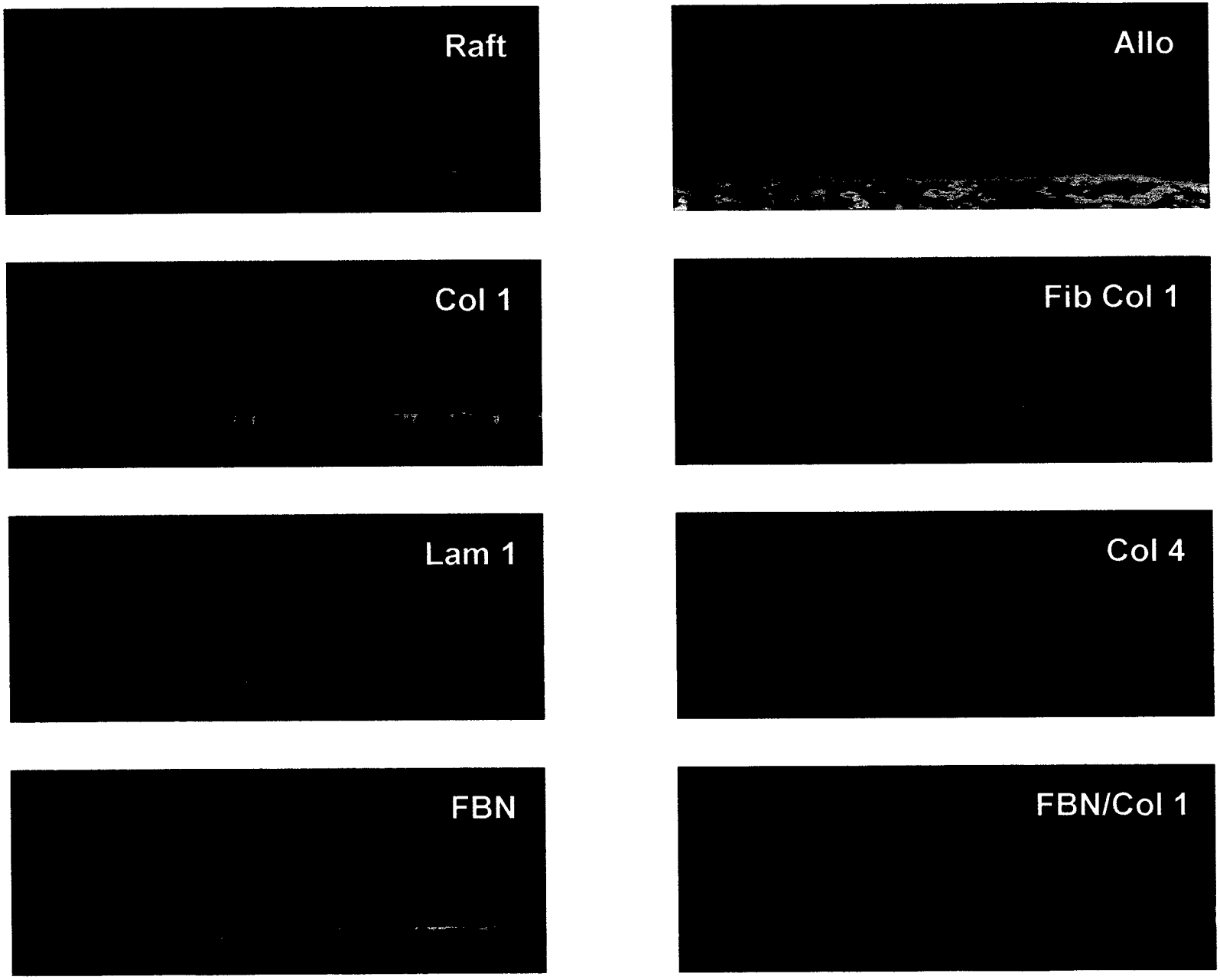

Figure 9

Alpha 6

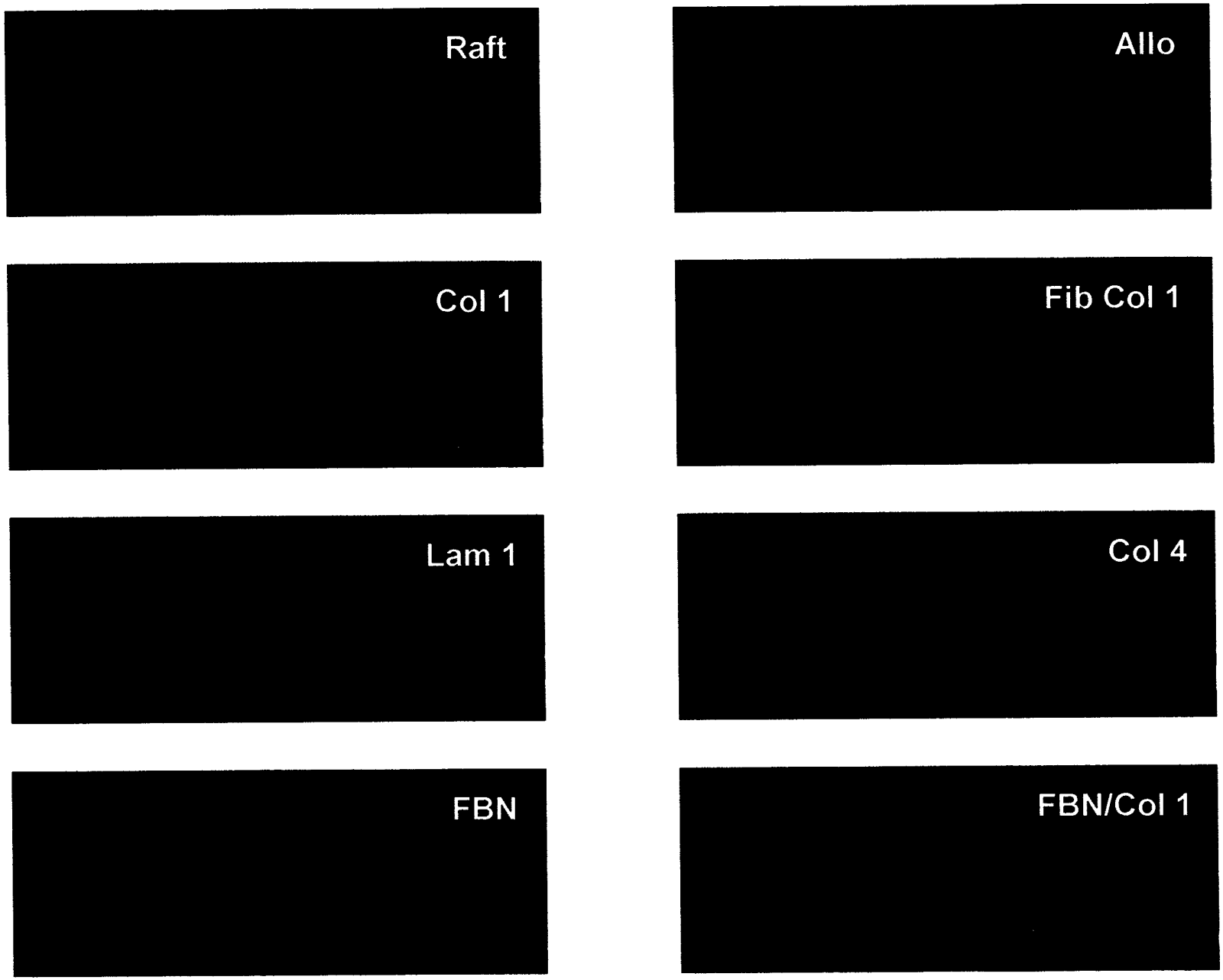

Figure 10

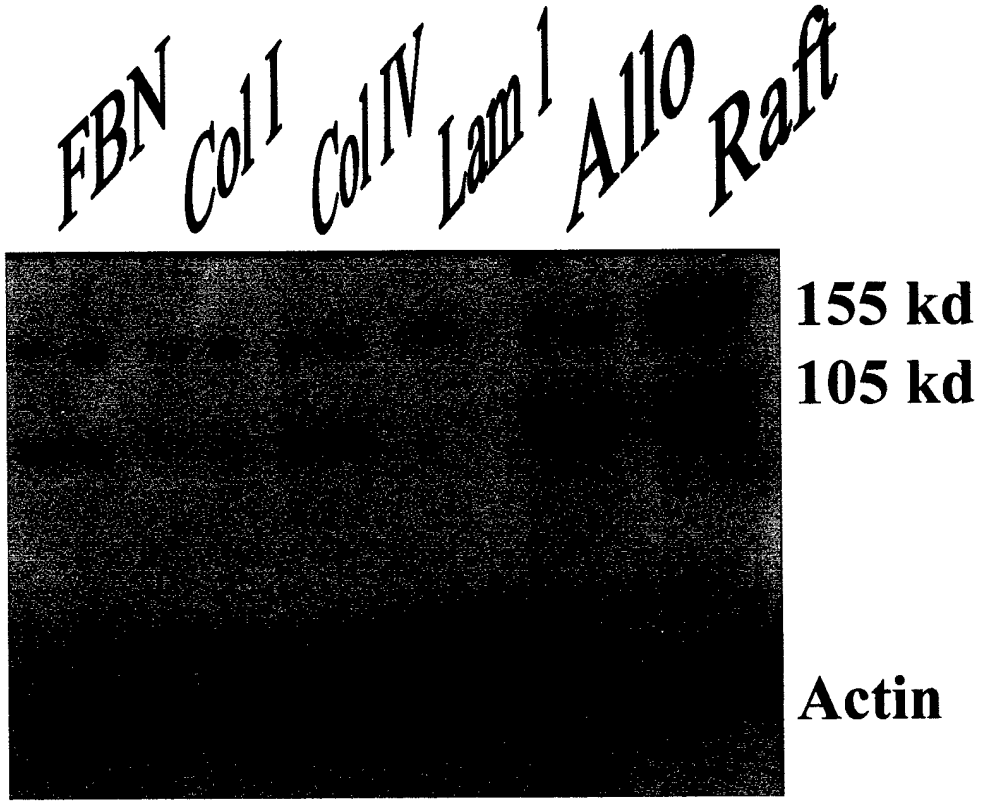

Figure 11 Phenotypic properties of epithelial tissues grown on ECM components

	Alloderm	Collagen Gel	Collagen I	Collagen IV	Fibronectin
Tissue Stratification	*****	*****	**	*****	***
Tissue Architecture	normal, well-polarized basal cells	loss of basal cell polarity	aberrant flat basal cell layer	normal, well-polarized basal cells	loss of basal cell polarity
Collagen. IV	linear	linear, patchy	linear, pc	linear, pc	linear, pc
Laminin 5	linear	linear	linear	linear	linear
Collagen VII	linear	patchy, pc	patchy, pc	linear, pc	linear, pc
Collagen IV	linear	linear, patchy	linear, patchy	linear	none
α6 integrin	linear	linear, patchy	pc	linear	none
Filaggrin	+++	+++	++	+++	+++
K1	+++	++	++	++	++
Brdu (LI)	28%	26%	15%	27%	16.5%
Gamma 2 Chain of Lam 5	linear, patchy	linear	linear	linear, pc	linear, patchy
% Tunel - positive basal cells	0	0	6%	0	17.5 %

BM – basement membrane, HFF human foreskin fibroblasts
***** - full stratification, *** - moderate stratification, ** - little stratification
pc – pericellular staining only, sb - suprabasal staining
+++ - strong staining, ++ - moderate staining

Figure 12

Laminin 1

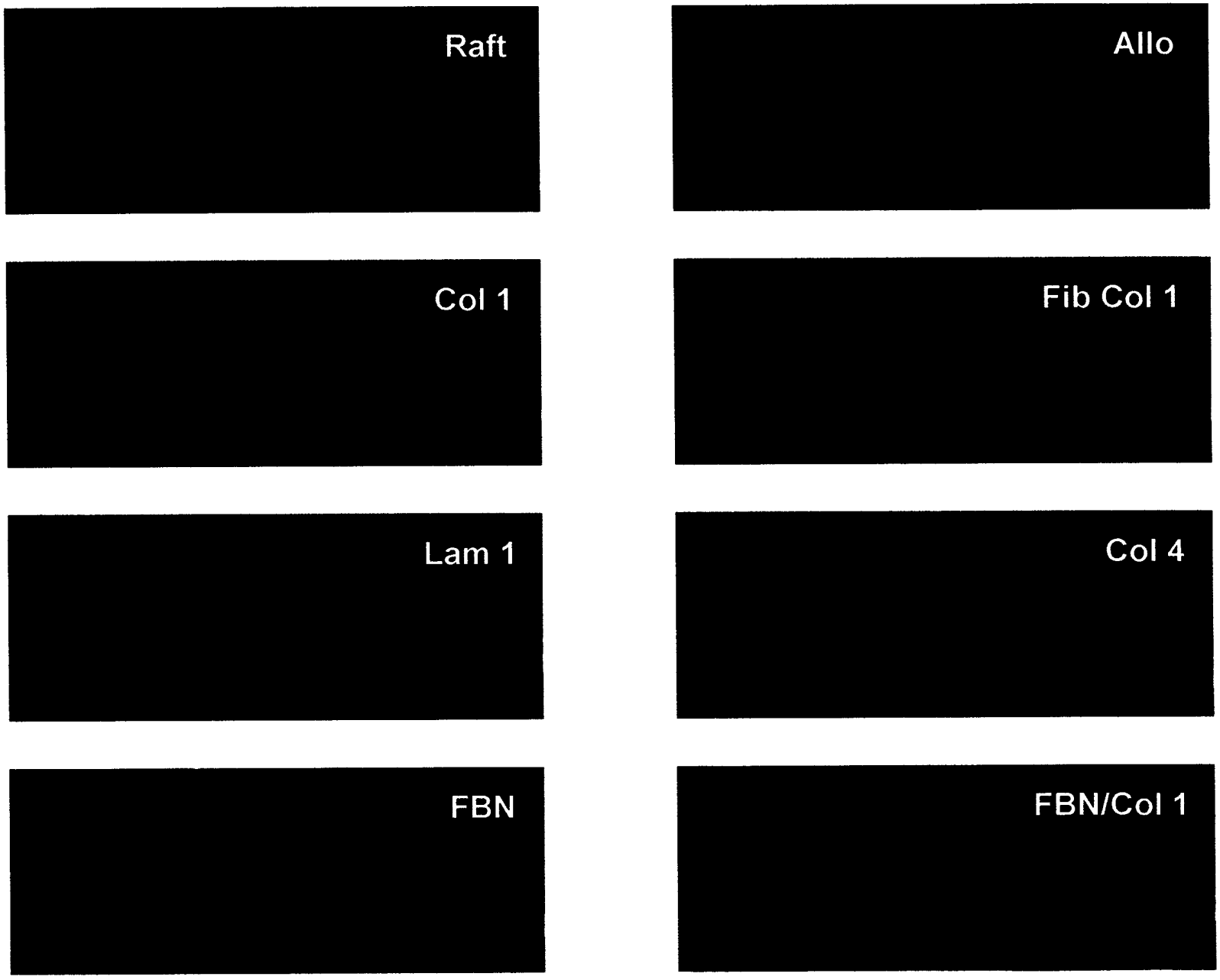

Figure 13

Collagen 7

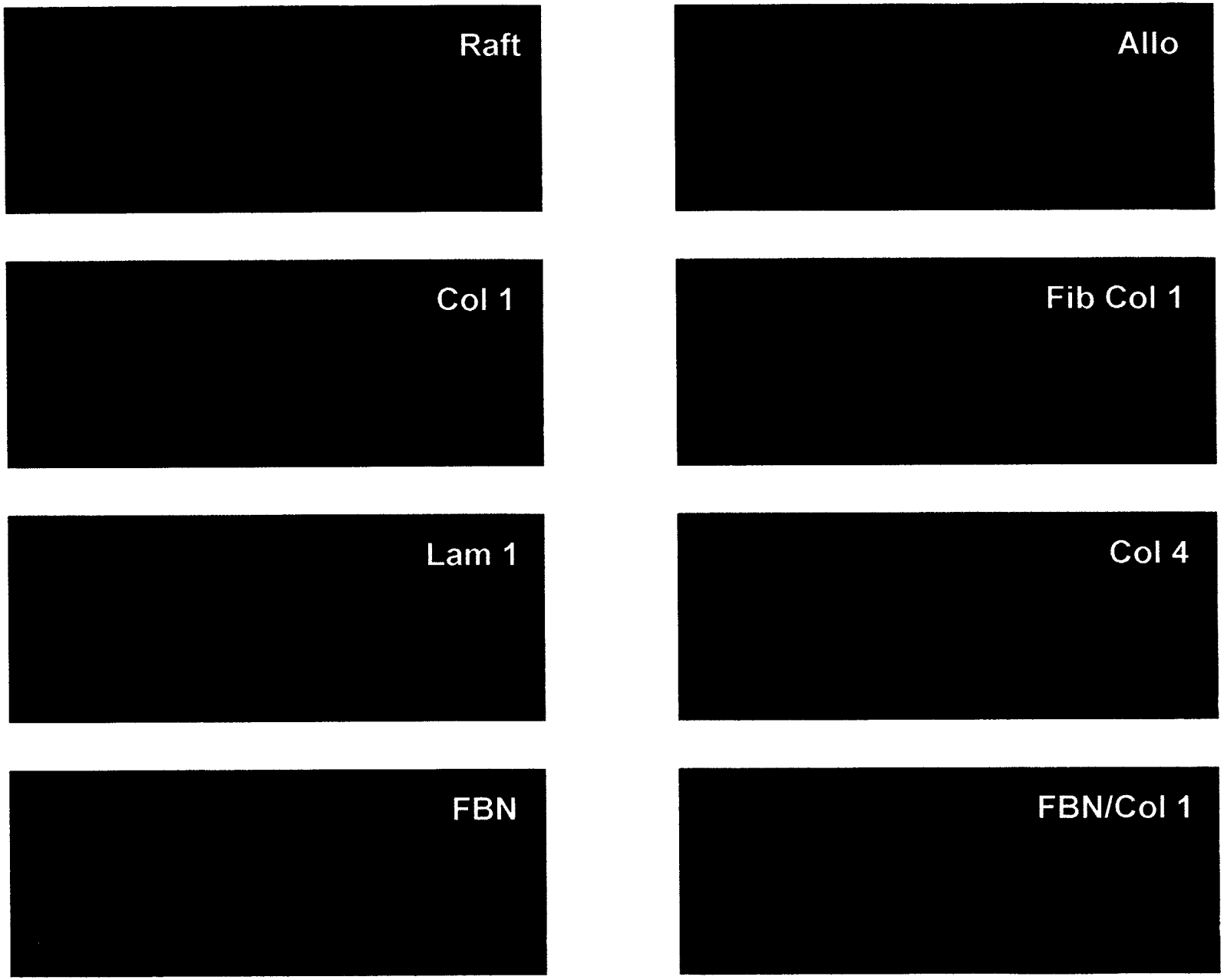

Figure 14

Collagen 4

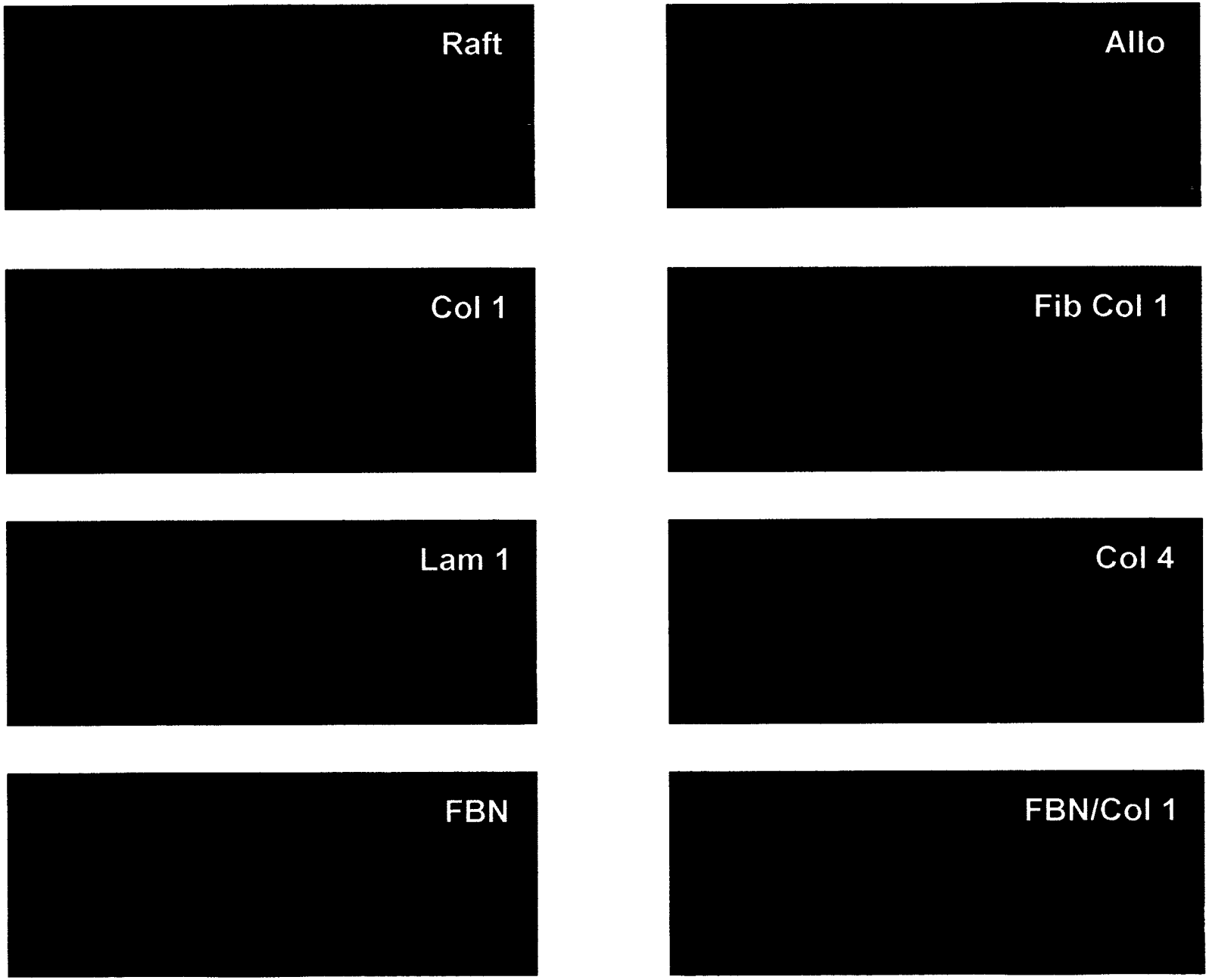

Figure 15

Keratin 1

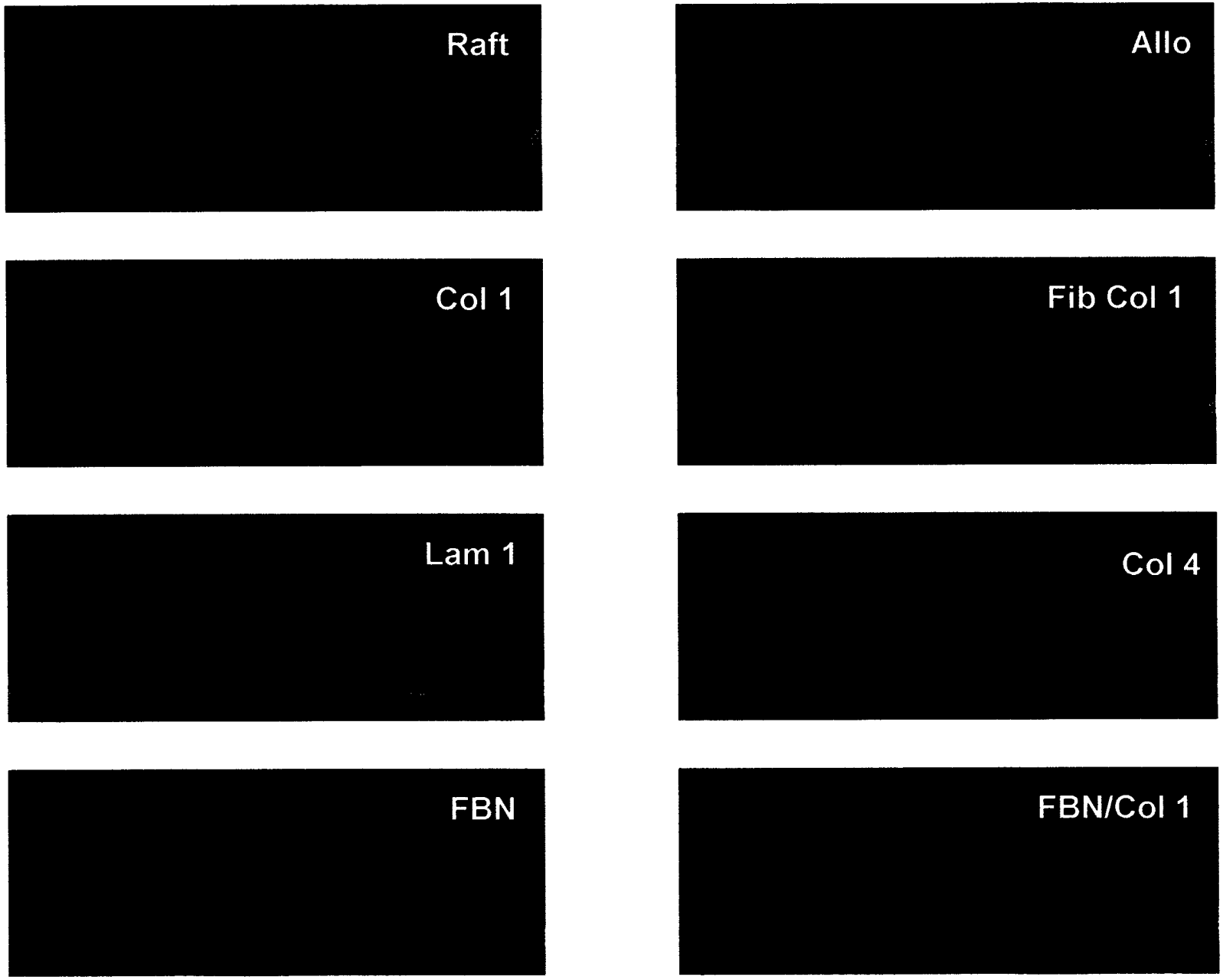

Figure 16

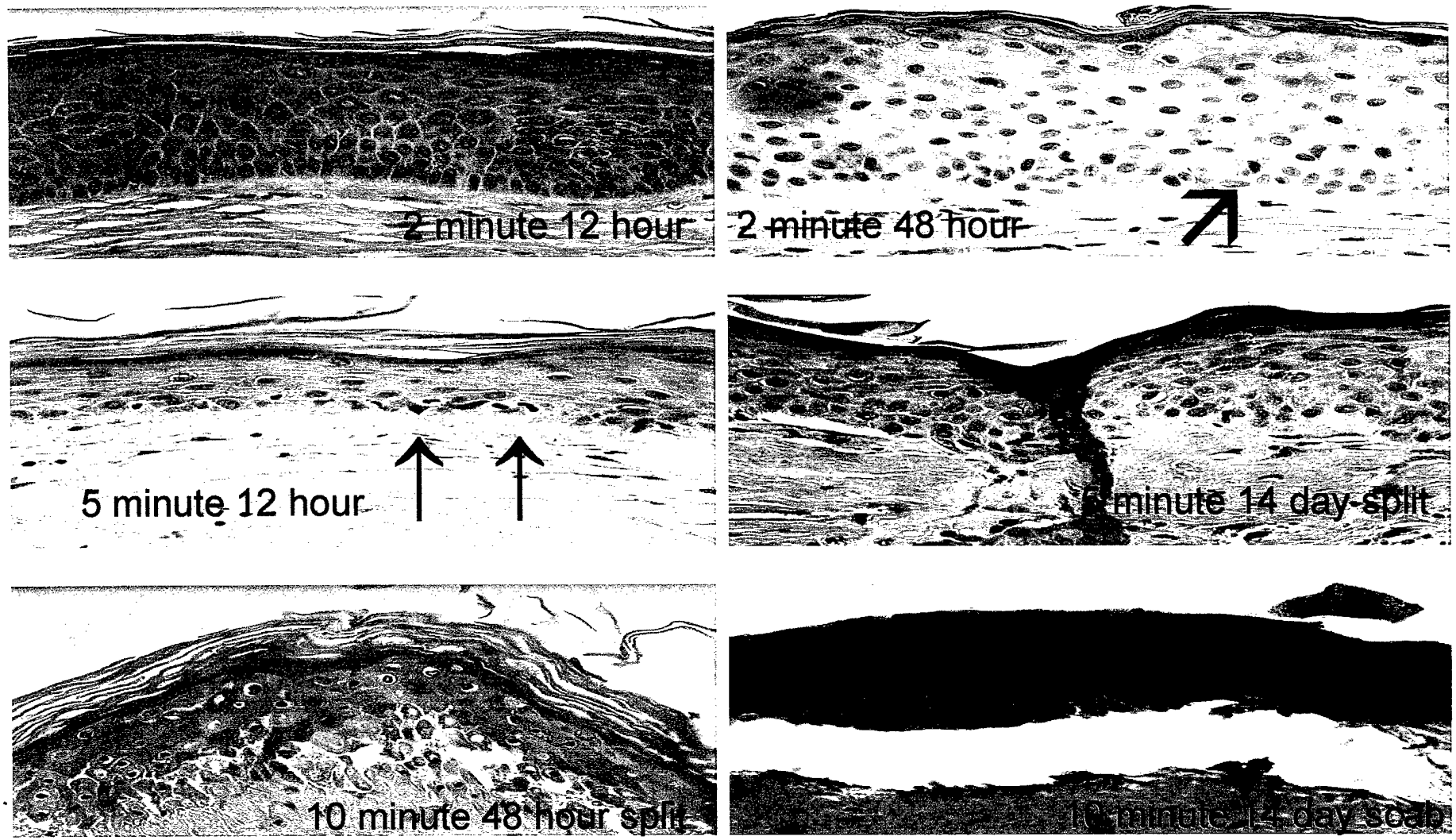
2 minute 12 hour
2 minute 48 hour
5 minute 12 hour
5 minute 14 day split
10 minute 48 hour split
10 minute 14 day soap

Figure 17

8 minutes 6 hour

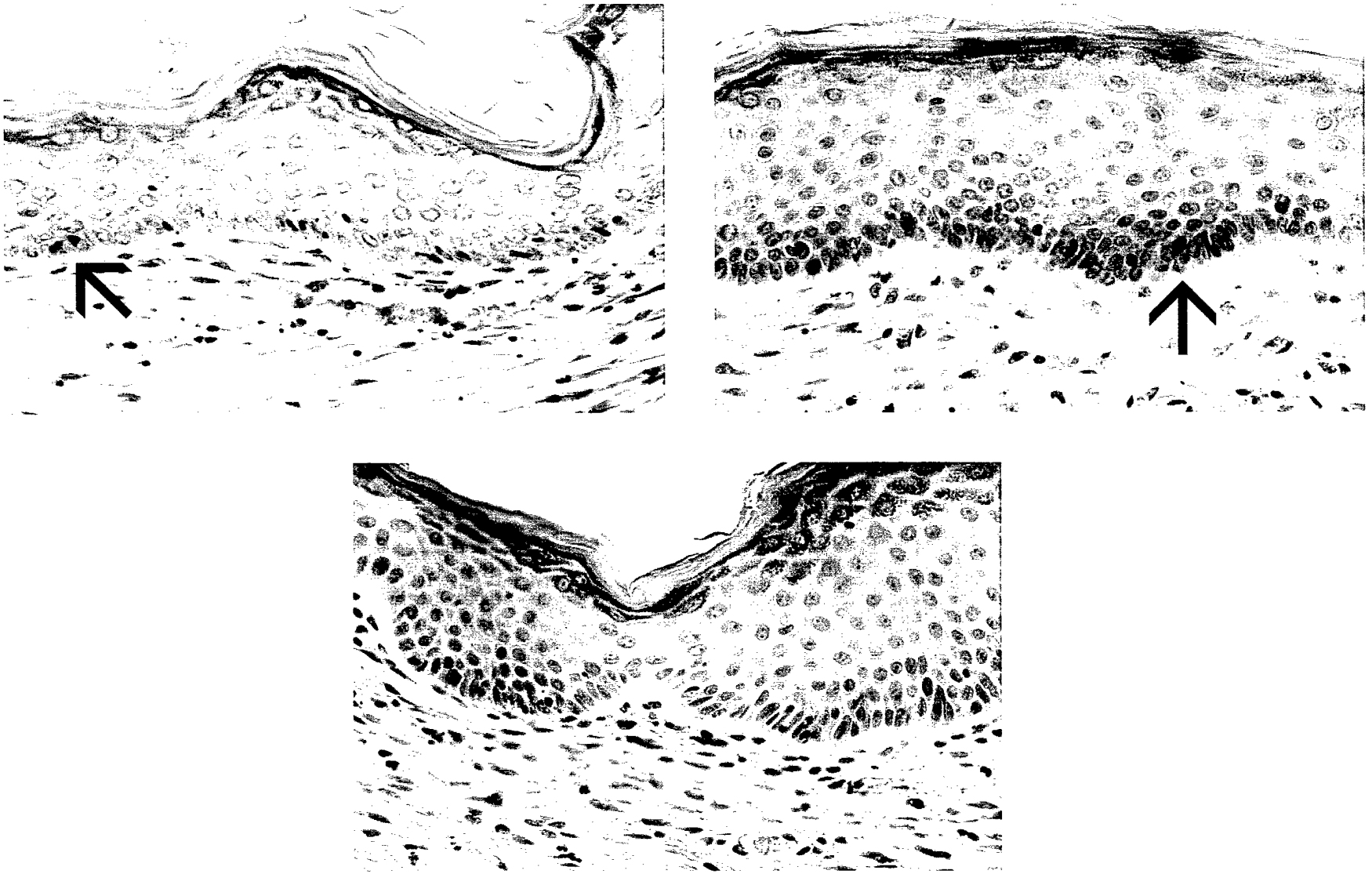

Figure 18

10 minutes 6 hour

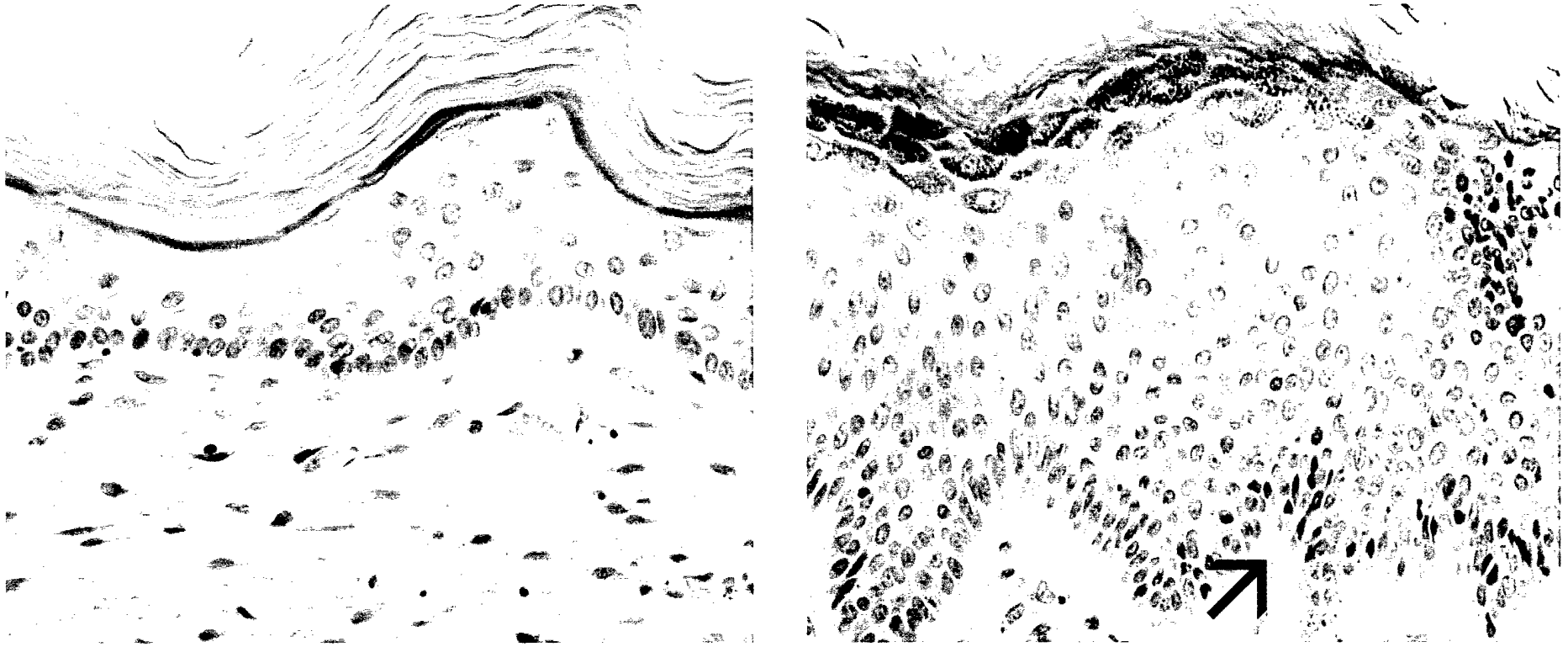

Figure 19

12 minute 6 hour

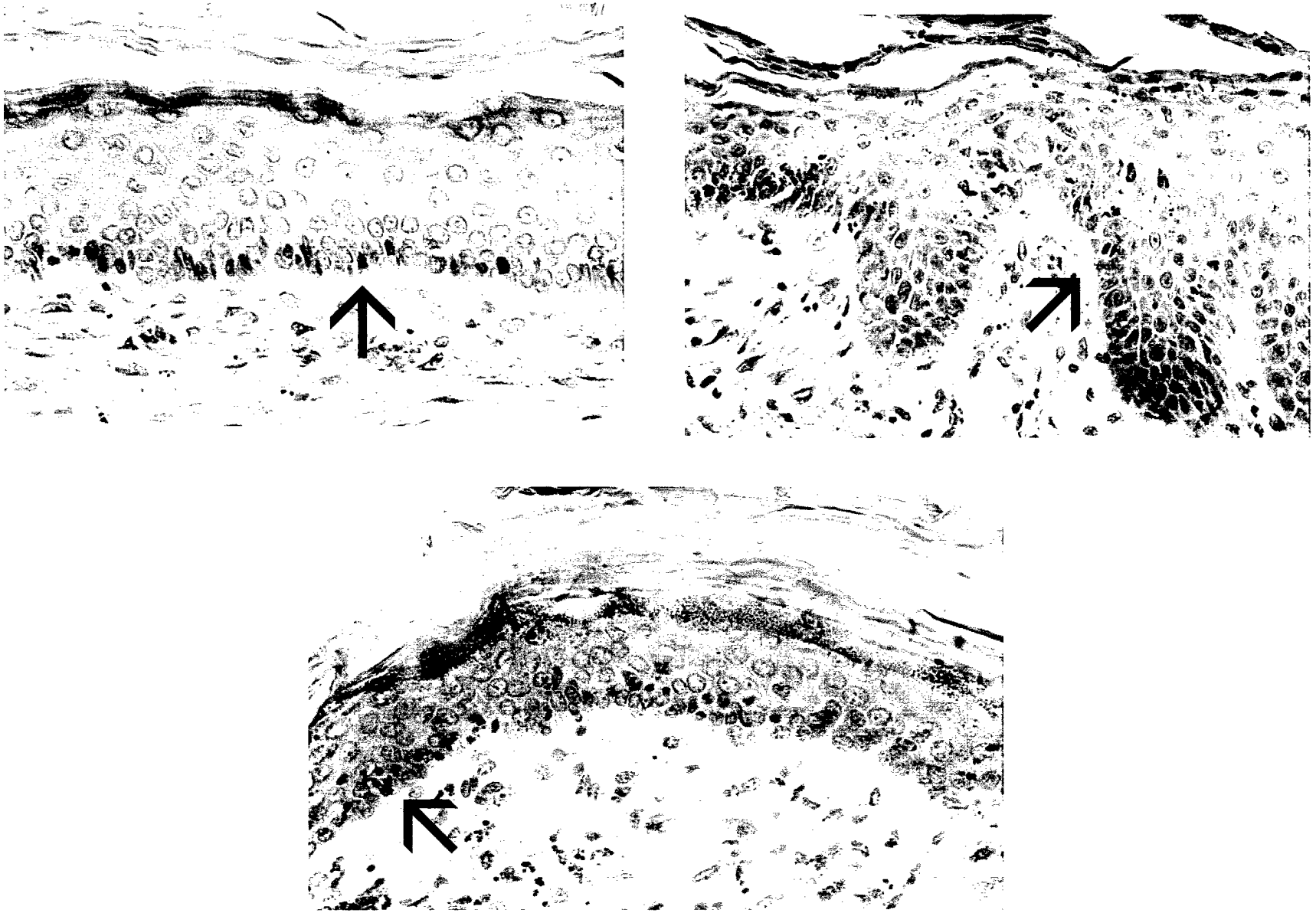

Figure 20

CONTROLS

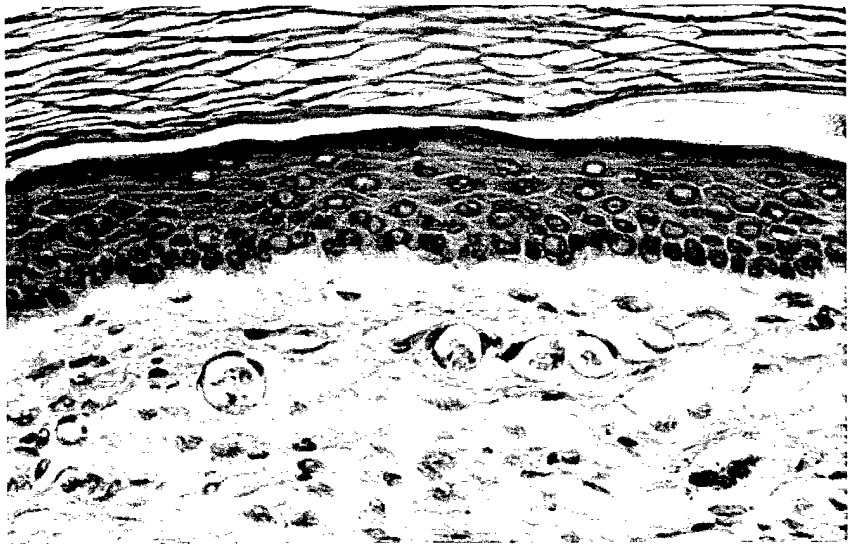

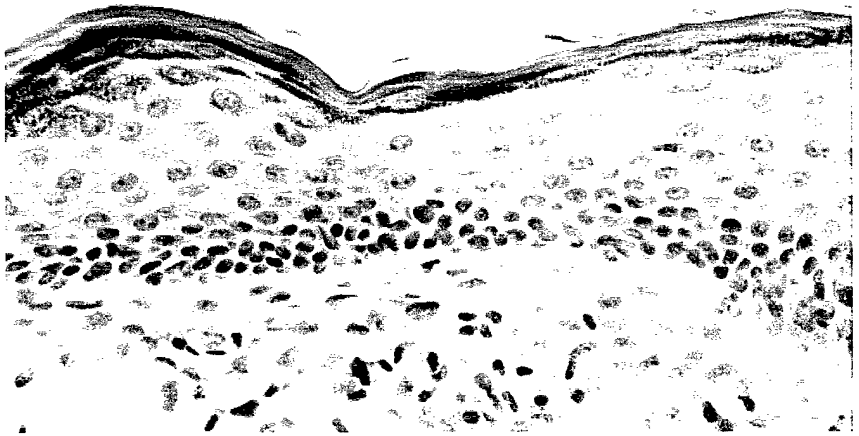

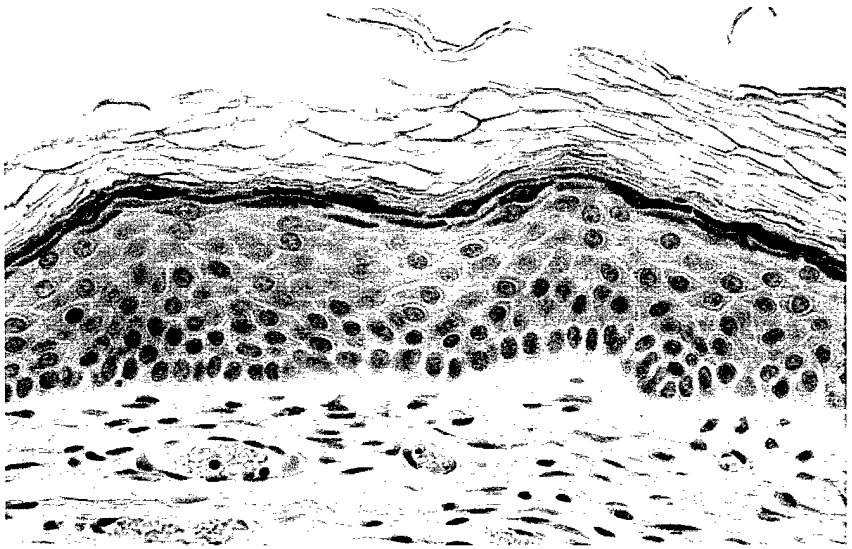

Figure 21

5 minute 24 hour

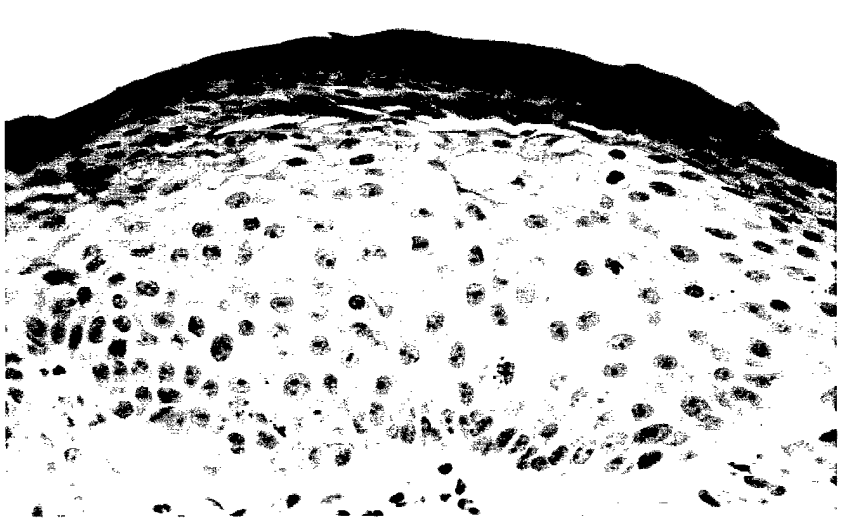

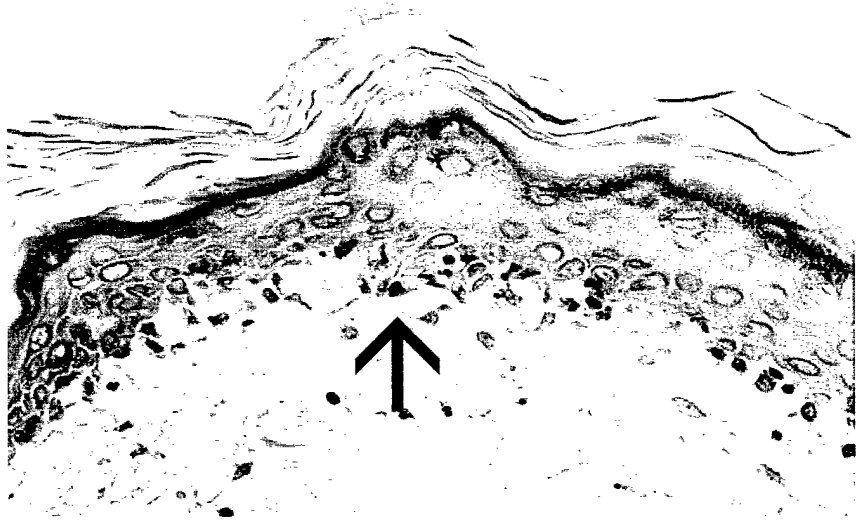

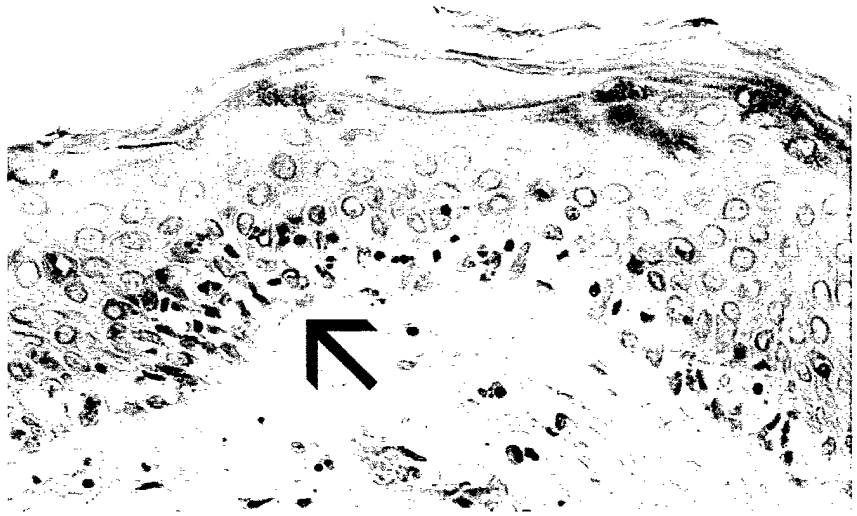

Figure 22

8 minute 24 hour

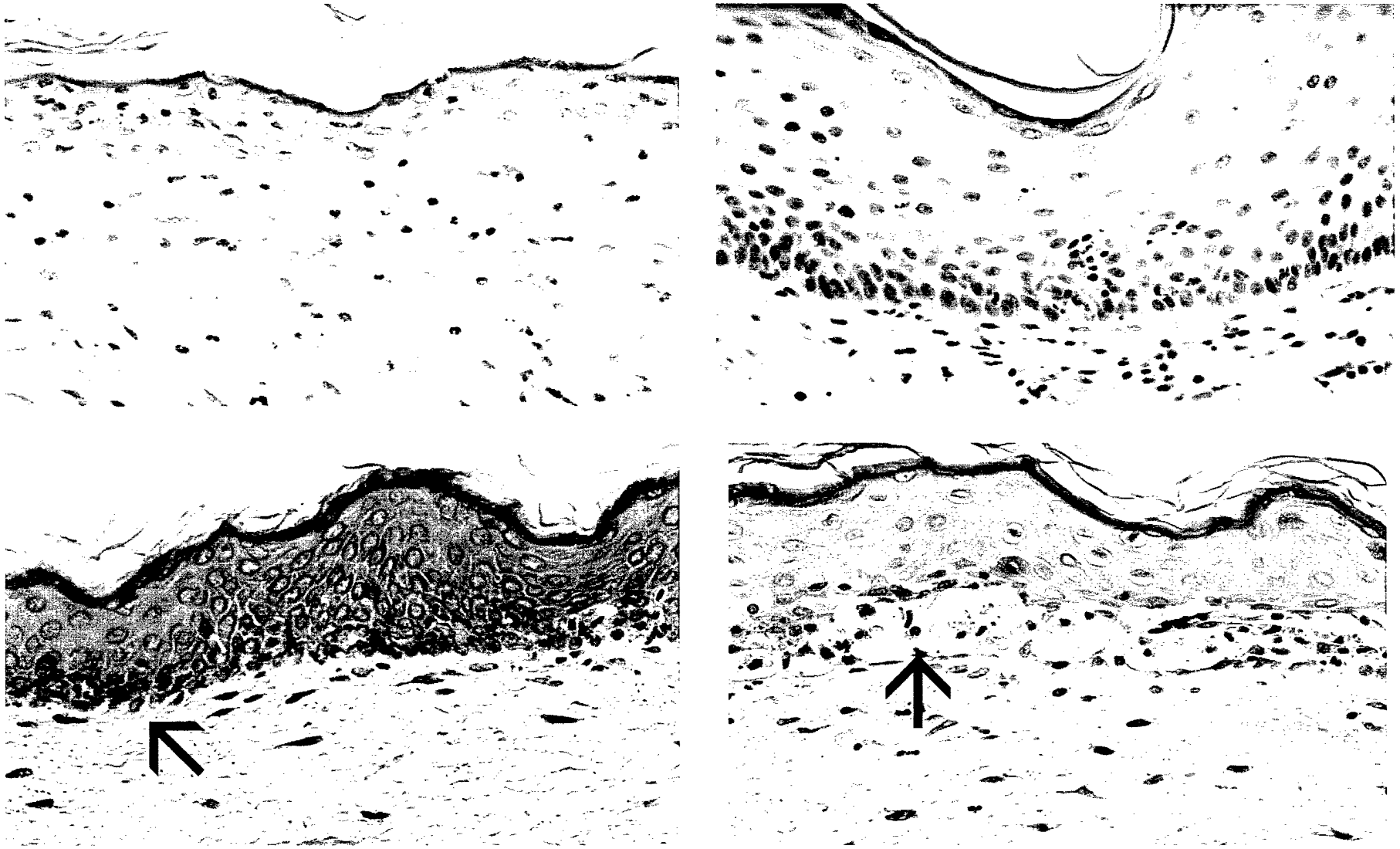

Figure 23

10 minute 24 hour

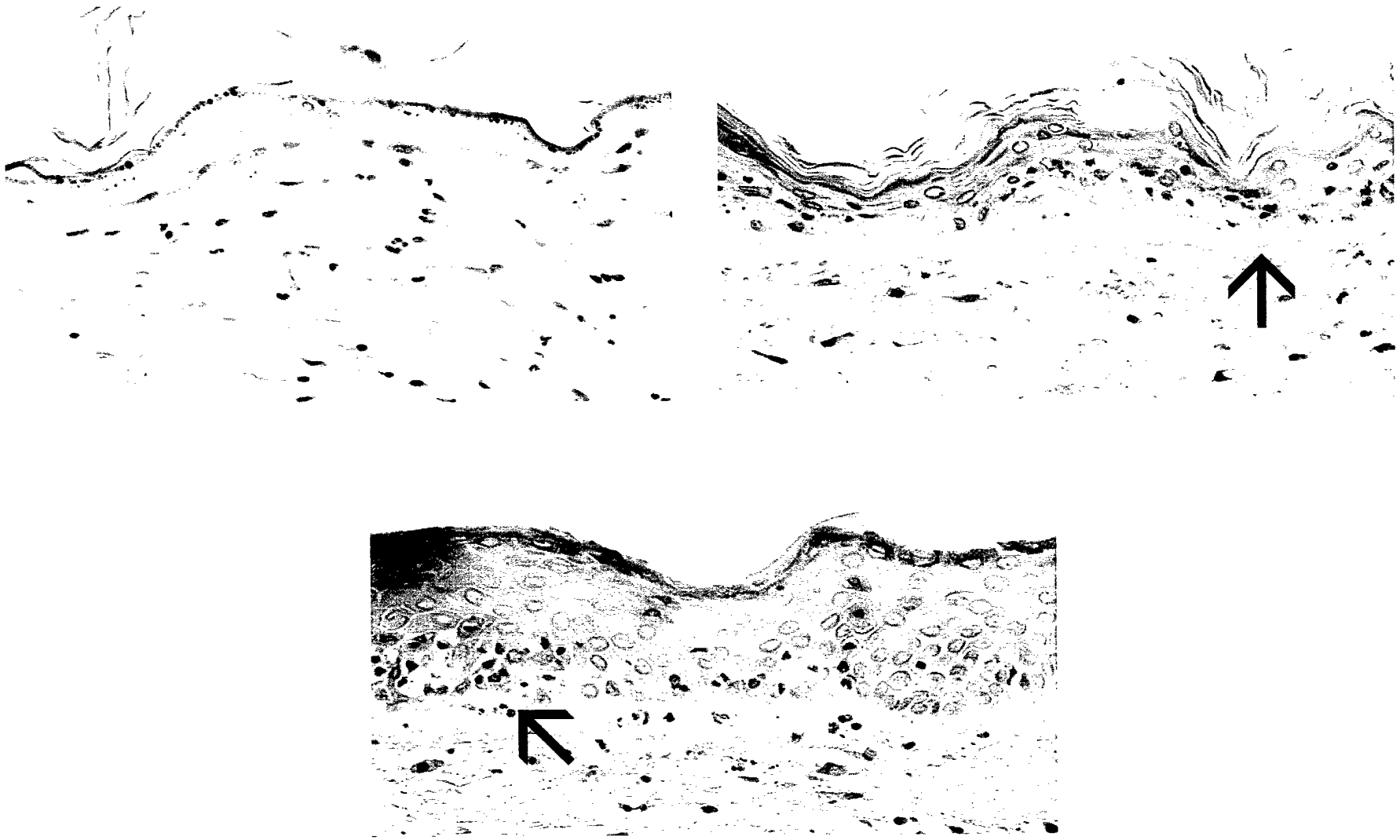

Figure 24

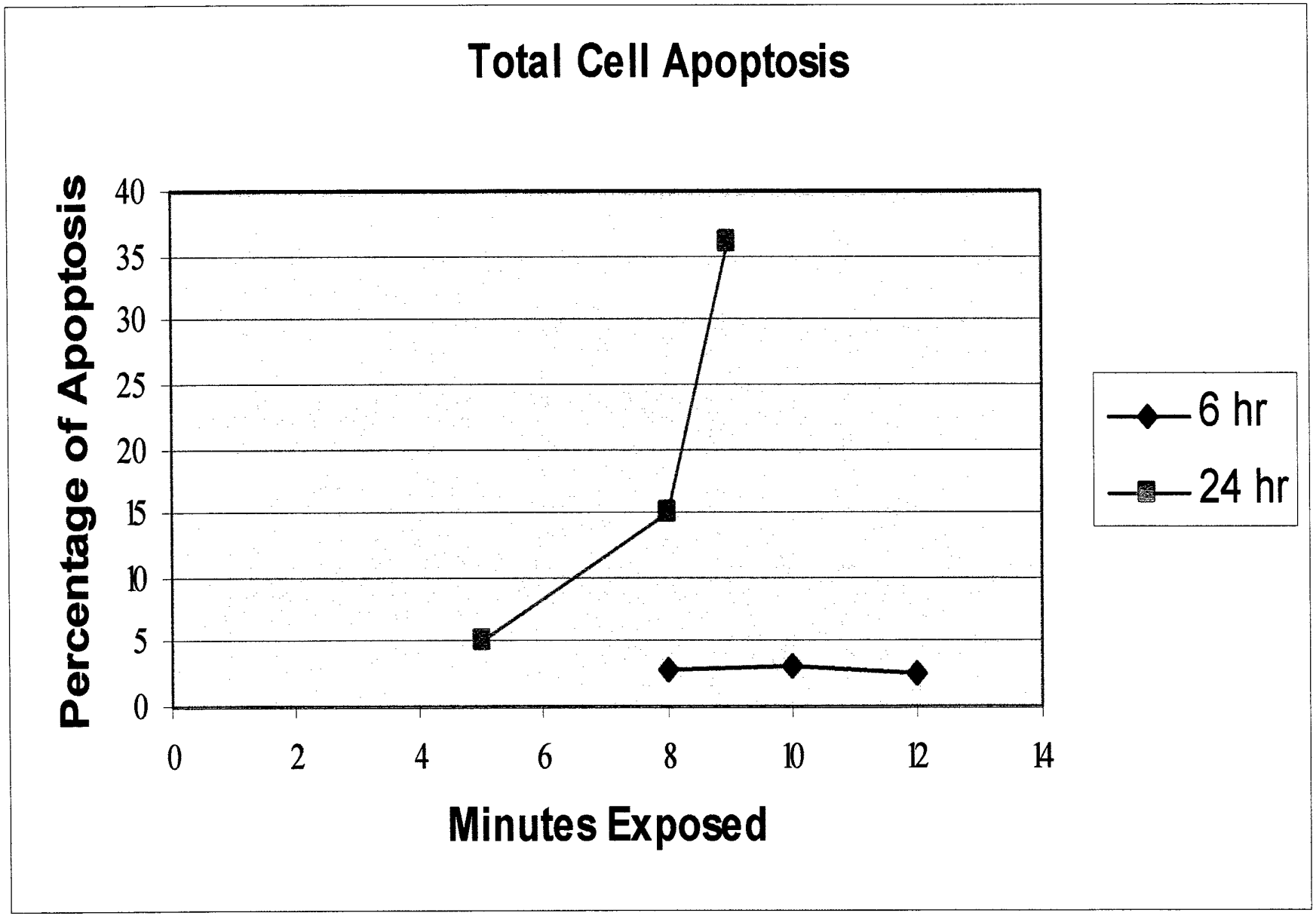
Total Cell Apoptosis
Percentage of Apoptosis
40
35
30
25
20
15
10
5
0
0
2
4
6
8
10
12
14
Minutes Exposed
6 hr
24 hr

Figure 25

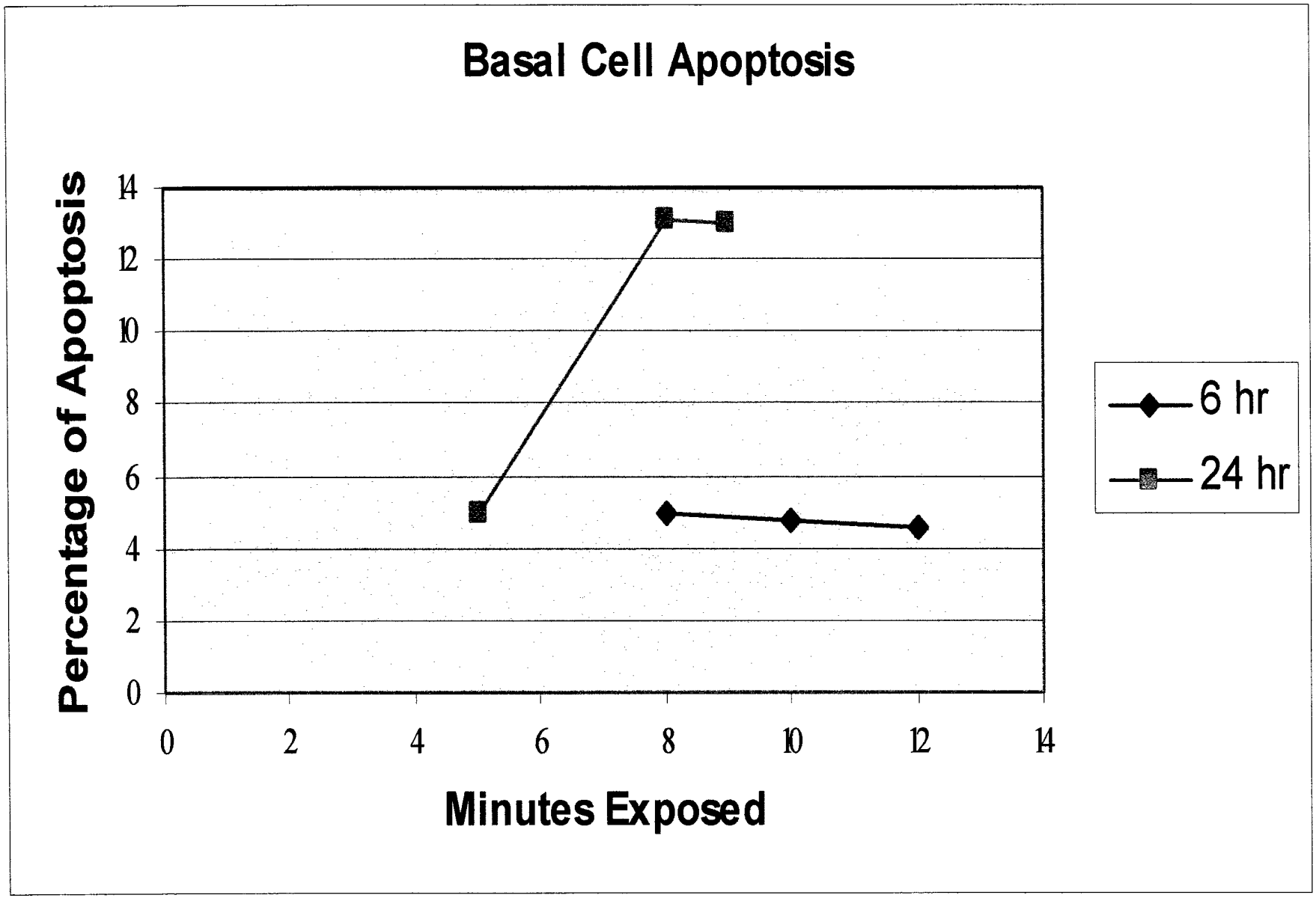
Basal Cell Apoptosis
Percentage of Apoptosis
0
2
4
6
8
10
12
14
Minutes Exposed
6 hr
24 hr

Figure 26

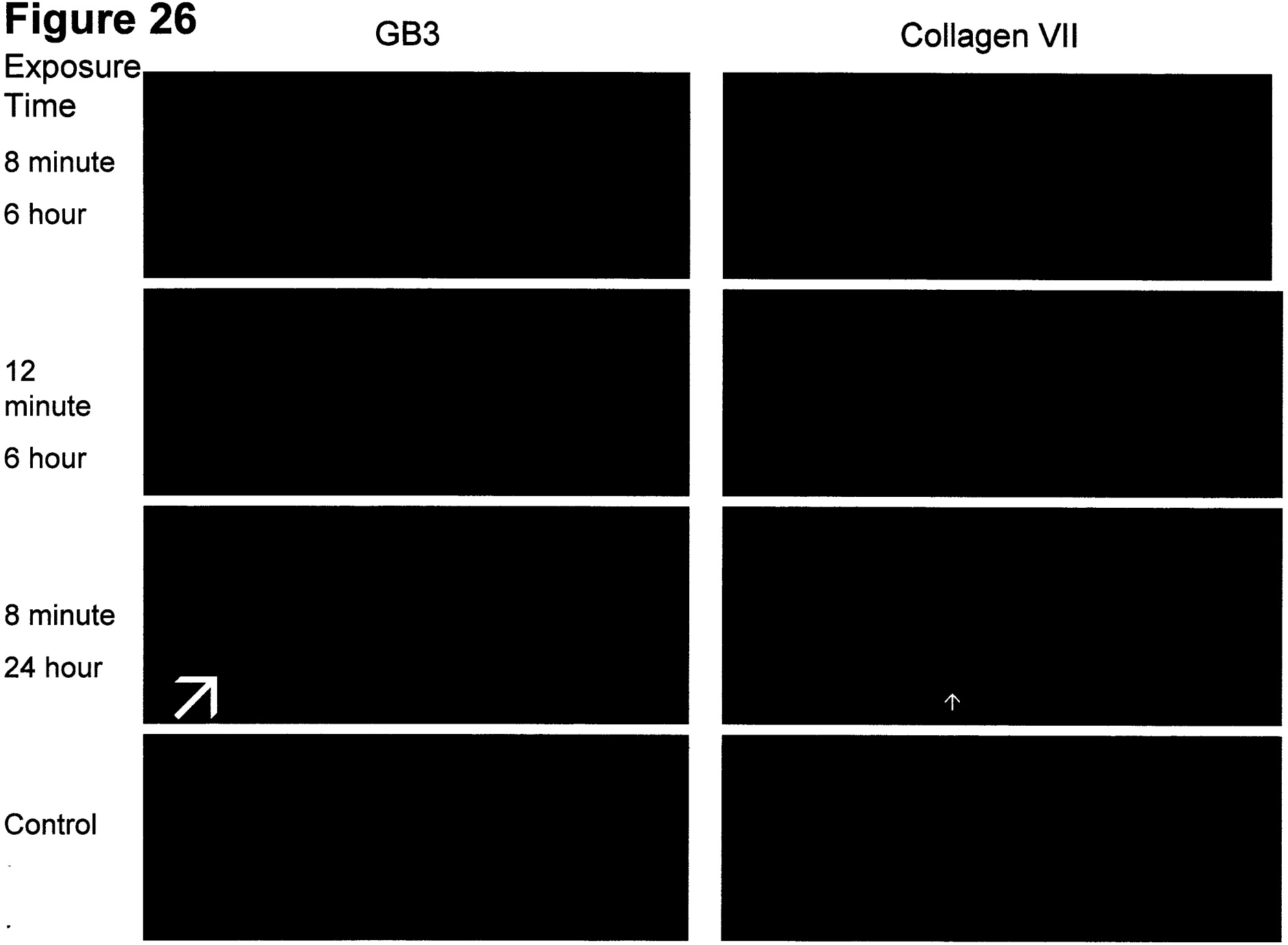
GB3
Collagen VII
Exposure Time
8 minute
6 hour
12 minute
6 hour
8 minute
24 hour
Control

Figure 27

Collagen IV

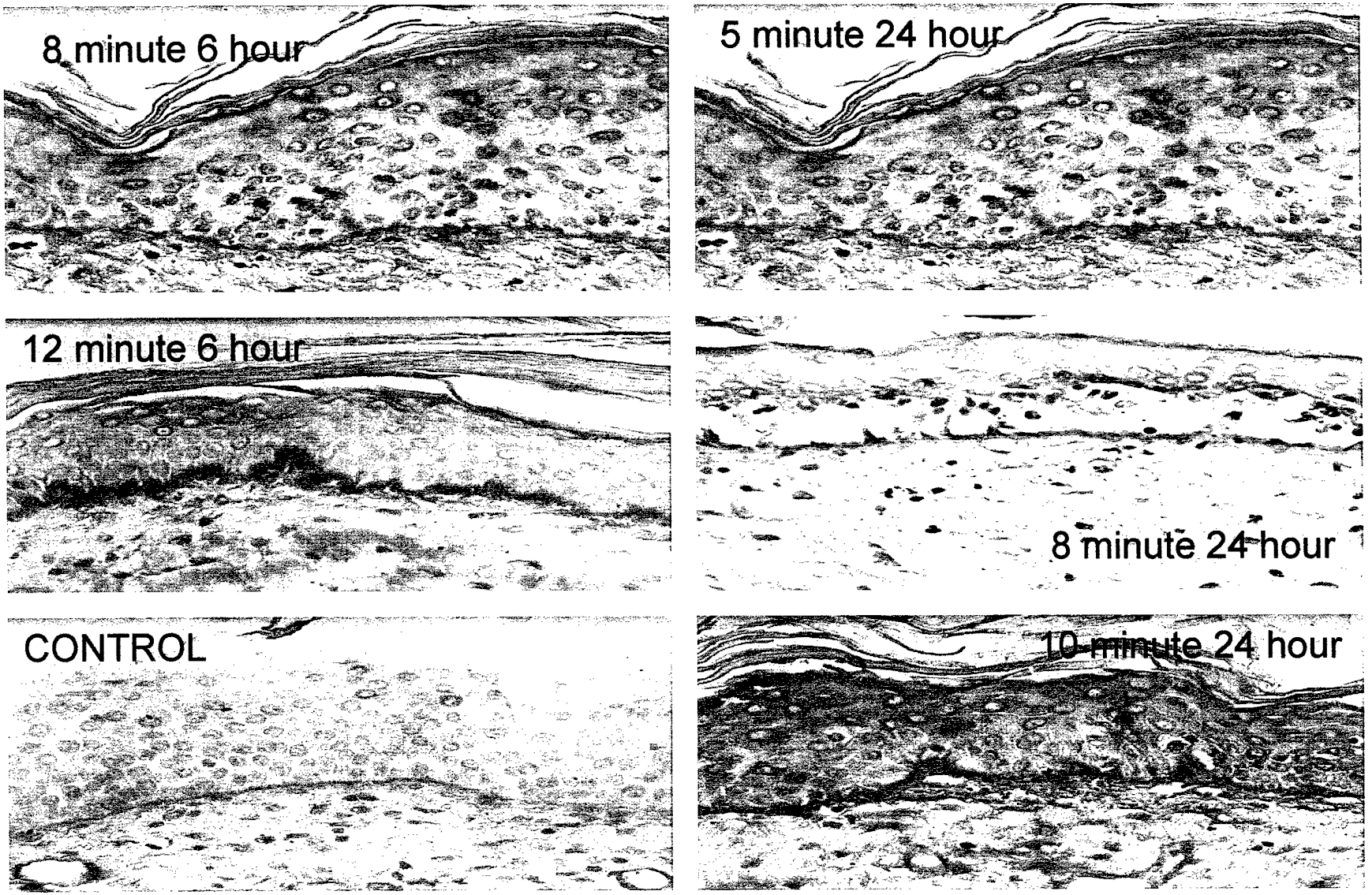

Figure 28

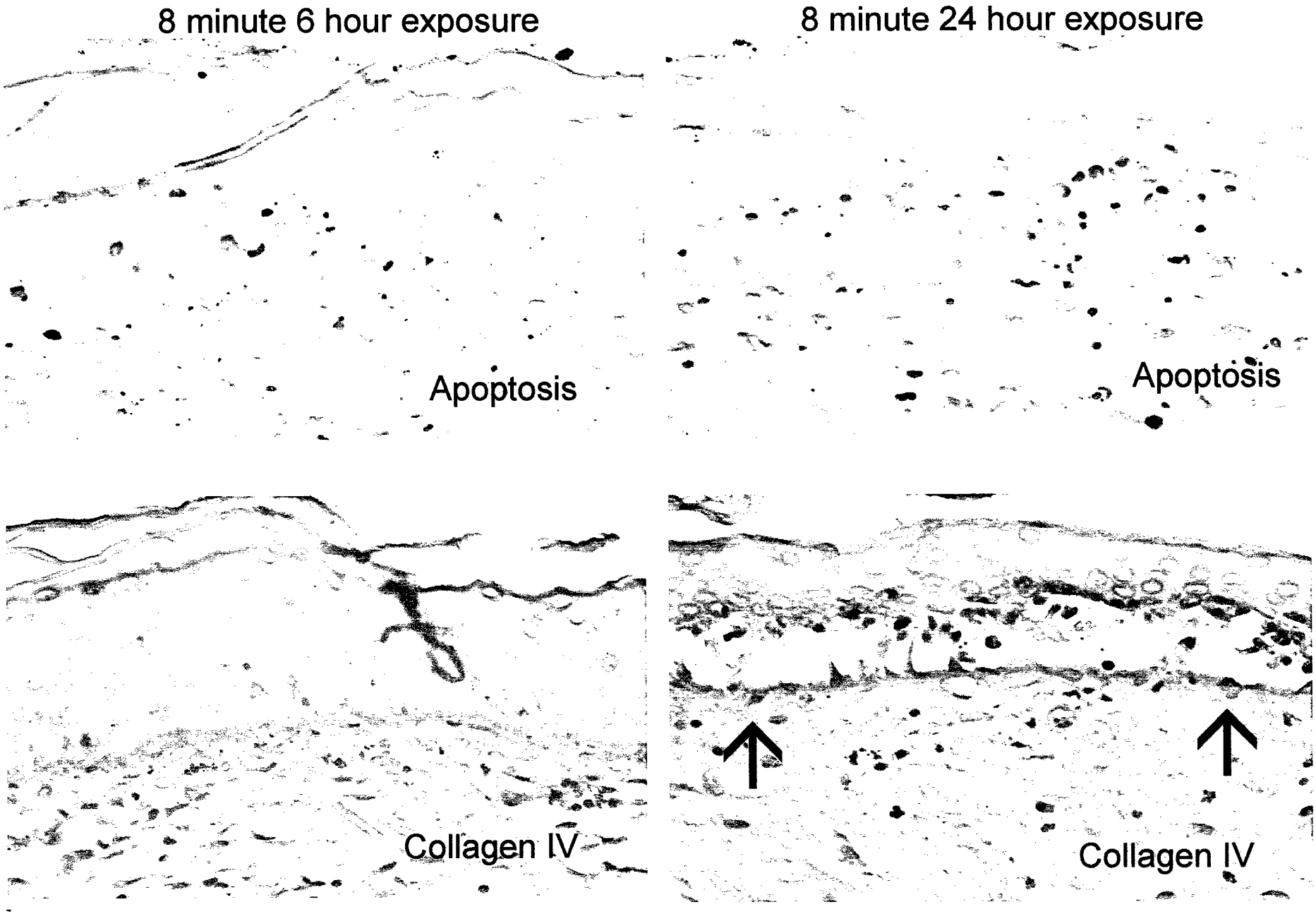
8 minute 6 hour exposure
8 minute 24 hour exposure
Apoptosis
Apoptosis
Collagen IV
Collagen IV

Figure 29

48 Hour 952-D PRP

2X

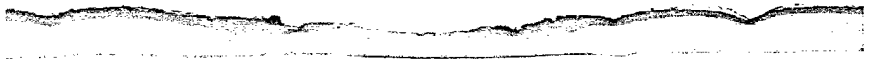

10X

10X

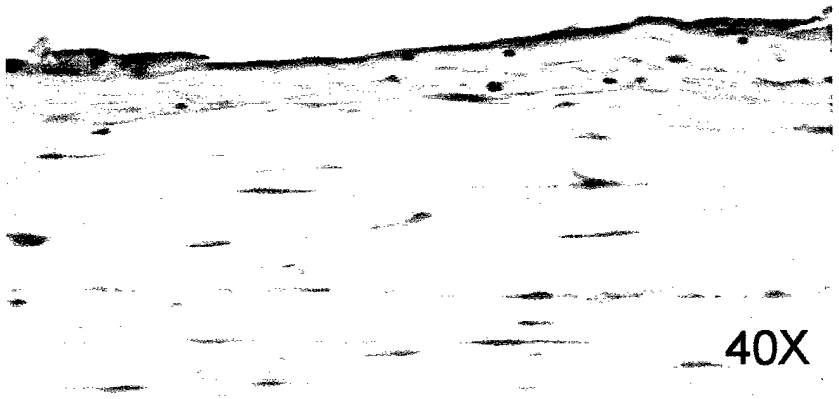

40X

Figure 30

48 Hour 953-A PPP

2X

10X

10X

40X

Figure 31

48 Hour 951-D No Tx

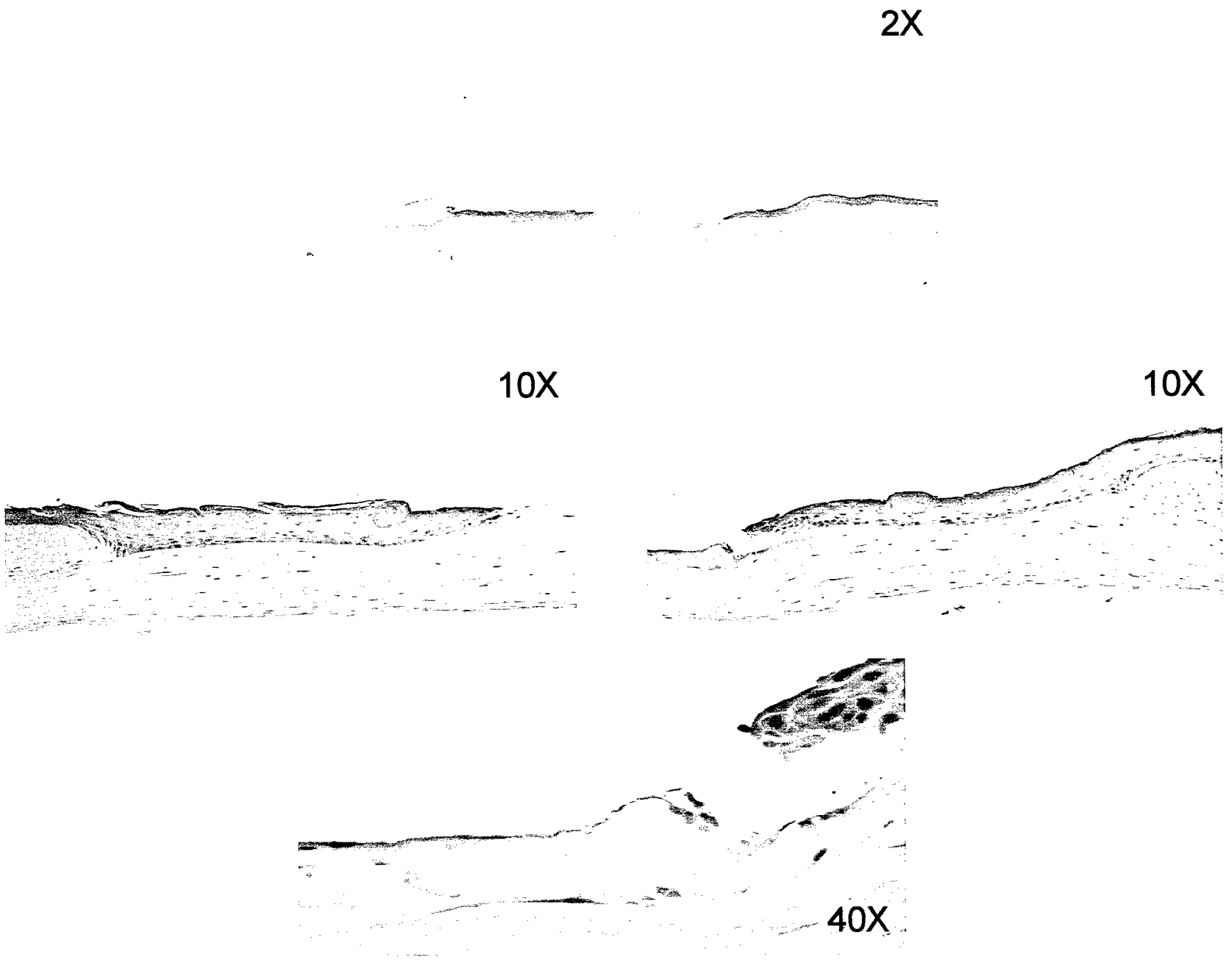

Figure 32

96 Hour 951-B PRP

2X

10X

10X

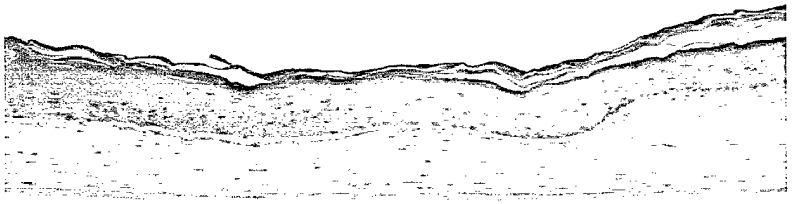

40X

Figure 33

96 Hour 953-F PPP

2X

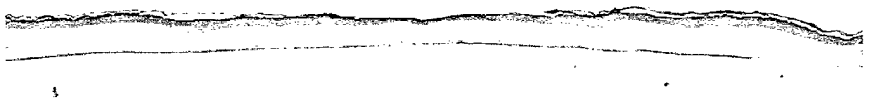

10X

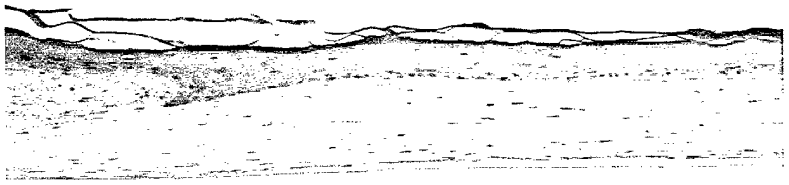

10X

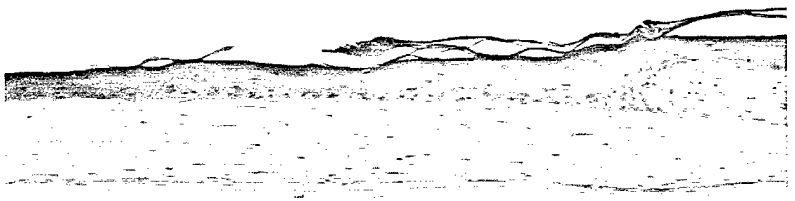

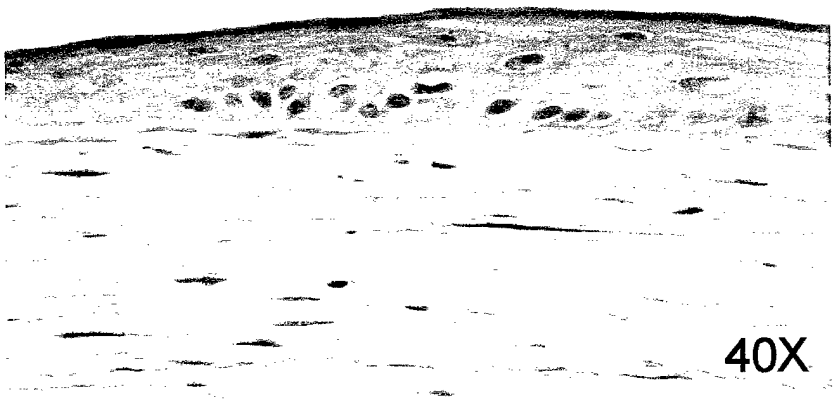

40X

Figure 34

96 Hour 951-C No Tx

2X

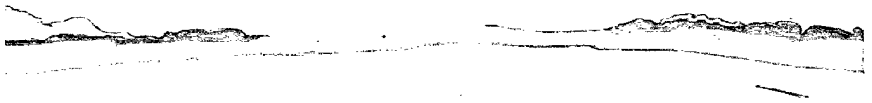

10X

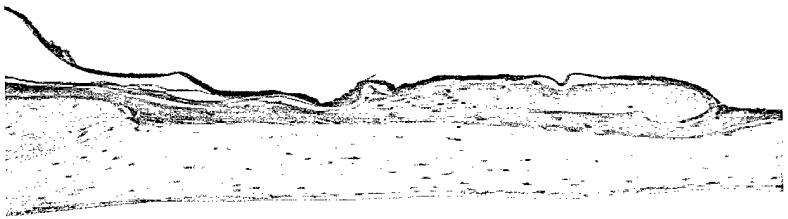

10X

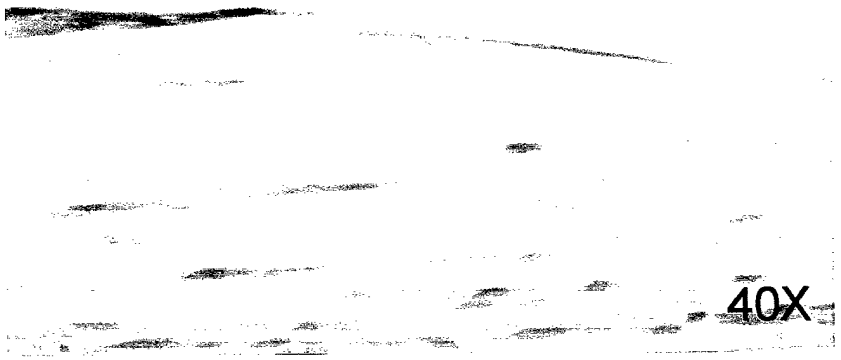

40X

Figure 35

48 Hour 951-D No Tx
GB3

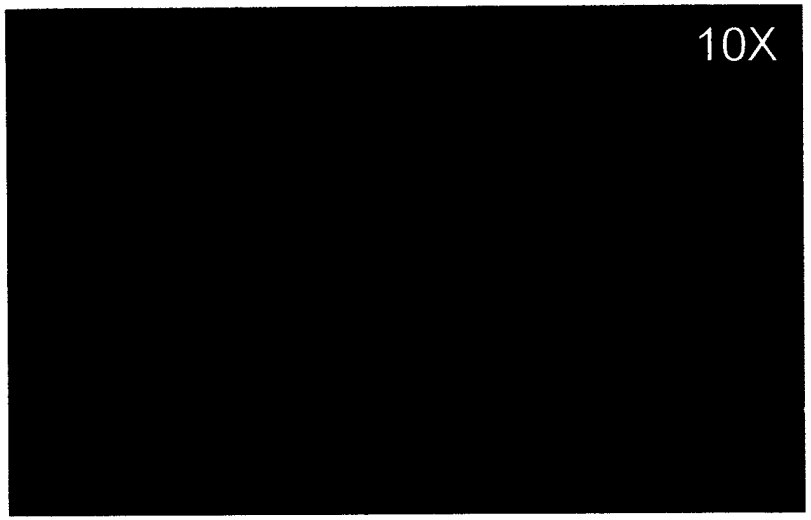

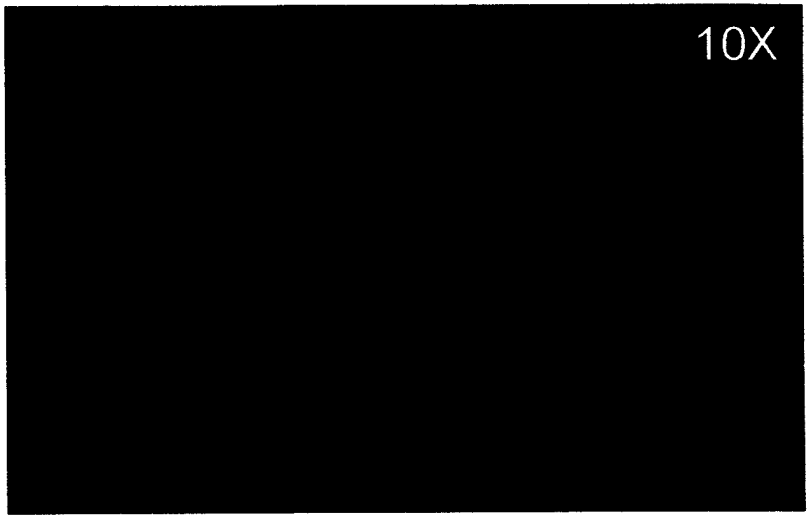

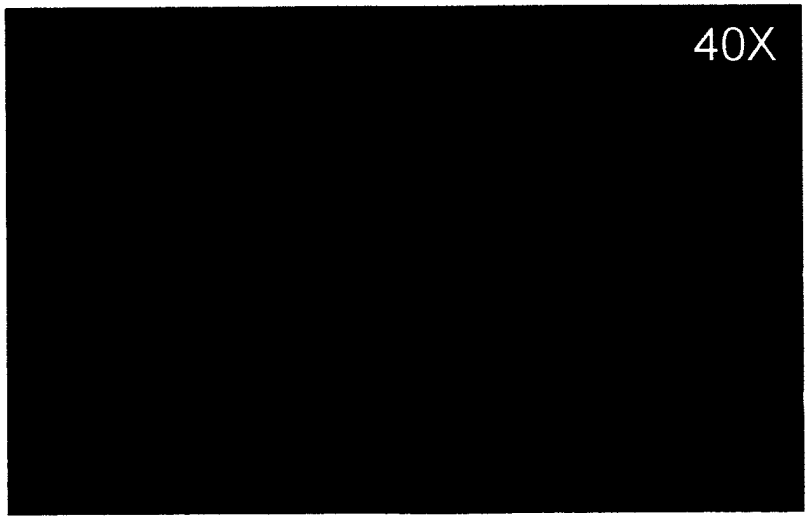

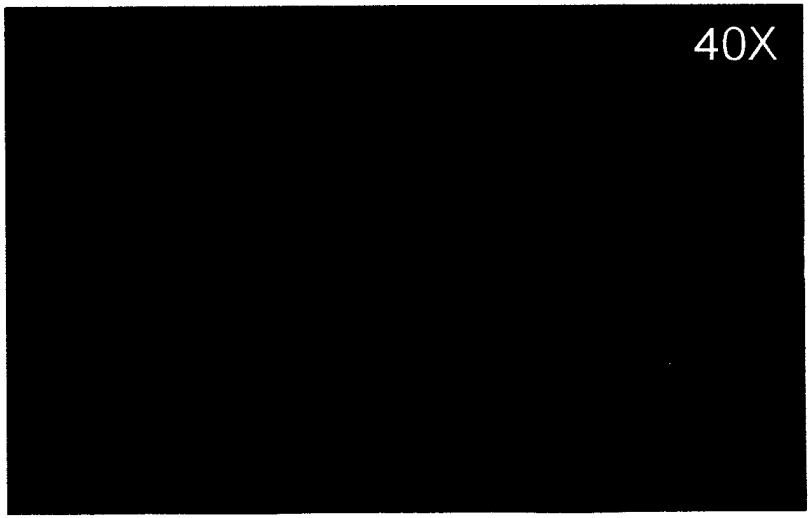

Figure 36

48 Hour 952-D PRP
GB3

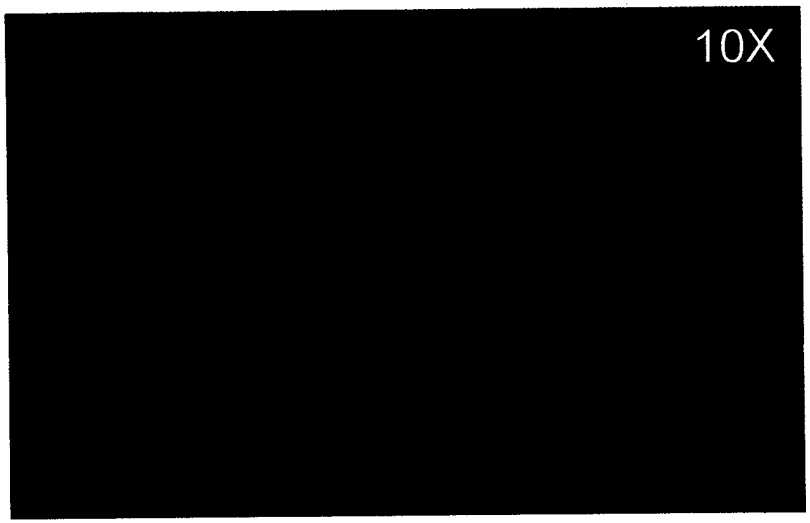

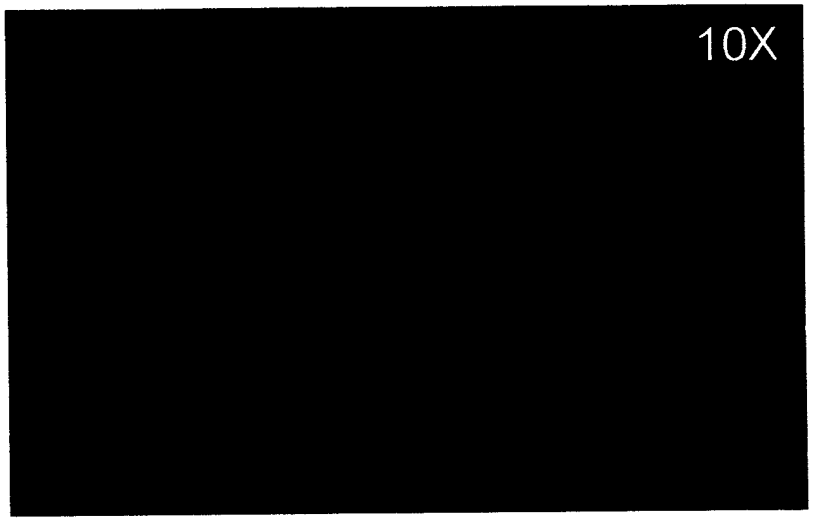

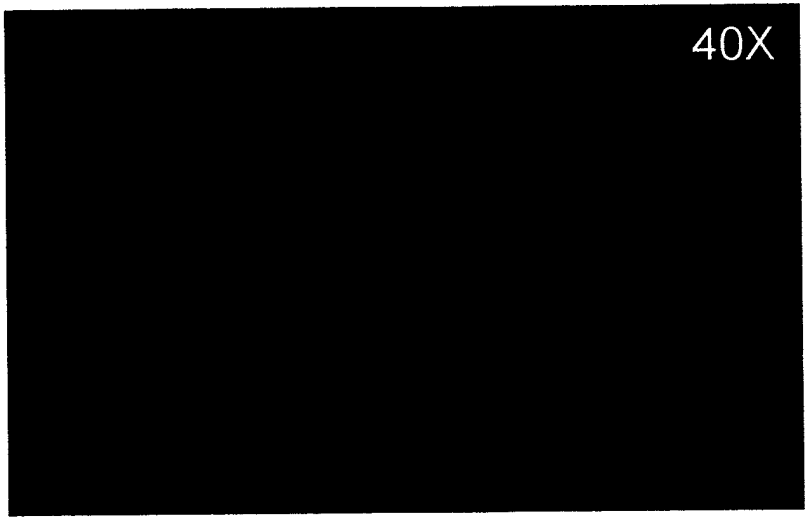

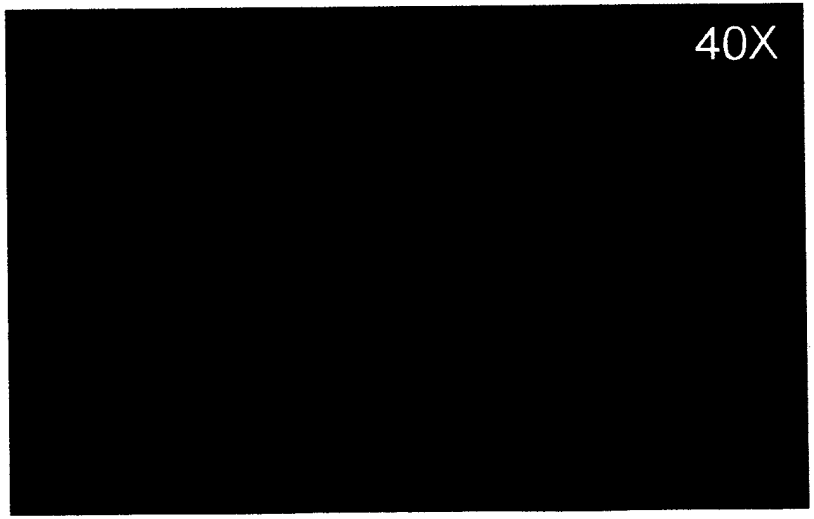

Figure 37

96 Hour 951-C No Tx
GB3

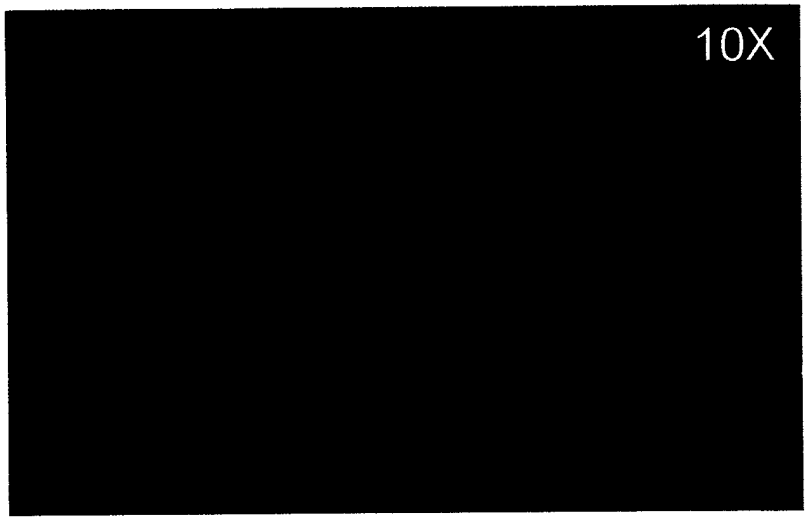

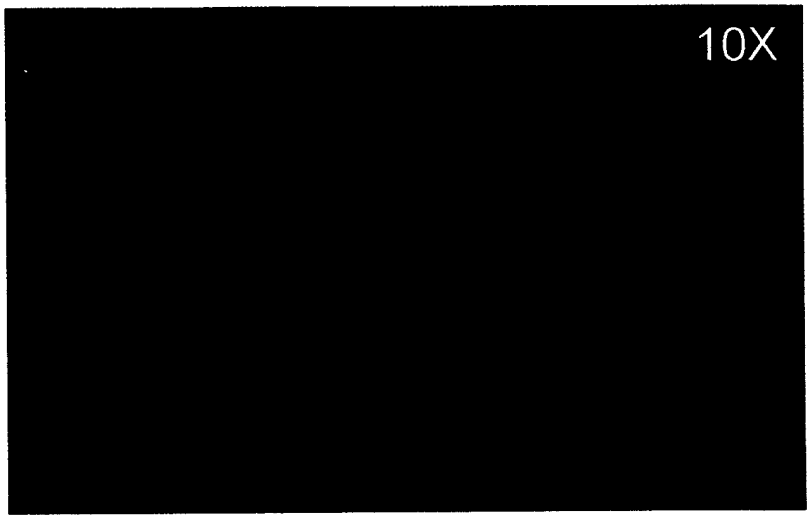

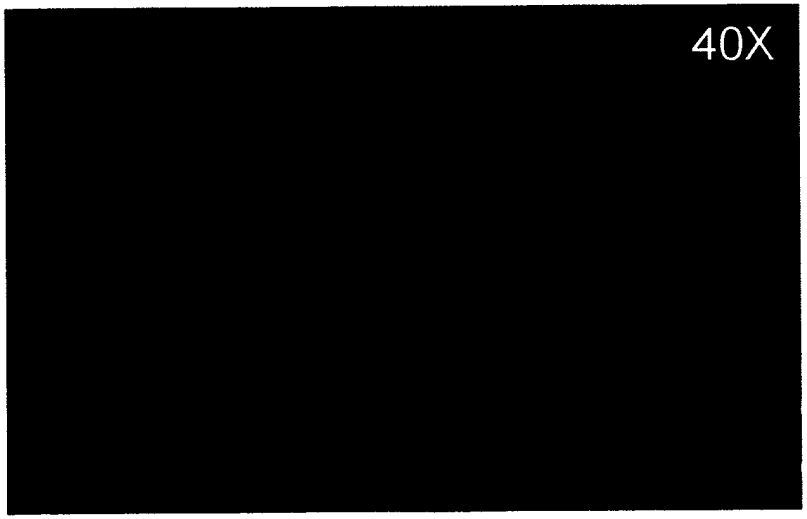

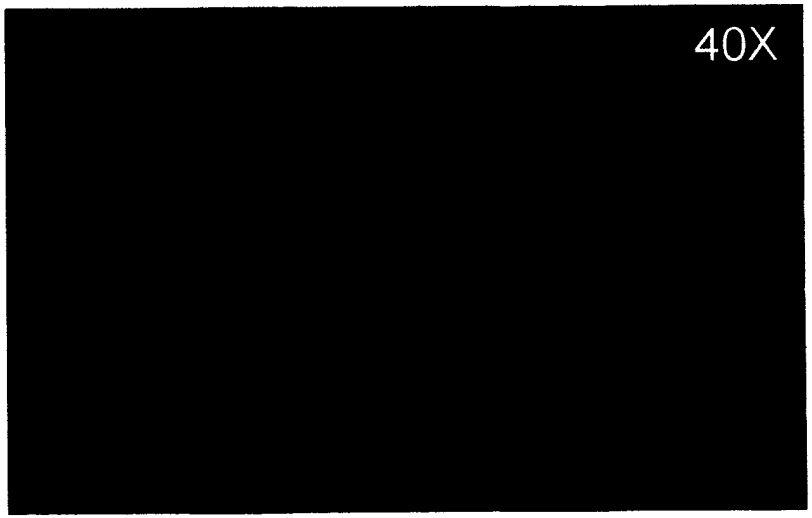

Figure 38

96 Hour 953-F PPP
GB3

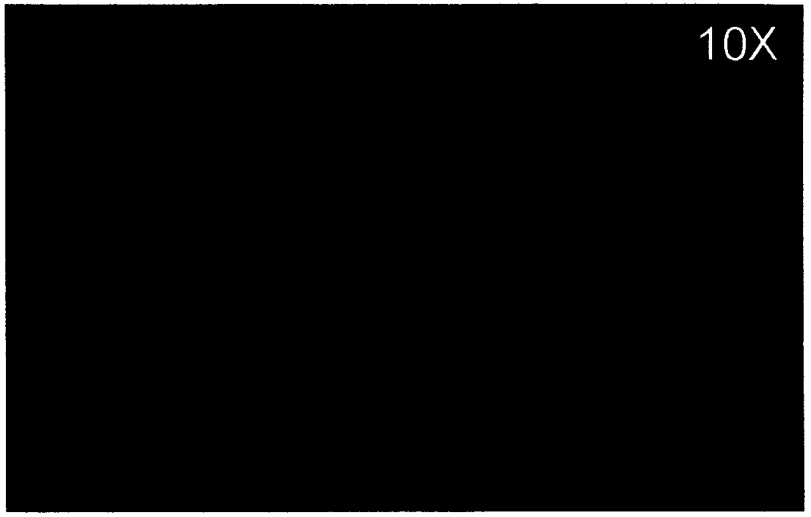

Figure 39

96 Hour 951-B PRP
GB3